Derek J. Smith

Candidate

Department of Computer Science

Department

This dissertation is approved, and it is acceptable in quality and form for publication on microfilm:

Approved by the Dissertation Committee:

, Chairperson

Accepted:

Dean, Graduate School

Date

The Cross-Reactive Immune Response:
Analysis, Modeling, and Application to Vaccine Design

by

Derek J. Smith

B.Sc., Computer Science, University of Bradford, 1982

M.Sc., Computer Science, University of New Mexico, 1994

Dissertation

Submitted in Partial Fulfillment of the

Requirements for the Degree of

Doctor of Philosophy

Computer Science

The University of New Mexico

Albuquerque, New Mexico

December 1997

For Dorothy, Mabel, and John.

Acknowledgments

Very special thanks to Dave Ackley, Will Attfield, Warren Bean, Susan Chasey, Dave Davis, Brian Divine, Steve Fisher, Stephanie Forrest, Ron Hightower, Jim Hollan, Terry Jones, Pentti Kanerva, Jeff Krueger, Ron Manson, Wendell Miller, Ron Moore, George and Pat Paice, Mr. Parr, Alan Perelson, Sheryl St. Germain, Francesca Shrady, Alan Smith, Ann Smith, Dorothy Smith, Jim Smith, John Smith, Mabel Smith, William Smith, Paul Stanford, Carla Wofsy, and Agnes Zander.

Also thanks to Pete Allen, Steve Armijo, Tom Barrow, James Battye, Ben Bederson, Sandi Blanton, Graham Birtwhistle, Richard Bodsworth, Pat and Chris Boswell, Paula Bramante, Jessica Brigidi, Joann Buehler, Rob C., Linda Cicarella, Chris and Karen Creedon, Nancy Cox, Sibylle Cseri, Dipankar Dasgupta, Lisa Desjarlais, Patrik D'haeseleer, Eva Encinas, Chris Faehl, Rob and Maura Farrow, Graham Heatherington, Steve Hofmeyr, Donato Forte, Mike Houlder, Peter Hraber, Deborah Gavel, Liz Gutierrez, Jon Helfman, Bhanu Kapoor, Jo Kelley, Ian Knight, Pauline Knight, Rod Lazorik, Stan Lee, George Luger, Terri MacKeigan, Lea Joe and Phil, Barbara Mansel, Doug Matzke, J Mehaffey, Melanie Mitchell, Mr. Moffatt, Bernard Moret, Ana Mosterín Höpping, Patrick Nagatani, Jad Nehme, Avidan Neumann, Tony Nicholas, Mihaela Oprea, Mr. Owen, Barak Pearlmutter, Teri Peterson, Vardit Ravitsky-Neumann, Steve Row, Henry Shapiro, Mahant-Shetti, Henry Shrady, Margret Shrady, John Skaras, Suzanne Sluizer, Deborah Smith, Tim Smith, Anil Somayaji, Jason Stewart, Tony Stockman, Bernhard Sulzer, Ron Thomas, Kathryn Vogel, Mr. Waterhouse, and Mr. Williams.

Financial support was orchestrated by Stephanie Forrest via the Joseph P. and Jeanne

M. Sullivan program in theoretical immunology and a graduate internship at the Santa Fe Institute, the University of New Mexico Computer Science Department AI and Digital Equipment fellowships, and grants ONR (N00014-95-1-0364) and NSF (IRI-9157644). This work was also supported by grants NIH (AI28433, RR06555), and the Los Alamos National Laboratory LDRD program. Portions of this work were performed under the auspices of the U.S. Department of Energy.

DEREK J. SMITH

The University of New Mexico
December 1997

The Cross-Reactive Immune Response: Analysis, Modeling, and Application to Vaccine Design

by

Derek J. Smith

Abstract of Dissertation

Submitted in Partial Fulfillment of the
Requirements for the Degree of

Doctor of Philosophy

Computer Science

The University of New Mexico

Albuquerque, New Mexico

December 1997

The Cross-Reactive Immune Response:
Analysis, Modeling, and Application to Vaccine Design

by

Derek J. Smith

B.Sc., Computer Science, University of Bradford, 1982

M.Sc., Computer Science, University of New Mexico, 1994

Ph.D., Computer Science, University of New Mexico, 1997

Abstract

The cross-reactive immune response occurs when an immune system is exposed to one pathogen and challenged with a related but different pathogen; for example, vaccination with one strain of influenza and challenge with a wildtype strain. In this way immunological memory functions as an associative memory. A discrete object model of the immune system was built to study the cross-reactive response. Parameters of the model were derived from immunological data, and lazy evaluation was used to make the simulation efficient. The model was used to understand annual vaccination against influenza. Influenza accounted for at least 10,000 deaths in each of the 19 epidemics in the United States between 1957 and 1986, and the medical and lost productivity cost of the epidemics in the 1960's was between two and four billion dollars. Vaccination against influenza is difficult because the virus continually changes—this requires the vaccine to be updated, sometimes on a yearly basis, and for individuals in high risk groups to be revaccinated each year. Vaccine efficacy in first-time vaccinees is usually 70-80%. However, vaccine efficacy in repeat-vaccinees varies widely from 0 to 80%. This variation has been observed for 20 years, yet is not fully understood. Experiments using the model described here offer an explanation

for this variation by showing how immunological memory to previous vaccines can interfere, both positively and negatively, with subsequent vaccination. The degree, and sign, of the interference depended on the antigenic differences between the vaccine strains and epidemic strains used in the experiments. Currently, new strains for the influenza vaccine are chosen to be close to the expected epidemic strains. The results reported here suggest that vaccine strains should also be chosen to be distant from previous vaccine strains.

Contents

List of Tables

List of Figures

Chapter 1

Introduction

We share our planet with an enormous variety of organisms, and as we live our lives the vast majority of them ignore us. Some however, mostly microorganisms such as bacteria and viruses, use our bodies as hosts for part or all of their life-cycles. With some we have a symbiotic relationship; for example, the bacteria in our stomachs synthesize vitamins and in return they get a free food supply. With others, such as the influenza virus, the relationship is parasitic, and our immune system has evolved to recognize such organisms and make life uncomfortable for them. Our immune system remembers pathogens it has seen before, and if it sees them again it can often eliminate them before they cause disease. This memory is why we only get some infectious diseases such as measles once, and is also the basis for vaccination. Vaccines are weakened or inactivated pathogens that do not cause disease, but which expose our immune systems to the pathogen and induce immunological memory to the pathogen.

Some pathogens change over time, and depending on how much they change, immunological memory to earlier variants might still recognize them, and attack them, though with reduced capacity. Vaccination is greatly complicated by such antigenically variable pathogens. For example, components of the influenza vaccine have to be updated, sometimes on a yearly basis, to maintain a reasonable correspondence with the virus, and individuals at risk from death or serious illness from influenza are revaccinated annually with the new vaccine strains. However, even then the effectiveness of annual influenza vaccination is highly variable. In some cases it is as good or a little better than first-time vaccination, but in other cases it is significantly worse—in some studies, annual vaccinees are no better protected than individuals who have never been vaccinated. The elderly are particularly at risk from death or severe illness from influenza, but vaccine efficacy in the elderly is often less than 50%. During the 19 influenza epidemics between 1957 and 1986, over 10,000 excess deaths were recorded during each epidemic. The variability of influenza vaccine efficacy in repeat vaccinees is not fully understood, though it has been observed for over 20 years.

This is an interdisciplinary dissertation in which I bring computer science techniques to the study of the immune response to antigenically variable pathogens. In particular, I address the question of annual vaccination against influenza, although the tools I build are also applicable to other areas. My approach is to use computer modeling. I also bring the perspective that immunological memory is a form of associative memory, and associative memories are well studied systems in computer science. My main emphasis is on answering questions related to public health, but along the way we will also see some spin-offs back to computer science.

1.1 Vaccines

Vaccination is a highly successful technique in preventive medicine. For example, in 1954, just before the introduction of the polio vaccine, there were 18,000 cases of paralytic polio in the United States, by 1961 there were 1,000 cases, and by 1985 there were 5. Similarly with smallpox, a sometimes deadly disease, cases dropped dramatically after the introduction of a vaccine, and it is believed that smallpox has now been eradicated from the planet. Protection by vaccination is potentially long lasting; for example, measles vaccination confers protection for life. Vaccination is also cost effective, with common vaccines costing less than 20 US dollars per person, and because of this vaccination is one of the few health measures available in many developing countries. Vaccination sometimes has side effects, sometimes very serious, and these have usually been caused by impurities in the vaccine. Modern vaccine manufacturing and testing techniques significantly reduce these risks. Although there are many cases of successful vaccines, there are many infectious diseases for which no effective vaccine exists. As discussed above, antigenic variability makes vaccination particularly difficult. Vaccination is a truly elegant process, it allows our immune system to learn to recognize a weakened version of a pathogen so it can better cope with the real thing. Contrast this with antibiotics that take over from our immune systems in the midst of disease, have to be taken four times a day for two weeks, and do nothing to protect us from future attacks. Incomplete treatment with antibiotics also risks the selection of antibiotic-resistant pathogens.

1.2 Models

Immunologists use a range of model systems which trade off accuracy for observability, controllability, and cost effectiveness. *In vivo* models are usually the most accurate, but it is difficult to observe and control what is happening inside an animal. Mice are the most common experimental animals, because their immune systems are similar to those of humans, they are easy to breed, cheap to keep, easy to handle, and most people don't get too worked up if humans experiment on them. However, for some diseases mice do not work well; for example, mice don't get human influenza, so much influenza work is done using ferrets. It is often a crucial step in studying a disease to find an animal model that behaves similarly to humans. A major difficulty with work on HIV for example is the lack of an animal model; chimpanzees are the closest to humans for HIV work, but chimpanzees are an endangered species, and are difficult to breed and work with, and most people are more concerned about humans experimenting on chimpanzees than they are about using mice. Only 600 chimpanzees were available for all forms of medical research in the United States in the early 1990's.

It is difficult to observe what is happening *in vivo*, primarily because the immune system is highly complex, highly detailed, and massively distributed. For example, for over 10 years, it was generally considered that during asymptomatic HIV infection the virus was mostly dormant, in a similar way that herpes virus lies dormant between outbreaks. However, it is now thought that a raging battle is going on during the asymptomatic period, with enormous viral replication and T cell killing by HIV, and enormous T cell replenishment and viral killing by the immune system. Thus, the steady state during the first 10 years is not due to the virus being dormant, but is a dynamic steady state of great activity.

Gene manipulation and organ transplant techniques greatly increase the variety of animal models. For instance SCID-human mice have no immune systems of their own, and have partial human immune systems. Gene manipulation can create ”knockout” mice, that have missing genes, and such models systems are useful to simplify aspects of the immune system so it can be studied more easily. For example, there are knockout mice that express only one B cell receptor specificity, whereas normal mice express 10 to 100 million specificities. Such genetically manipulated animal models are very useful, but accuracy is reduced from experiments in normal mice because the natural environment of the immune system has been altered. Whether this matters depends on the experiment. Situations arise where experiments in one model system contradict the results of another, and the reasons are sometimes due to reduced accuracy in model systems.

Another modeling technique that simplifies the immune response is to use model antigens. Bacteria and viruses are complex organisms, and the immune response to them is often multifaceted. Thus, the use of a simplified antigen such as a small protein coated with small regular chemicals called haptens simplifies the immune response and thus makes it easier to observe. Again, accuracy is reduced, but it is a useful trade-off.

In vitro experiments are a further abstraction from *in vivo* experiments, as they take place in a petri dish or a test tube. The cells under study are removed from their natural environment and thus accuracy is reduced; however, such experiments are much more controllable and observable, and often much cheaper and faster, than *in vivo* experiments.

In vitro experiments are a very useful tool, but like any model system, care must be taken when translating the model results into what would be expected *in vivo*. For example, syncytia formation (cells clumping together) was seen early on in the study of HIV *in vitro*, and it was thought that it might be a mechanism that caused depletion of T cells *in vivo*. It is now thought that this is not the case.

In machina experiments are potentially powerful new model systems for immunologists. They are maximally observable and controllable—every detail of a computer simulation can be recorded and any simulated cell or molecule can be manipulated in any way at any time. However, they are also potentially low in accuracy. The accuracy of an *in machina* model is limited by how much is programmed into the model and by immunological knowledge. Important details of the immune response, such as how the memory population is maintained, what controls cell differentiation, and the mapping from protein sequence to tertiary structure, are not fully understood. Thus model designers must guess at these processes, or abstract away from them. For instance, in the *in machina* model built for this study, the memory population is maintained by long-lived cells, cell differentiation is a probabilistic process, and sequence and structure are equivalent; all of these are abstractions from reality. However, such a model may still be useful—it depends on whether the aspects of the immune system that have been abstracted away are critical for what the model is being used to study. If the behavior of the system depends on the high level behavior of an ensemble of components, as opposed to the details of the behavior of a single component, and if that high-level behavior is captured in the model, then the model can be useful. *In machina* experiments are particularly suited to understanding the system level behavior of ensembles of components over time. This is because the simulation is transparent, and can be examined at whatever level of detail is desired, without affecting the simulation. This is in contrast to an *in vivo* experiment in which the animal often has to be killed and dissected to observe what has happened.

Like *in vivo* animal models, genetically manipulated animal models, systems using model antigens, and *in vitro* models, the results from *in machina* models must be treated carefully, and tested with more accurate models. Testing in more accurate, but difficult to work with, models is very important, and has guided my research toward an application that is testable with current immunological techniques. The bottom line is that if a model is compelling, and its results can be tested, then it will be used.

1.3 The Rest of the Story

The next chapter shows that immunological memory functions as an associative memory, and explains why it is associative. In an associative memory, recall does not require exactly the same stimulus that was used to write to the memory; this is in contrast to a computer memory which requires an exact match of a stimulus to recall what was written. This chapter also introduces the concept of *shape space* and an antigen's *ball of stimulation*, and shows that the volume of the intersection of balls of stimulation is important for understanding cross-reactive memory. This abstract view enables prediction, at an abstract level, the immune response to multiple cross-reactive antigens. To make this abstract view somewhat more real, I then proceed to build a model of the immune system that can be used to simulate the cross-reactive immune response. Chapters three and four are about making the model sufficiently accurate and computationally efficient.

In chapter three, *deriving shape space parameters from immunological data,* I set parameters for the model. I show that the intersection of balls of stimulation (and thus the cross-reactive immune response) is sensitive to the parameters of shape space, and I derive those parameters from immunological data. The results of this derivation indicate that a realistic-size repertoire of 10^7 B cells should be used in simulations. In chapter four I describe how *lazy evaluation* can be used to make simulations of such a large number of B cells computationally tractable.

In the remainder of the dissertation I focus on application of the model. There are potential applications wherever the understanding of pathogenesis or vaccine design is complicated by antigenic variability of the pathogen; for example, in influenza, tuberculosis, and HIV. I have chosen to concentrate on annual vaccination against influenza, and this is described in the fifth chapter, *annual vaccination against influenza: an* in machina *study*. The model shows good qualitative agreement with existing knowledge, and analysis of phenomenon seen in the model provides potential explanations of previously contradictory experimental results, and might help in vaccine strain selection.

The sixth chapter, *further work*, details results on using the model for vaccine strain selection, and for multivalent vaccine design, and also gives a mathematical analysis of cross-reactive memory, and details wet experiments that could be done to test the predictions from the influenza work.

Chapters two, three, four, and five, are written as journal publications, and are at various stages of acceptance and submission.

Chapter 2

Immunological Memory is Associative*

Abstract

We show that immunological memory is in the class of sparse distributed associative memories along with Kanerva's *Sparse Distributed Memory*, Albus's *Cerebellar Model Arithmetic Computer*, Marr's *Theory of Cerebellar Cortex*, and Aleksander *et. al's WISARD*. These memories derive their associative and robust nature from a sparse sampling of a huge input space by recognition units (B and T cells in the immune system) and a distribution of the memory among many independent units (B and T cells in the memory population in the immune system).

2.1 Introduction

In an *associative* memory, data is stored at an address and is retrieved by reading the memory at the same address, or a similar address. This process is called *associative recall* and is in contrast to a *point* memory (such as the random access memory of a traditional computer) in which the write and read addresses must be identical. Associative memories are useful computational devices in noisy or imprecise environments and have been used

*A prior version of this chapter was published as Smith *et al.* (1996)

in many applications including: speech recognition (Prager & Fallside, 1989; Danforth, 1990), character recognition (Sabourin & Mitiche, 1993; Manevitz & Zemach, 1997), and robot control (Albus, 1981; Commuri *et al.*, 1997). Associative memories are also typically *robust*, not only to noise in a read address but also to failure of components of the memory—the signal-to-noise ratio of the output decreases proportionally to noise in the address or the number of failed components. Many implementations of associative memory have been proposed including: Marr (1969), Albus (1981), Willshaw (1981), Hopfield (1982), Kohonen (1984), Aleksander *et al.* (1984), Kanerva (1988).

Immunological memory is associative—it responds to antigens similar, but not necessarily identical, to ones it has seen before. The associative memory properties of the immune system were explicitly used 200 years ago when Jenner (1798) vaccinated with cowpox to protect humans from smallpox. The modern investigation into associative recall of immunological memory began with the observation that antibodies induced during an influenza infection often had greater affinity to prior strains of influenza than to the infecting strain—suggesting that the antibodies were generated by memory of prior infections—a phenomenon was called original antigenic sin (Francis, 1953; Davenport *et al.*, 1953). Gilden (1963) and Fazekas de St. Groth & Webster (1966) investigated original antigenic sin by injecting laboratory animals with one antigen and recalling the memory of that antigen by injection of a related antigen. Some researchers considered associative recall "a degeneracy in the secondary immune response" because it showed that not every exposure was remembered uniquely (Eisen *et al.*, 1969). However, as research continued, and associative recall was observed in many animals with many different antigens, it became clear that it was a general feature of immunological memory (Virelizier *et al.*, 1974; Ivanyi, 1972; Deutsch & Bussard, 1972; Fish *et al.*, 1989; Nara & Goudsmit, 1990; Smith, 1994). Immunologists refer to associative recall as a *cross-reactive* or *heterologous* secondary immune response. Immunological memory was explicitly identified as an associative memory by Farmer *et al.* (1986).

This paper refines the observation that immunological memory is associative by showing that it is a member of the class of *sparse distributed* associative memories (Kanerva, 1992). We do this by showing the high level correspondences between immunological memory and the archetypal member of the class—Sparse Distributed Memory (Kanerva, 1988). This class is characterized by, and derives its associative and robust properties from a sparse sampling of the input space by recognition units, the activation of a subset of recognition units by an input address, and a distribution of data to the activated recognition units. When interpreted as neural networks, this class correspond to three layer networks with a large hidden layer with fixed weights between the first and second layers. Other members of this class include Marr (1969)'s *Theory of Cerebellar Cortex*, the *Cerebellar Model Arithmetic Computer* (CMAC) (Albus, 1981), *WISARD* (Aleksander *et al.*, 1984) and *Sparse Distributed Memory* (SDM) (Kanerva, 1988) (and its variations (Jaeckel, 1989a; Jaeckel, 1989b)). The details of the implementation of each memory varies widely—from mathematics and logic (SDM and CMAC), to neurobiology (Marr), to immunobiology (described here).

2.2 Immunological Memory

The immune system recognizes a large number of cells and molecules (antigens) it has never seen before, and decides how to respond to them. Some antigens, such as viruses, bacteria, parasites and toxins generate mixtures of T cell and antibody responses. Other antigens, such as those that make up the individual's body, must not be attacked[1]. The immune system remembers antigens it has seen before and when it sees them again is often capable of eliminating them before disease occurs—this is the basis for vaccination, and the reason why we do not get many infectious diseases more than once. The immune system is complex, highly detailed, and not fully understood—thus the following brief exposition is necessarily simplified and incomplete.

[1]Diseases such as multiple sclerosis, rheumatiod arthritis and insulin-resistant diabetes are examples of autoimmune diseases where the immune system attacks the body it usually protects.

Recognition. Vertebrate immune systems use a large number of highly specific B and T cells to recognize antigens. An individual has the genetic material and randomizing mechanisms to potentially express more than 10^{10} distinct B cell receptors (Berek & Milstein, 1988), and at any time actually expresses a subset of 10^7 to 10^8 distinct B cell receptors (Köhler, 1976; Klinman *et al.*, 1976; Klinman *et al.*, 1977). The number of possible distinct antigens is difficult to calculate, but it is thought to be in the range 10^{12} to 10^{16} (Inman, 1978). B and T cells can be stimulated by antigen if their affinity for the antigen is above some threshold. Typically 10^{-5} to 10^{-4} of an individual's B cells can be stimulated by an antigen (Edelman, 1974; Nossal & Ada, 1971; Jerne, 1974), these B cells are said to be in the *ball of stimulation* of the antigen (Perelson & Oster, 1979) (Figure 2.1a).

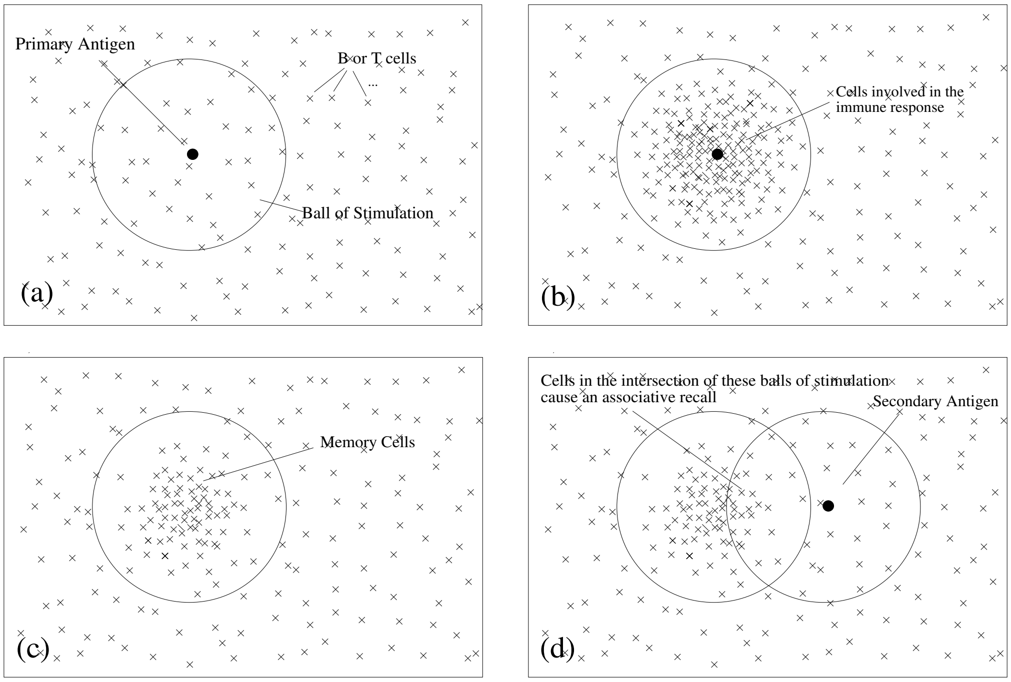

Figure 2.1: (a) A two dimensional illustration of (a high dimensional) sparse distribution of B or T cell receptors ($\times$) in a space where distance is a measure of affinity for an antigen ($\bullet$). B and T cells within some threshold affinity can bind the antigen and become activated. The region the antigen activates is called the *ball of stimulation* of the antigen. (b) Activated B cells replicate and mutate and the higher affinity ones are selected. (c) After the antigen is cleared a memory population persists. (d) A second exposure to the same antigen, or here a related antigen, restimulates the memory population and results in associative recall.

Response. When B and T cells are stimulated by antigen they divide. The B cell receptor sometimes mutates on cell division and this can increase the affinity of its daughter cells for the antigen, a process called affinity maturation. Toward the end of a response, when antigen becomes scarce, higher affinity B cells have a fitness advantage over lower affinity B cells and are preferentially selected in a process similar to natural selection (Figure 2.1b) (Burnet, 1959). During the replication of cells in response to antigen, some B cells differentiate into plasma cells and secrete antibodies which can eliminate the antigen. In the case of a viral infection, some T cells differentiate into cytotoxic T lymphocytes (CTLs), which can kill virus-infected cells.

After the antigen is cleared, the B cell and T cell populations decrease, but a persistent sub-population of memory cells remains (Figure 2.1c) (discussed further in section 2.5). These memory cells implement immunological memory—if the same antigen is seen again, the memory population is restimulated, and because of its size quickly produces large quantities of antibodies (or CTLs). This is called a *secondary* immune response, and often clears the antigen before the antigen causes disease. If the secondary antigen is slightly different from the primary antigen, its ball of stimulation might intersect part of the memory population created in a response to the primary antigen (Figure 2.1d). Memory cells in the intersection can bind the secondary antigen and produce antibodies and/or CTLs to remove it. The strength of a secondary immune response is related to the number of memory cells stimulated by the antigen (Gerhard, 1978; East *et al.*, 1980).

2.3 Sparse Distributed Memory (SDM)

Kanerva's SDM is a member of the class of sparse distributed associative memories (Kanerva, 1992). SDM, like random access memory, is written to by providing a binary address and data, and read from by providing a binary address. Unlike random access memory, the address space of SDM is very large, sometimes 1,000 bits, giving $2^{1,000}$ possible addresses. SDM cannot instantiate such a large number of address-data locations so it instantiates a randomly chosen subset of say 1,000,000 address-data locations. These instantiated address-data locations are called hard locations and are said to *sparsely* cover the input space (Kanerva, 1988).

When an address is presented to the memory, hard locations that are within some threshold Hamming distance of the address are activated. This subset of activated hard locations are said to be in the *access circle* of the address (Figure 2.2a). On a write, each

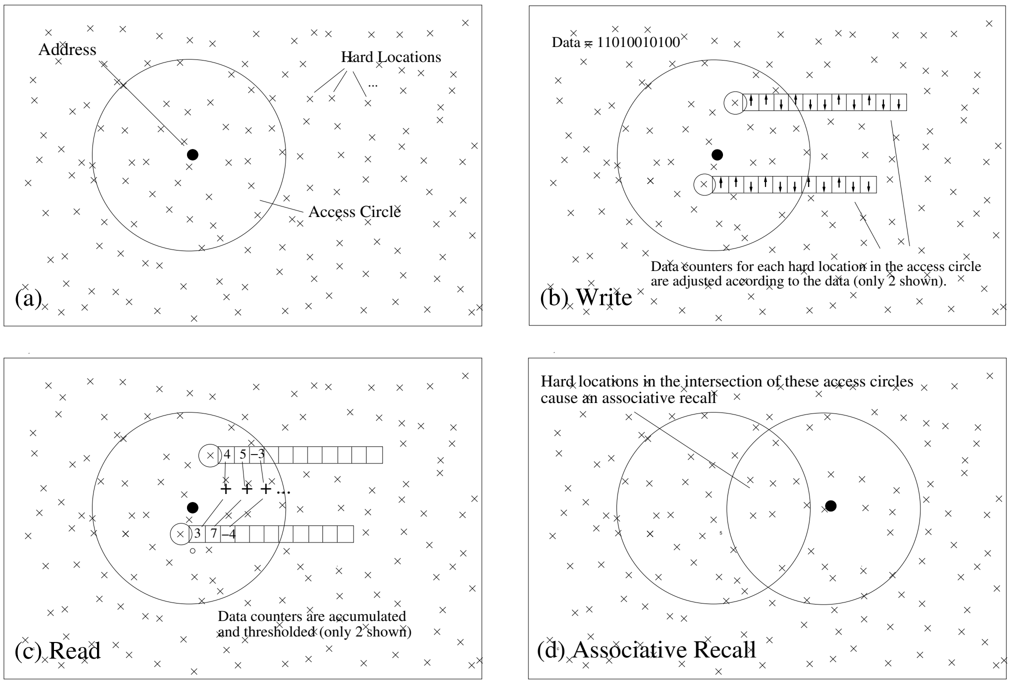

Figure 2.2: (a) A two dimensional illustration of hard locations sparsely and randomly distributed in a high dimensional binary input space. Distance in the space represents Hamming distance between hard locations. Hard locations within some radius of an input address are activated and form an access circle. (b) Activated hard locations adjust their data counters on a write and (c) accumulate and threshold them on a read. (d) The access circle of a similar address might include some hard locations from the prior write and induce an associative recall.

bit of the input data is stored independently in a counter in each activated hard location. If the i^{th} data bit is a 1, the i^{th} counter in each hard location is incremented by 1, if the i^{th} data bit is a 0 the counter is decremented by 1 (Figure 2.2b). On a read, each bit of the output is composed independently of the other bits. The value of the i^{th} counter of each activated hard location are summed. If the sum is positive the output for the i^{th} bit is a 1, if the sum is negative the output is a 0 (Figure 2.2c).

The distribution of data among many hard locations makes the memory robust to the loss of some hard locations, and it permits associative recall of the data if a read address is slightly different from a prior write address. If the access circle of the read address intersects the access circle of the write address, hard locations in the intersection give an associative recall of the write data (Figure 2.2d).

2.4 Correspondence between Immunological Memory and SDM

Table 2.1 summarizes the correspondence between immunological memory and SDM. Both immunological memory and SDM use detectors to recognize an input. In the case

SDM	Immunological memory
Hard location	B/T Cell
Access circle	Ball of stimulation
Hamming distance	Affinity
Write	Primary response
Read	Secondary response
Associative recall	Cross-reactive response
Address	Antigen
Data	B/T cell receptor, antibody class, T cell homing receptor, response/tolerance.

Table 2.1: The structural and functional correspondence between immunological memory and SDM.

of SDM, hard locations recognize an address, in the case of immunological memory, B and T cells recognize an antigen. In both systems the number of possible distinct inputs is huge, and due to resource limitations the number of detectors is much smaller than the number of possible inputs—both systems *sparsely* cover the input space. In order to respond to all possible inputs, detectors in both systems do not require an exact match with the input, but are activated if they are within some threshold distance of the input. Thus, in both systems an input activates a subset of detectors. In SDM, this subset is called the access circle of an input address, in immunological memory, it is called the ball of stimulation of an antigen.

In SDM the distance between a hard location and an address is defined to be Hamming distance. In the immune system, the equivalent of distance is a function of the binding *affinity* of an antibody, or B or T cell receptor, for an antigen. Binding is a complex physical chemical process involving, among other things, shape and charge complementarity. Even though the mechanism of the distance calculation in the immune system is very different from that in SDM, the function is the same—to activate a subset of detectors that will be involved in a read or write of the memory.

In both systems detectors store data associated with each input. In the case of SDM the data is an exogenously supplied bit string. In the case of immunological memory the data is the B or T cell receptor that can bind the antigen, the class of antibody or CTL response, and whether to respond to the antigen at all.

Both systems *distribute* data to each activated detector. In the case of SDM the data is used to adjust counters; in the case of immunological memory, memory cells are created which in the case of B cells have undergone genetic reconfigurations that determine the class of antibodies they will produce, and in the case of T cells might have homing receptors for the part of the body which the antigen infected. Because the data is stored in each detector, each detector can recall data independently of the other detectors. In both memories, the strength of the output (the signal) is an accumulation of the data in each activated detector. Thus, when only a subset of detectors are activated, either due to a noisy address (Figures 2.1d and 2.2d) or failure of some detectors, the output signal degrades gracefully, and the signal strength is proportional to the number of activated detectors. Thus, the distributed storage of information makes both systems robust.

2.5 Discussion

We have shown that B and T cells in the immune system perform an high level function analogous to hard locations in SDM—B and T cells perform a sparse coverage of all possible antigens in the same way that hard locations perform a sparse coverage of all possible addresses in a SDM. Also, data are distributed among many independent B and T cells in immunological memory as they are among many independent hard locations in a SDM. These high level correspondences between immunological memory and SDM characterize immunological memory as a member of the class of sparse distributed associative memories. Along with other members of this class, immunological memory is associative and robust precisely because it is sparse and distributed.

The idiotypic network theory (Jerne, 1974) has been central in previous discussions of the associative properties of immunological memory (Farmer *et al.*, 1986; Gibert & Routen, 1994). However, we regard the network theory as but one of the potential mechanisms that maintain the population of memory B cells; other theories include long-lived cells (Mackay, 1993), retained antigen (Tew & Mandel, 1979; Tew *et al.*, 1980), and cross-reactions with environmental antigen (Matzinger, 1994). Our explanation of why immunological memory is associative is independent of whichever of these mechanisms maintains the memory population.

A consequence of our description is to focus attention on the intersection of balls of stimulation. The number of clones in the intersections of balls of stimulation might be useful in explaining and predicting aspects of the cross-reactive immune response, in the same that the number of hard locations in the intersection of access circles is useful in explaining and predicting the behavior of SDM (Kanerva, 1988). For example, Figure 2.1d provides a qualitative understanding of why a cross-reactive response becomes weaker as two antigens become less alike—because the number of memory cells in the intersection of the balls of stimulation becomes smaller. Similarly, Figure 2.3 provides a qualitative understanding of how a prior infection can reduce the effectiveness of a vaccination against an epidemic challenge.

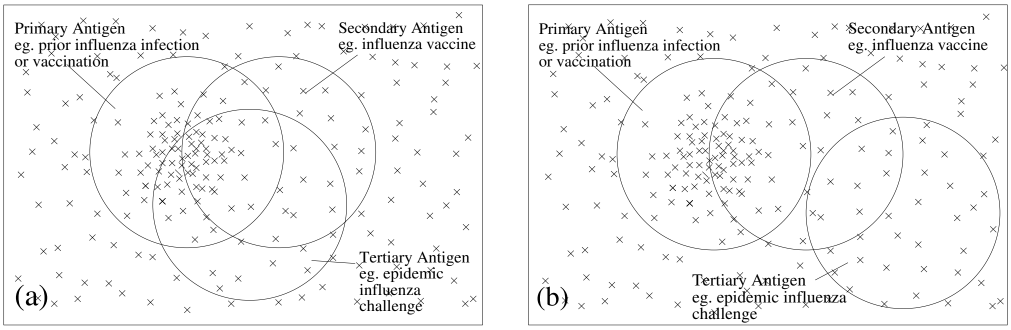

Figure 2.3: Associative recall of a prior exposure (primary antigen) can cause a vaccine (secondary antigen) to fail. If the ball of stimulation of a vaccine intersects the memory of a prior exposure, the vaccine may be cleared by associative recall of the prior exposure and fail to make highly specific memory to the vaccine strain. If the ball of stimulation of a subsequent epidemic challenge (tertiary antigen) also intersects memory of the prior exposure, it too can be cleared quickly by an associative recall (Figure 2.3a). However, if there is no intersection between the prior and epidemic strains, there will be no memory to clear the epidemic strain quickly, and the epidemic challenge might cause disease (Figure 2.3b).

To make these qualitative observations somewhat more quantitative, we have derived approximations of the dimensionality and cardinality of the space of B cell and antibody receptors (Smith *et al.*, 1997d). We showed that a five dimensional Euclidean space, or a twenty dimensional Hamming space with a four letter alphabet, are reasonable approximations given current immunological data on the cross-reactive immune response. This allows us to approximate the number and affinity distribution of cells in the intersection of balls of stimulation as a function of the distance between antigens. We have used the twenty dimensional Hamming space to model and analyze the cross-reactive immune response between two antigens (Figure 2.1) (Smith *et al.*, 1997a) and between three antigens (Figure 2.3) (Smith *et al.*, 1997b). In both cases we show good qualitative correspondence with existing data, offer explanations of data that were previously considered contradictory, and make predictions.

Chapter 3

Deriving Shape Space Parameters from Immunological Data*

Abstract

We present a method for deriving shape space parameters that are consistent with immunological data, and illustrate the method by deriving shape space parameters for a model of cross-reactive memory. Cross-reactive memory responses occur when the immune system is primed by one strain of a pathogen and challenged with a related, but different, strain. Much of the nature of a cross-reactive response is determined by the quantity and distribution of the memory cells, raised to the primary antigen, that cross-react with the secondary antigen. B cells with above threshold affinity for an antigen lie in a region of shape space that we call a *ball of stimulation*. In a cross-reactive response, the intersection of the balls of stimulation of the primary and secondary antigens contains the cross-reactive B cells and thus determines the degree of cross-reactivity between the antigens. We derive formulas for the volume of intersection of balls of stimulation in different shape spaces and show that the parameters of shape space, such as its dimensionality, have a large impact on the number of B cells in the intersection. The application of our method for deriving

*Journal of Theoretical Biology (in press) shape space parameters indicates that, for Hamming shape spaces, twenty to twenty-five dimensions, a three or four letter alphabet, and balls of stimulation of radius five or six, are choices that match the experimental data. For Euclidean shape spaces, five to eight dimensions and balls of stimulation with radius about twenty percent of the radius of the whole space, match the experimental data.

3.1 Introduction

Cross-reactive memory is observed when an individual develops memory to one strain of a pathogen and is challenged with a related strain. Vaccination with cowpox to protect against smallpox is an example of an early use of cross-reactive memory (Jenner, 1798; Ada, 1993). Cross-reactive memory also occurs in the natural immune response to pathogens that mutate. Francis (1953) observed that the immune response to influenza was often a recall of the response to a prior influenza infection, and called the phenomenon "original antigenic sin". Subsequent studies revealed that some memory cells specific for the primary antigen were also cross-reactive with the secondary antigen (Fazekas de St. Groth & Webster, 1966b; Deutsch & Bussard, 1972; Gerhard, 1978; Yarchoan & Nelson, 1984). Cross-reactive memory is often useful in that memory to a one strain of a pathogen can protect against other strains. It has also been suggested that memory to the primary antigen may be maintained by challenge with cross-reactive antigen (Angelova & Shvartsman, 1982; Matzinger, 1994). However, cross-reactive memory can also be a problem because memory cells highly specific for the secondary antigen are not formed if the antigen is cleared too quickly by memory cells of the primary antigen. The same effect can potentially cause vaccine failure; a vaccine might be cleared by memory cells of a prior infection without inducing memory to the vaccine components.

Most of the experimental work on cross-reactive memory has been performed using two strains of a single organism, or two related haptens, as primary and secondary antigens. Experiments on more than two antigens would be useful in order to better understand, for example, sequential infections with influenza (Angelova & Shvartsman, 1982), pathogenesis of HIV, and multivalent vaccine design. We have developed a model and computer simulation of cross-reactive memory in order to perform *in machina* multi-antigen experiments with the goal of helping to understand the immune response to mutating pathogens and sequential multivalent vaccines. An advantage of computer simulations is that all of the data in the simulation are easily measured; a disadvantage is that the simulation may omit or distort important aspects of the system being modeled. We describe some of our efforts to calibrate a model with immunological data to make it closer to the *in vivo* reality.

Much of the character of a cross-reactive response is determined by the quantity and distribution of the population of memory cells, raised to the primary antigen, that also react with the secondary antigen. Figure 3.1 shows that if we consider the cells that respond to the primary and secondary antigens as sets, then the cells that react with both antigens, the cross-reactive cells, lie in the intersection of the sets. If the antigens are closely related, then there are a large number of cells in the intersection and there will probably be a strong cross-reactive response. If the antigens are less closely related, then the number of cells in the intersection is small, and there will probably be only a weak cross-reactive response. Because the number and distribution of cells in the intersection plays a significant role in the cross-reactive response, it warrants careful study in a model being used to study cross-reactive responses. We would like to know how the intersection varies as a function of the antigenic differences between the primary and secondary antigen. The number of cells in the intersection will depend on how we choose to model antibody-antigen interactions, and what parameters values we choose for this aspect of the model. In this paper we derive parameters, from experimental data, for a model of cross-reactive memory.

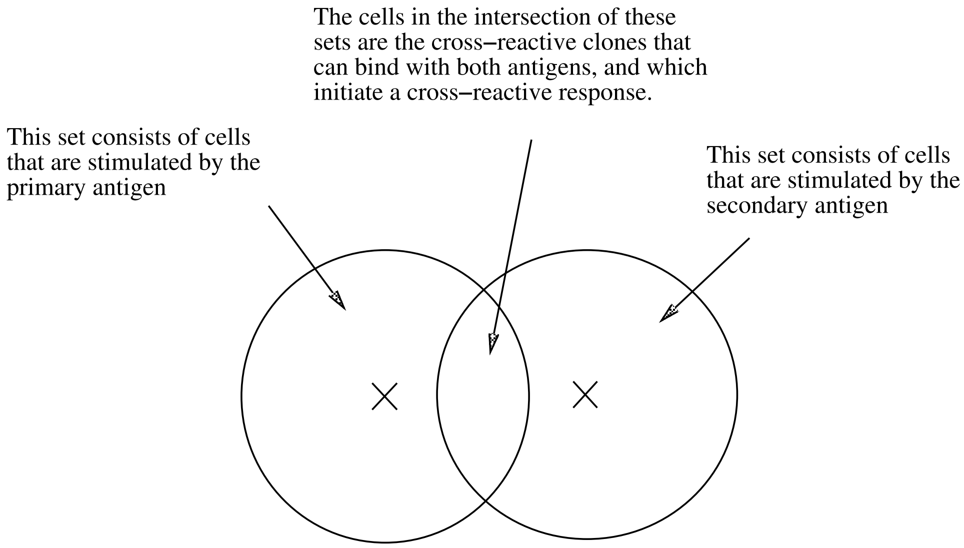

Figure 3.1: The cells that cause a cross-reactive response are those in the intersection of the set of cells stimulated by the primary antigen and the set of cells stimulated by the secondary antigen.

3.2 Shape Space Model of Antibody-Antigen Interactions

Antibody-antigen binding affinity[1] is based on complementarity between regions of the antigen and antibody. An abstract model of this was introduced by Perelson & Oster (1979). In this model antibodies and antigens are considered as points in a "shape space" and the distance between an antibody and an antigen is a measure of their affinity for each other. Thus, antibodies within an affinity cutoff for clonal selection by an antigen form a ball in shape space called a ball of stimulation. In a cross-reactive response, each antigen forms such a ball and the intersection of the balls contains the cross-reactive antibodies, thus determining the degree of cross-reactivity between the antigens. Consequently, the Venn diagram representation in Figure 3.1 can also be interpreted as a shape space diagram.

In order to make shape space more quantitative Perelson & Oster (1979) represented

[1]We refer to the binding of antibodies and antigen, however, this analysis could also be applied to the binding of the T cell receptor with antigen presented on MHC.

the "generalized shape" of antibodies and antigens with a set of real valued coordinates $<a_1, a_2 \ldots a_n>$. Thus, mathematically, each antibody and antigen could be regarded as a point in an n-dimensional real-valued space. The affinity between an antigen and antibody was related to the distance between them, which was measured as the square root of the sum of the squares of the distances between the values in each dimension. For example, if the coordinates of an antibody are $<a_1, a_2 \ldots a_n>$ and the coordinates of an antigen are $<b_1, b_2 \ldots b_n>$, the distance between them is $\sqrt{\{(a_1 - b_1)^2 + (a_2 - b_2)^2 + \ldots + (a_n - b_n)^2\}}$. Shape spaces that use real-valued coordinates, and that measure distance this way, are called *Euclidean* shape spaces (Segel & Perelson, 1988; DeBoer *et al.*, 1992b).

An alternative to Euclidean shape space is *Hamming* shape space, in which antigens and antibodies are represented as sequences of symbols (Farmer *et al.*, 1986; DeBoer & Perelson, 1991; Seiden & Celada, 1992; Weisbuch & Oprea, 1994; Hightower *et al.*, 1995; Perelson *et al.*, 1996; Detours *et al.*, 1996). Such sequences can be can loosely interpreted as peptides and the different symbols as properties of either the amino acids or of equivalence classes of amino acids of similar charge or hydrophobicity. The mapping between sequence and shape is not fully understood, so for the purposes of this paper we assume that sequence and shape are equivalent. This assumption is reasonable in some situations, for example Champion *et al.* (1975) showed that for azurins, lysozymes, and alpha subunits of tryptophan synthetase, that sequence difference was correlated with the degree of antigenic difference. However, for some antigenic determinants, a single amino acid change can cause a large change in antigenic difference. For such cases a different type of analysis would be needed.

In order to measure the affinity between sequences, we need to define what symbols are complementary so the Hamming distance can be calculated. Any choice is equivalent mathematically, hence for simplicity we choose symbols to be complementary to themselves. For example, let CADBCADB be an antigen and CBDBCDDB an antibody, these are "complementary" in six out of eight places, and thus have a reasonably high affinity for each other. Shape spaces which measure contiguous complementary symbols (Percus *et al.*, 1993), or use other rules for complementarity between symbol sequences (Weisbuch & Oprea, 1994; Detours *et al.*, 1996), have also been used.

A shape space will have different properties depending on the number of dimensions, n, the radius of a ball of stimulation, r, and, in the case of Hamming shape space, on the number of symbols in each dimension, k. As an example of how some properties are sensitive to n, k and r, Figure 3.2 plots the volume of the intersection of two balls of stimulation, as a function of the sequence difference between the antigens. The formula for the intersection volume is derived in appendix A. Thus, in a model where the volume of the intersection is important, as in a model of cross-reactive memory, shape space parameters must be chosen carefully.

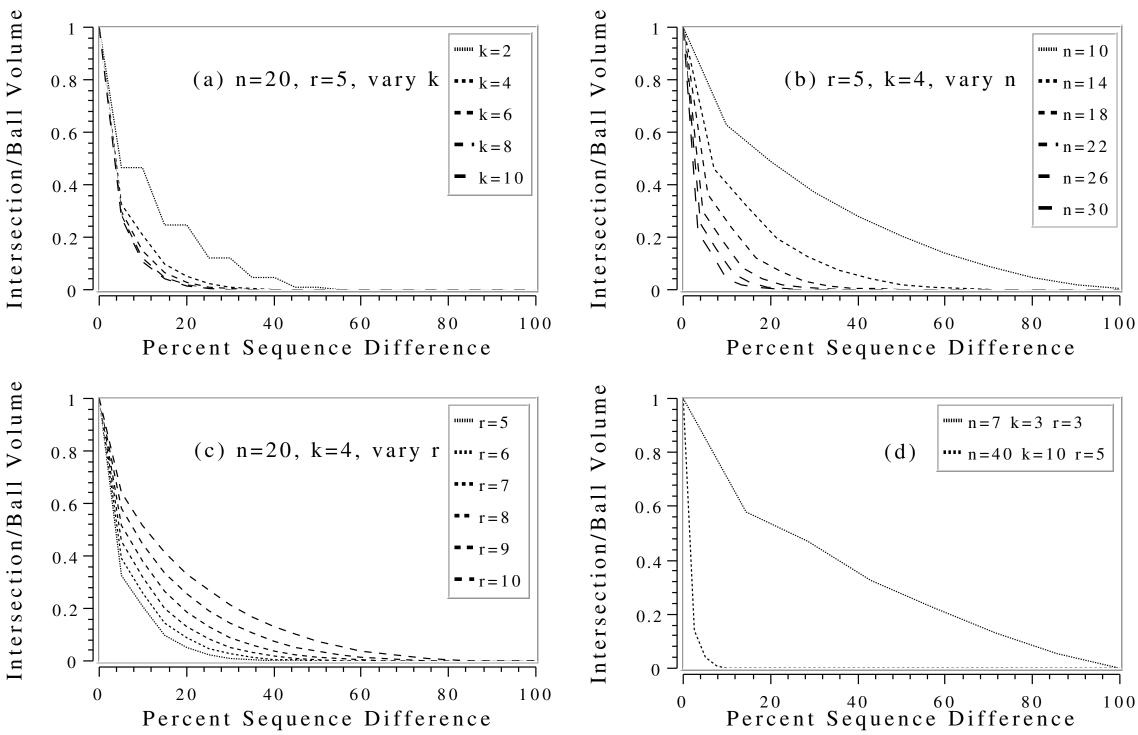

Figure 3.2: Panels (a), (b) and (c) show that as n or k increase, or as r decreases, the intersection volume, as a function of the sequence difference, falls off more quickly. Panel (a) shows that the binary alphabet, $k = 2$, has an unusual property—every other increase in sequence difference does not cause a decrease in the intersection volume (Kanerva, 1988). Panel (d) shows n, k, and r set at extreme values to illustrate how much the curves can differ.

3.3 The Method and its Application

The method of deriving shape space parameters from immunological data consists of the following steps: (i) determine properties that are important to represent correctly in the model, (ii) estimate data values, from immunological experiments, that characterize these properties, (iii) derive equations for these data values as a function of the parameters of the model, (iv) equate the immunological data values with the model equations, and (v) solve the equations for the model parameters. For a model of cross-reactive memory, an important property to represent correctly is cross-reactivity, and the ideal data values would be the number of B cells in the intersection of the balls of stimulation of antigens of varying sequence differences.

When the sequence difference is zero, the intersection volume is the volume of a ball of stimulation. What has been measured experimentally is the proportion of B cells that respond to an antigen, and from this we can estimate the absolute number of B cells in a ball of stimulation. Estimates for the proportion, P_{exp}, range from 10^{-5} to 10^{-4} (Edelman, 1974; Nossal & Ada, 1971; Jerne, 1974). The equation from the model for the proportion, P, of B cells responding, is volume of a ball of stimulation divided by the volume of the space. Equating the experimental data values and the formula from the Hamming space model we have

$$\frac{\sum_{0 \leq i \leq r} \binom{n}{i} (k-1)^i}{k^n} = 10^{-5} \text{ to } 10^{-4}. \tag{3.1}$$

The size, S, of the shape space needs to be sufficiently large to be able to represent all possible antibodies. Based on the number of gene segments used to encode antibodies, the number of possible antibodies, S_{exp} is thought to be at least 10^{10} (Berek & Milstein, 1988; Lodish *et al.*, 1995). Including the effects of somatic hypermutation the number of possible antibodies is many orders of magnitude higher (Lodish *et al.*, 1995); for example it might be as high as 10^{16}. Again equating the experimental data values and the formula from the model we have

$$k^n = 10^{10} \text{ to } 10^{16}. \tag{3.2}$$

Another data value that can be extracted from experiment is the sequence difference at which the intersection volume of the balls of stimulation goes to zero, i.e. the sequence difference at which two antigens no longer cross-react. We call this distance the "cross-reaction cutoff". It is more intricate than the above equations and is derived in the following subsection.

3.3.1 Cross-Reaction Cutoff

The experimental data for the cross-reaction cutoff comes from two sources: East *et al.* (1980) and Champion *et al.* (1975). East *et al.* (1980) primed rabbits[2] with beef myoglobin and split them into five groups. Each group received a second injection of myoglobin from one of beef, sheep, pig, whale or chick. The antibody titer to beef myoglobin was plotted against the percent sequence difference between the myoglobins given in the primary and secondary injections. These data are almost ideal, but not quite. The antibody titer was measured at the peak of the secondary response, however we need the number of cells at the beginning of the secondary response. These values are related, but the dynamics of the immune response makes the relation complex. When there are no cross-reactive antibodies, the relation is simple; we can assume there were no cross-reacting cells at the beginning of the response, and thus determine the cross-reaction cutoff. East *et al.* (1980) estimate this point, C_{exp}, to occur in the range of 33 to 42% sequence difference between the primary and secondary antigens.

A second source of the data value for the cross-reaction cutoff comes from Champion *et al.* (1975). In these experiments, seven groups of rabbits were primed with one of seven bacterial azurins. At ten to twelve weeks the rabbits were boosted with the same strain with which they were primed. At twenty to twenty-five weeks the rabbits were boosted again on three successive days, with the same strain, and then bled one week later and the antisera purified. Micro-complement fixation assays were used to determine how

[2] Values for our other parameters were taken from experiments in mice, however this parameter is taken from experiments in rabbits.

well each antisera fixed complement to each of the heterologous azurins. As with East *et al.* (1980), these data are almost ideal, but not quite. The problem is that the distribution of antibodies is not uniform, as it has been biased by affinity maturation during the hyperimmunization. In order to use these data we would need to know the bias due to affinity maturation, and that is not available. We can however again determine the cross-reaction cutoff, which this time is at 40% sequence difference between the antigens.

In order to properly match the model to the experimental cross-reaction cutoff, we need to take into account that memory B cells are more easily stimulated than naive B cells. Fish *et al.* (1989) showed that clonal expansion of memory B cells required a lower affinity antibody-antigen interaction than clonal expansion of naive B cells. In their experiments, A/J mice primed with *p*-azophenylarsonate (Ars) responded predominantly with clones derived from a single V_H gene segment, $V_H Id^{CR}$, and when primed with *p*-azophenylsulfonate (Sulf), no such clones were elicited. However, in mice primed with Ars and challenged with Sulf, clones originally encoded by the $V_H Id^{CR}$ were present. We take this greater sensitivity of memory B cells into account by increasing the radius of the ball of stimulation of the secondary antigen as shown in Figure 3.3. Thus, when we calculate the volume of the intersection in the model, we must take the radius of the first (naive) ball of stimulation as r, and the radius of second (memory) ball of stimulation as $r \times M_{exp}$.

Two further factors need to be taken into account before relating the cross-reaction cutoff in experiments with that in the model. First, vertebrate immune systems only express a portion of their total number of possible B cell specificities at any one time. For the mouse, this number, the expressed repertoire, E_{exp}, is in the range 10^7 to 5×10^7 (Köhler, 1976; Klinman *et al.*, 1976; Klinman *et al.*, 1977). In contrast the formulas in the model give answers in terms of the number of all possible B cell specificities. Second, an experiment might not be able to detect less than a critical number of B cells in the intersection of balls of stimulation, whereas the model can detect a single B cell. We take these factors into account by equating the ratio of the intersection volume and shape space volume in the

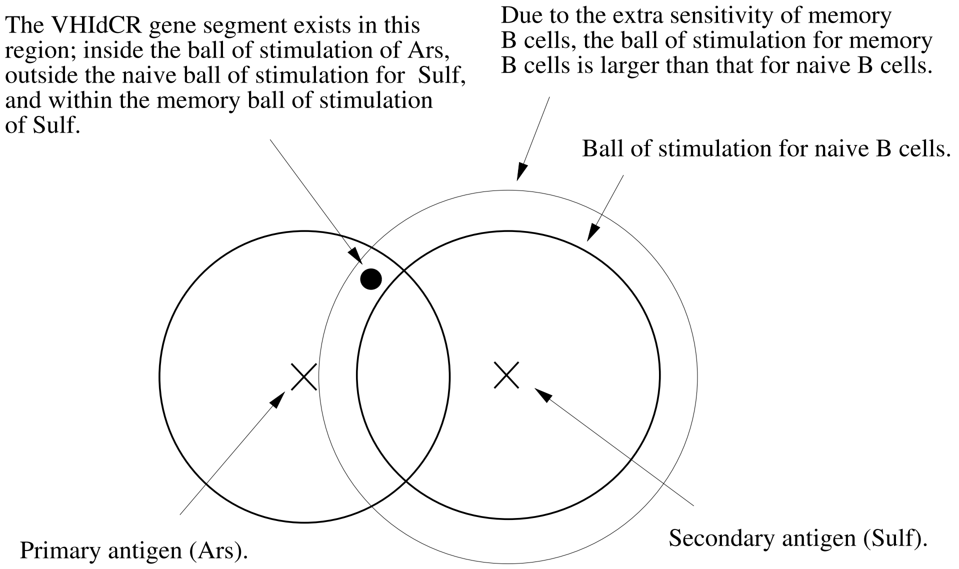

Figure 3.3: The extra sensitivity of memory B cells results in a ball of stimulation for the secondary antigen that is larger than that of the primary antigen. The amount that the memory ball of stimulation is greater than the naive ball of stimulation is the value M_{exp} as explained in the main text.

model, with the ratio of the number of B cells an experiment can detect in the intersection (which we assume to be a single B cell specificity) and the size of the expressed repertoire. Thus we have

$$\frac{I(n,k,r,rM_{exp},c)}{k^n} = \frac{1}{10^7 \text{ to } 10^8}, \tag{3.3}$$

where c ranges from 33 to 42% sequence difference, and where the intersection volume, I, is defined in appendix A.

3.3.2 Solving for Shape Space Parameters

Given values from experiments for M_{exp}, P_{exp}, E_{exp}, S_{exp} and C_{exp}, Equations 3.1 through 3.3 can be solved[3] for the Hamming shape space parameters n, k and r. For example, rea-

[3]We obtain solutions be considering k's in the range 2 to 20, and for each k, derive a real valued n from Equation 3.2, select an integer r that gives a ball of stimulation closest to the desired size from Equation 3.1,

sonable values to choose from current immunological data are $C_{exp} = 0.33 - 0.42, P_{exp} = 10^{-5}, S_{exp} = 10^{12}, M_{exp} = 1.2$ and $E_{exp} = 10^{7}$, which give shape space parameters $\{n = 20, k = 4, r = 5\}$ or $\{n = 25, k = 3, r = 6\}$. Table 3.1 shows solutions for different values of the immunological data.

			$S = 10^{10}$	$S = 10^{12}$	$S = 10^{14}$	$S = 10^{16}$
			$k - n - r$	$k - n - r$	$k - n - r$	$k - n - r$
$M = 1.0$	$P = 10^{-5}$	$E = 10^{7}$	6-13-3 7-12-3 8-11-3	5-17-5 6-15-5 8-13-4 9-13-4 10-12-4 11-12-4	4-23-7 5-20-7 6-18-6 7-17-6 8-16-6	4-27-9 5-23-8 6-21-8 8-18-7 9-17-7
		$E = 10^{8}$	3-21-4 4-17-3	3-25-6		3-34-10
	$P = 10^{-4}$	$E = 10^{7}$	2-33-6		2-47-10	2-53-13
		$E = 10^{8}$	2-33-6	2-40-8	2-47-10	
$M = 1.2$	$P = 10^{-5}$	$E = 10^{7}$	3-21-4 4-17-3	3-25-6 4-20-5		
		$E = 10^{8}$			2-47-9	2-53-11
	$P = 10^{-4}$	$E = 10^{7}$	2-33-6	2-40-8	2-47-10	
		$E = 10^{8}$				

Table 3.1: The values for k, n and r, that satisfy the immunological data, in a Hamming shape space, for different values of M_{exp}, P_{exp}, E_{exp}, and S_{exp}. Multiple entries indicate multiple solutions and blank entries indicate no solutions.

3.4 Using the Same Method on Euclidean Shape Space

The method for deriving shape space parameters can be applied to other shape spaces, other experimental data, and other properties we choose to satisfy. As an example, we now use the method to derive parameters for a Euclidean shape space.

After Perelson & Oster (1979), we place a limit on the magnitude of each shape space parameter and normalize distances with respect to this distance, so that radii are in

find values for c that bound the right hand side of Equation 3.3 (using n rounded to an integer), interpolate for an exact c, and accept solutions that give c between 0.33 and 0.42.

the range zero to one. We map sequence difference directly onto the Euclidean distances 0 to 1.[4] We use $\hat{r}$ for the normalized radius and $\hat{c}$ for the normalized cross-reaction cutoff.

For Euclidean shape space, equation 3.1 becomes

$$\hat{r}^n = 10^{-5} \text{ to } 10^{-4}, \tag{3.4}$$

where the left hand side of this equation is derived at the end of appendix B, and equation 3.3 becomes

$$\frac{I(n, \hat{r}, \hat{r}M, \hat{c})}{\text{Ball}(n, 1)} = \frac{1}{10^7 \text{ to } 10^8}, \tag{3.5}$$

where $\hat{c}$ ranges from 0.33 to 0.42, I is now the Euclidean intersection volume and Ball$(n, 1)$ is the volume of the n-dimensional Euclidean shape space normalized to radius 1; both quantities are derived in appendix B.

			$C = 0.33$	$C = 0.36$	$C = 0.42$
			$n/\hat{r}$	$n/\hat{r}$	$n/\hat{r}$
$M = 1.0$	$P = 10^{-5}$	$E = 10^7$	7/0.19	8/0.24	9/0.28
		$E = 10^8$	6/0.15	7/0.19	8/0.24
	$P = 10^{-4}$	$E = 10^7$	5/0.16	5/0.16	6/0.22
		$E = 10^8$	5/0.16	5/0.16	6/0.22
$M = 1.1$	$P = 10^{-5}$	$E = 10^7$	7/0.19	7/0.19	8/0.24
		$E = 10^8$	6/0.15	7/0.19	7/0.19
	$P = 10^{-4}$	$E = 10^7$	5/0.16	5/0.16	6/0.22
		$E = 10^8$	5/0.16	5/0.16	5/0.16
$M = 1.2$	$P = 10^{-5}$	$E = 10^7$	6/0.15	7/0.19	8/0.24
		$E = 10^8$	6/0.15	6/0.15	7/0.19
	$P = 10^{-4}$	$E = 10^7$	5/0.16	5/0.16	5/0.16
		$E = 10^8$	4/0.10	5/0.16	5/0.16

Table 3.2: Solutions of Equations 3.4 and 3.5, for the model parameters n and $\hat{r}$, that satisfy the immunological data in a Euclidean shape space, for different values of $M_{exp}, P_{exp}, E_{exp}$, and C_{exp}.

Solutions of Equations 3.4 and 3.5 (Table 3.2) indicate that n, the number of dimensions, is not very sensitive to the biological values; five to eight dimensions is about

[4] An alternative Euclidean space would wrap each dimension and have a toroidal total volume. This has the advantage of eliminating edge effects of the spherical total volume.

right for a Euclidean shape space that satisfies the immunological data for a cross-reactive memory model. In general, the number of dimensions increases as: C_{exp} increases, E_{exp} decreases, P_{exp} decreases, or M_{exp} decreases.

3.5 Discussion

The intersection volume between balls of stimulation for primary and secondary antigen encounters plays an important role in cross-reactive memory responses. Choices of shape space parameters have a significant effect on the intersection volume predicted by our model. Thus, care must be taken when choosing shape space parameters. We have selected immunological data that are important for a model of cross-reactive memory, and have shown how we can derive shape space parameters from these data. A comparison of our findings for Euclidean and Hamming shape spaces (Figure 3.4) shows agreement in the intersection volume at zero sequence difference and zero intersection as would be expected as these were the data points for which the equations were solved. However, the intersection volumes differ between these points.

Experiments could be done to test the qualitative relationships in this paper, if we assume that antigenic difference is proportional to sequence difference. Ideal data would give the intersection volume, at various sequence differences, for multiple antigens. As an example, Gerhard (1978) measured the degree of cross-stimulation between various strains of influenza with known sequence differences. Such data could be used to further determine the appropriate choice of shape space parameters.

In prior work, Perelson & Oster (1979) estimated the number of dimensions for a Euclidean shape space to be between five and ten. This agrees well with our calculations which suggest five to eight dimensions (Table 3.2). Percus *et al.* (1993) used a variation on Hamming shape space in which the complementary symbols had to be contiguous. Using self-nonself discrimination arguments, they predicted about a fifteen symbol binding region for strings made from a three symbol alphabet, and a nineteen symbol binding region when

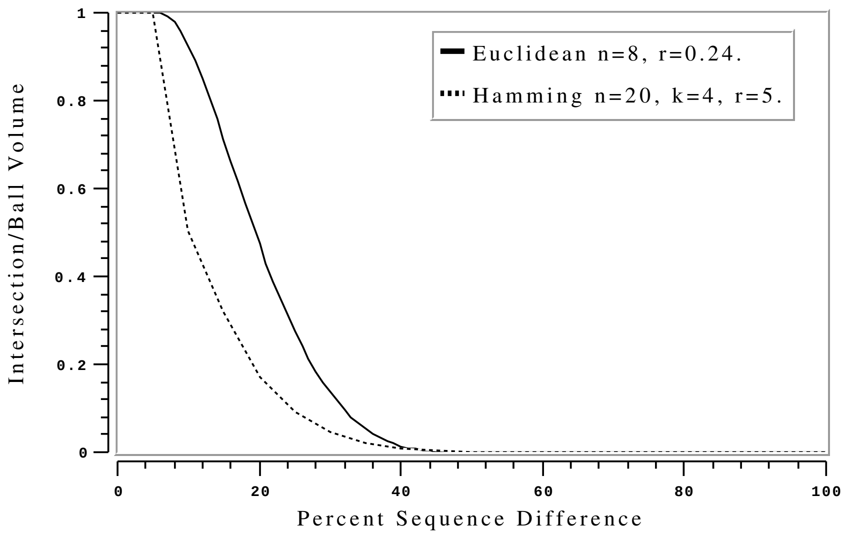

Figure 3.4: A comparison of the intersection volume, as a function of sequence difference, for a Euclidean and Hamming shape space. For both spaces, the shape space parameters were derived from the immunological data $M_{exp} = 1.2, P_{exp} = 10^{-5}, E_{exp} = 10^{7}, C_{exp} = 0.42$, and, for Hamming space, $S_{exp} = 10^{12}$.

the complementary symbols could be in two contiguous regions. Here we find that a twenty symbol binding region, with a four symbol alphabet and balls of stimulation of radius five, which gave a minimum binding region of fifteen symbols, or a twenty-five symbol binding region, with a three symbol alphabet and balls of stimulation of radius six, which gave a minimum binding region of nineteen symbols, to be consistent with immunological data on cross-reactivity. X-ray crystallographic analysis has shown that a typical antibody-antigen binding site is about seventeen amino acids (Amit *et al.*, 1986), and that there might some gaps in the binding. This matches well with our derivation of a twenty symbol binding region, and a ball of stimulation of radius five.

Segel & Perelson (1988) and DeBoer *et al.* (1992) simulated immunological processes in one and two dimensional Euclidean spaces because it facilitated analysis and comprehension of the dynamics. However, our calculations suggest that a Euclidean shape space between five and eight dimensions is more consistent with the immunological data on cross-reactivity. Binary alphabets are common when Hamming shape spaces are used. Seiden & Celada (1992) used a Hamming space with a binary alphabet and eight to fourteen dimensions. This allowed them to express the complete repertoire which was important for their experiments. Farmer *et al.* (1986) used a binary alphabet and thirty-two dimensions, and Hightower *et al.* (1995) used a binary alphabet and sixty-four dimensions. Binary alphabets with a multiple of thirty-two dimensions are an obvious choice for the efficiency of computer simulations. However, binary alphabets have a stair-step intersection volume, as shown in Figure 3.2a, and thus might not be a good choice for a model of cross-reactive memory.

It may be tempting to suggest that real antibodies and antigens can be characterized by five to eight Euclidean parameters, or by twenty or so four-symbol Hamming parameters. Either of these statements may or may not be true, but they should not be inferred by the work presented here. What this work shows is how to choose Hamming and Euclidean shape space parameters of a model so that they will match a chosen set of immunological observations.

We have shown, for Hamming shape space, that alphabet sizes of three and four, with the number of dimensions in the mid to low twenties, and balls of stimulation of radius five to six, are good parameters for use in a model of cross-reactive memory. For Euclidean shape space we have shown that, for a wide range of immunological data, five to eight dimensions and balls of stimulation of normalized radius 0.15 to 0.22 are good parameters. We have also shown that, for Hamming shape space, binary alphabets have a stair-step intersection volume, and that large alphabets only satisfy the constraints for extreme values of the immunological data.

Chapter 4

Using Lazy Evaluation to Simulate Realistic-Size Repertoires in Models of the Immune System*

Abstract

We describe a method of implementing efficient computer simulations of immune systems that have a large number of unique B and/or T cell clones. The method uses an implementation technique called *lazy evaluation* to create the illusion that all clones are being simulated, while only actually simulating a much smaller number of clones that can respond to the antigens in the simulation. The method is effective because only 0.001% to 0.01% of clones can typically be stimulated by an antigen, and because many simulations involve only a small number of distinct antigens. A lazy simulation of a realistic number of clones and 10 distinct antigens is 1,000 times faster and 10,000 times smaller than a conventional simulation—making simulations of immune systems with realistic-size repertoires computationally tractable.

*Accepted with minor modifications to Bulletin of Mathematical Biology

4.1 Introduction

The B and T cell repertoires of vertebrate immune systems can recognize and respond to almost all foreign antigens, even laboratory derived ones that almost surely have never been seen in evolutionary history. The repertoire can also distinguish, at a fine level of detail, between foreign antigens and the components of the body it protects. To achieve this broad yet detailed coverage, the immune system maintains a large number of highly specific clones, where a clone is a set of cells derived from a single precursor and which almost assuredly have a unique B or T cell receptor. In this paper we discuss only the B cell repertoire; however, the method is also applicable to the T cell repertoire.

The murine B cell repertoire maintains 10^7 to 10^8 distinct clones (Köhler, 1976; Klinman *et al.*, 1976; Klinman *et al.*, 1977), each of which typically can be stimulated by only 10^{-5} to 10^{-4} of all possible antigens (Edelman, 1974; Nossal & Ada, 1971; Jerne, 1974). In order for an antigen to stimulate a B cell it must bind to antigen-specific receptors on the surface of the B cell.

The binding affinity between receptors and antigens is based on complementarity at the molecular level. Perelson & Oster (1979) introduced an abstract model of binding in which molecules are considered as points in a "shape space" and affinity is measured as a function of the distance between such points. Modelers have used a variety of methods to represent molecules in shape space. Segel & Perelson (1988) and DeBoer *et al.* (1992) examined one and two dimensional shape spaces in which the shape of molecules was represented by one or two real numbers, e.g. the depth or depth and width of a binding cleft or protrusion on a molecule. Affinity was then measured as a function of the Euclidean distance[1] between the shapes. Seiden & Celada (1992), Forrest & Perelson (1991), and Perelson *et al.* (1996) (after Farmer *et al.* (1986)), represented molecules as strings of 8, 32, and 64 bits respectively and measured affinity as a function of the Hamming distance[2] (or a variation on it) between them. Weisbuch & Oprea (1994) and Detours *et al.*

[1]Euclidean distance is the familiar square root of the sum of the squares of the differences in each dimension. The Euclidean distance between receptors $a_1, a_2 \ldots a_n$ and $b_1, b_2 \ldots b_n$, is $\sqrt{\sum_{1 \leq i \leq n} (a_i - b_i)^2}$

[2]Hamming distance is a count of the number of locations in which the receptors differ. The Hamming

(1996) represented molecules as strings of digits chosen from a 4 and 16 letter alphabet respectively. Smith *et al.* (1997d) determined that representing molecules as strings of 20 symbols, with each symbol chosen from a 4 letter alphabet, and affinity measured as a function of Hamming distance, as well as using a realistic-size repertoire of 10^7 B cell clones, gave good fits to immunological data important for a model of cross-reactive memory.

To make simulations of 10^7 clones computationally tractable, we use a technique called *lazy evaluation* (Friedman & Wise, 1976; Henderson & Morris, 1976). This technique (as illustrated in the next section) delays calculations, and the building of data structures, until they are needed. When not all calculations and data structures affect the result of a program, and when the relevant ones can be identified efficiently, lazy evaluation can result in significant savings in run time and memory usage. In the case of the immune system, lazy evaluation can be effective because only 0.001% to 0.01% of all clones are usually stimulated by any particular antigen, and because many simulations involve only a small number of distinct antigens.

Lazy evaluation can be programmed explicitly in traditional programming languages, or implicitly by using languages in which all evaluations are performed lazily (Turner, 1979; Turner, 1985; Hudak *et al.*, 1992). Lazy evaluation has been applied in numerous domains including: animation (Elliott & Hudak, 1997), simulation of integrated circuits (Dunne *et al.*, 1993) (and a production simulator based on Yoshino *et al.* (1987)), sound synthesis (Dannenberg *et al.*, 1992), and dictionary lookup (Lucas, 1995). In this paper we describe how lazy evaluation can be programmed explicitly in models of the immune system.

4.2 Algorithm

In a conventional *eager* approach to immune system simulation, computation time is taken and memory space explicitly allocated to generate all clones at the start of the simulation

distance between the receptors AB$\underline{\text{D}}$CCDAD$\underline{\text{D}}$A and AB$\underline{\text{A}}$CCDAD$\underline{\text{C}}$A is 2 because they differ in the two underlined locations.

(Figure 4.1a). When an antigen is introduced, the clones that can be stimulated by it (said to be within its *ball of stimulation* (Perelson & Oster, 1979)), already exist and the simulation proceeds (Figure 4.1b). In the modified *lazy* simulation, no clones are generated at the start of the simulation (Figure 4.2a). Instead, when an antigen is introduced, the simulation is suspended while clones within the ball of stimulation of the antigen are generated (Figure 4.2b). In this way, all clones that could be stimulated by the antigen appear and act as in an eager simulation. The absence of the remaining clones has no effect on the simulation other than making it run faster and take less memory. Clones must not be added to regions of a ball of stimulation where they have already been created by the introduction of previous antigens—this would result in too many clones in the intersections of balls of stimulation (Figure 4.2c).

For a lazy simulation to be functionally equivalent to an eager simulation, clones generated within a ball of stimulation must be added in the same distribution they would have had in an eager simulation. The correct distribution depends on how receptors and antigens are represented, and how affinity between them is measured. Here we describe a lazy algorithm for receptors represented as strings of symbols, and affinity measured as a function of the Hamming distance between receptors. In an eager simulation using this representation, receptors are generated by choosing each symbol from a uniform distribution—loosely mimicking the random genetic process used by vertebrate immune systems to generate clonal diversity (Leder, 1991).

For the lazy simulation, clones must be generated only within balls of stimulation. To do this we develop a method to generate clones at radius i from the center of a ball of stimulation, and then repeat the method at radii 0 through r, where r is the radius of a ball of stimulation. The probability, p_i, that a randomly selected clone in an eager simulation is radius i from the center of a ball is given by $p_i = \binom{d}{i}\left\{\frac{(k-1)}{k}\right\}^i\left\{\frac{1}{k}\right\}^{(d-i)}$, where d is the number of symbols in the string representation of the receptor, and k is the number of possible symbols at each location in the string. Further, in an eager simulation with n clones, the probability of j clones at radius i is given by the binomial $B(n, p_i) = \binom{n}{j}\{p_i\}^j\{1-p_i\}^{n-j}$.

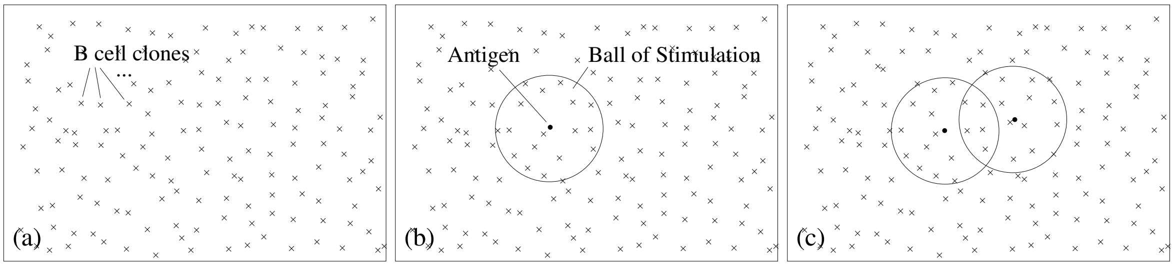

Figure 4.1: (a) In an eager simulation, all clones ($\times$) are generated at the start of the simulation. (b) & (c) When antigens ($\bullet$) are introduced, clones already exist and no new ones need to be generated.

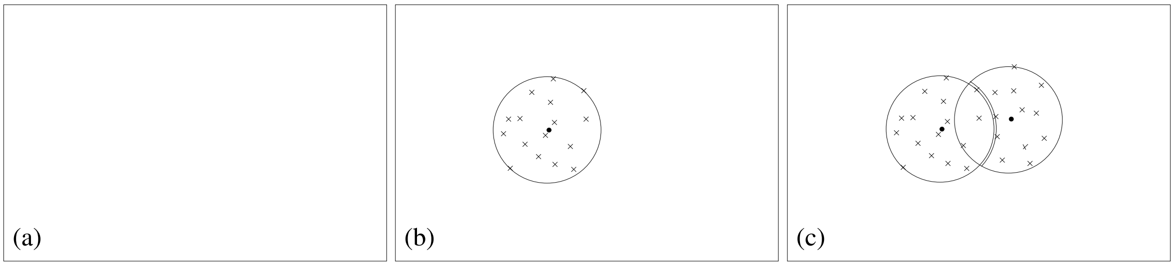

Figure 4.2: (a) In a lazy simulation, no clones are generated at the start of the simulation. (b) When an antigen ($\bullet$) is introduced, the simulation is temporarily halted while clones ($\times$) within its ball of stimulation are created. (c) When the ball of stimulation of a new antigen intersects that of an existing antigen, no additional clones need to be generated in the intersection as it has already been adequately populated.

Thus, the number of clones, $\hat{j}$, to generate at radius i from the center of a ball should be sampled from this binomial distribution. Each of the $\hat{j}$ clones is generated by changing i distinct symbols in the string that represents the receptor at the center of the ball of stimulation.

To avoid multiply generating clones in the intersections of balls of stimulation, each new clone is added to the lazy repertoire only if it is outside the balls of stimulation of all antigens already in the simulation. In the next two sections we verify that the lazy algorithm generates clones in the same distributions as the eager algorithm, and compare the algorithmic costs of the lazy and eager algorithms.

When a new antigen is added to the simulation

```
loop for i from 0 to r do
     loop for j from 1 to num-clones(i) do
          let clone = mutate(center, i)
              if {clone is outside the ball of stimulation
                        of all previously added antigens}
                 then {add clone to the simulation}
```

where `r` is the radius of a ball of stimulation;

where `num-clones(i)` produces a random number from the binomial distribution $B(n, p_i)$, where n is the number of clones in an eager simulation, and p_i is the probability that a clone is a radius i from an antigen;

and where `mutate(center, i)` mutates `i` distinct locations of the string representing the center of the ball of stimulation.

Figure 4.3: Pseudo-code describing the lazy algorithm for generating clones.

4.3 Verification

We generated a complex test case to check whether the lazy algorithm generates clones in the same distributions as the eager algorithm, especially in the case of multiply overlapping balls of stimulation. Following Smith *et al.* (1997d), molecules in the test were represented by strings of 20 symbols, each symbol was chosen from a four letter alphabet, and balls of stimulation had radius 5. A *seed* antigen was generated by randomly selecting each of its symbols from a uniform distribution, and 10 test antigens were generated in a cluster around the seed. Each test antigen was generated by mutating m randomly selected unique symbols of the seed, where m was chosen from a uniform distribution in the range zero to three so the balls of stimulation of the test antigens would have intersections of various sizes. Clones were generated, according to the lazy algorithm, and the number of clones at radii 0 through 5 for each antigen were counted. The experiment was replicated 100,000 times. For 10,000 of these experiments, the algorithm was metered to record the balls of stimulation that a newly generated clone fell within. These data were used to determine how much of each ball of stimulation was populated with clones generated by previous antigens.

Table 4.1 shows that the 10 antigens were at varying Hamming distances from each other and thus had varying overlaps. Table 4.2 shows that these overlaps resulted in many different proportions of balls of stimulation being populated by clones generated by prior antigens, and were thus a reasonable test of the lazy algorithm. Figure 4.4 shows that the observed and expected distributions are the same when compared visually, and Table 4.3 shows they are the same when compared statistically. Thus, the lazy algorithm worked correctly.

4.4 Algorithmic Cost

In this section we compare the algorithmic cost of the lazy and eager algorithms. The number of clones generated in a lazy simulation is $g{\times}p{\times}n$, where g is the number of distinct antigens in the simulation, p is the proportion of the repertoire that can be stimulated by an antigen, and n is the total number of clones in the eager simulation. Each of these clones needs to be checked to see if it falls within the ball of stimulation of any previously added antigen. Thus, the total number of checks after adding g antigens is $pn \sum_{0 \leq j < g} j = \frac{(g(g-1))}{2} pn$. If we assume that the cost of generating a clone is approximately the same as the cost of checking if a clone is in the ball of stimulation of an antigen, then the total cost of generating the lazy repertoire for g antigens is $gpn + \frac{g(g-1)}{2} pn = \frac{g^2+g}{2} pn$. The cost of the eager method is n because it generates n clones and does not have to do any checks. Comparing the cost of the lazy and eager algorithms, the lazy method is more efficient than the eager method when g is less than approximately $\sqrt{\frac{2}{p}}$.

For a realistic-size repertoire with $n = 10^7$ and $p{=}10^{-5}$, in a simulation with 10 distinct antigens, the lazy algorithm will create less than 0.01% of the clone repertoire at 0.1% of the cost of the eager algorithm. For less than 447 distinct antigens, and the same realistic-size repertoire, the lazy algorithm is lower cost than the eager algorithm (Figure 4.5). Simulations of more than 447 antigens, which would probably include simulations of immune networks, would be more efficient using an eager algorithm.

Antigen	Hamming distance to other antigens										Antigen string
	1	2	3	4	5	6	7	8	9	10	
1	0	4	2	1	4	4	2	3	3	2	CCBDDDBCCCABDCCDADAD
2	4	0	4	3	6	6	4	4	5	4	BCBDDDBCCCADDCCDAAAC
3	2	4	0	1	3	4	2	3	3	2	CCBDDDBCCCABACCDADAC
4	1	3	1	0	3	3	1	2	2	1	CCBDDDBCCCABDCCDADAC
5	4	6	3	3	0	6	4	5	5	4	CCCDDDBCCCABCCCDDDAC
6	4	6	4	3	6	0	3	4	5	3	CCBCDDBCCCBBDCCCADAC
7	2	4	2	1	4	3	0	1	3	2	CCBDDDBCCCDBDCCDADAC
8	3	4	3	2	5	4	1	0	4	3	CCBDDDBCCCDBDCCDACAC
9	3	5	3	2	5	5	3	4	0	3	CCBDDCDCCCABDCCDADAC
10	2	4	2	1	4	3	2	3	3	0	CCBBDDBCCCABDCCDADAC

Table 4.1: The pairwise Hamming distances between the 10 test antigens used in the experimental verification of the algorithm. The table is symmetric about the main diagonal because Hamming distance is commutative. The table shows that the antigens were at various Hamming distances from each other.

Antigen	Proportion of clones generated by each antigen									
	1	2	3	4	5	6	7	8	9	10
1	1.00	-	-	-	-	-	-	-	-	-
2	0.05	0.95	-	-	-	-	-	-	-	-
3	0.21	0.03	0.77	-	-	-	-	-	-	-
4	0.33	0.06	0.17	0.45	-	-	-	-	-	-
5	0.05	0.01	0.06	0.02	0.86	-	-	-	-	-
6	0.05	0.01	0.03	0.05	0.00	0.86	-	-	-	-
7	0.21	0.03	0.09	0.13	0.01	0.02	0.51	-	-	-
8	0.10	0.03	0.05	0.09	0.01	0.02	0.14	0.57	-	-
9	0.01	0.01	0.05	0.10	0.01	0.01	0.02	0.01	0.71	-
10	0.21	0.03	0.09	0.13	0.01	0.02	0.05	0.01	0.02	0.44

Table 4.2: The balls of stimulation of the 10 test antigens all overlapped each other; thus, many of the clones within a ball of stimulation were generated by the lazy algorithm operating on prior overlapping antigens. The proportions generated by each antigen are shown in this table. For example, for the fourth antigen, on average, 0.33 of the clones in its ball of stimulation were already generated by the first antigen, 0.06 by the second antigen, 0.17 by the third antigen, and 0.45 were generated *de novo* by the lazy algorithm on injection of the fourth antigen. The data were calculated by metering the lazy algorithm to record which balls of stimulation a newly generated clone fell within. The varying proportions suggest that the 10 antigens were a reasonable test of the lazy algorithm.

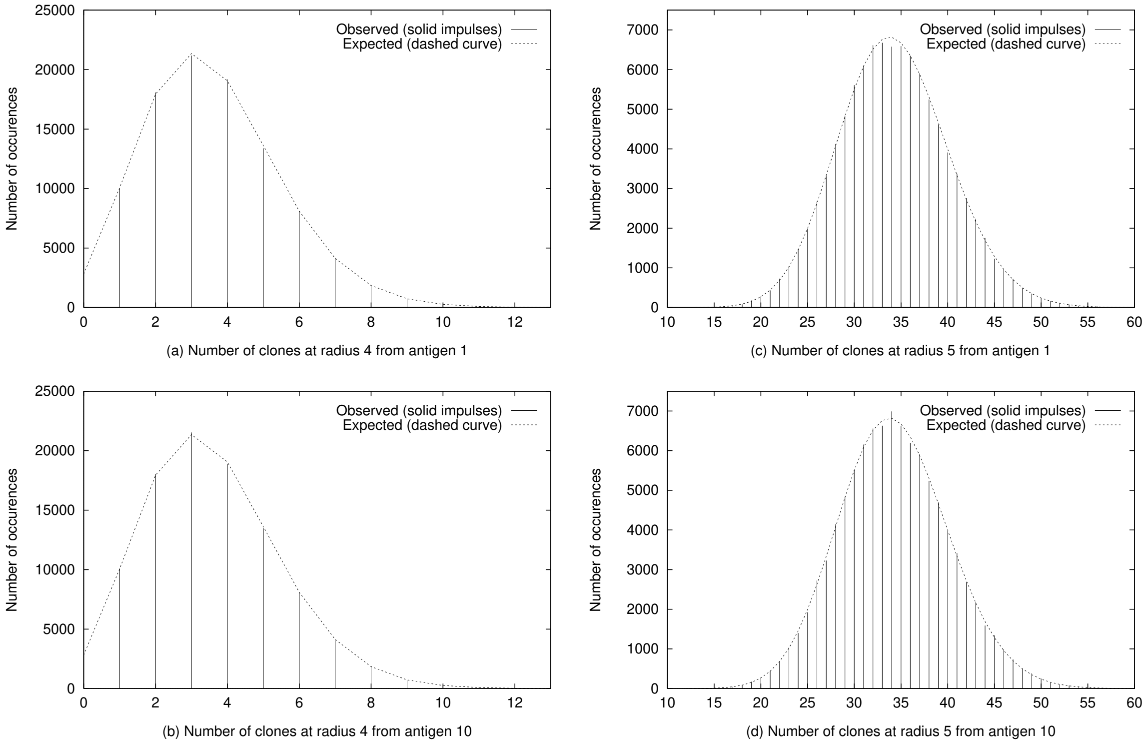

Figure 4.4: The expected (dashed curve) and observed (solid impulses) distributions of the number of clones at radii 4 and 5 from antigens 1 and 10. These data were collected from the application of the lazy algorithm to the sequential introduction of the 10 test antigens in 100,000 independent simulations and counting the number of clones at each radius within the ball of stimulation of each antigen. Antigens 1 and 10 are shown because they had the least and most number of clones, respectively, generated by prior antigens. Plots showing the distributions for the other antigens, and other radii, showed similar visual correspondence between the observed and expected distributions.

Radius	Observed χ^2 goodness-of-fit values for each antigen at each radius										Degrees	Critical
	1	2	3	4	5	6	7	8	9	10	of freedom	χ^2
1	0.00	0.11	0.00	1.34	0.23	0.04	0.11	0.23	1.02	0.12	1	3.84
2	4.36	1.50	0.89	3.08	1.19	2.61	1.71	4.55	0.48	1.04	2	5.99
3	5.15	3.06	5.40	0.43	0.60	2.14	4.13	4.87	3.20	1.69	4	9.49
4	13.57	10.68	22.36	17.71	6.44	11.24	12.10	7.33	17.46	10.08	12	21.03
5	39.47	44.45	31.72	31.74	45.25	39.95	35.96	48.35	28.22	54.58	40	55.76

Table 4.3: All observed χ^2 values (except one) were below their respective critical χ^2 value. Thus, there is no evidence (p=0.05) for rejecting the hypothesis that the observed data were in their expected distributions, and we conclude the lazy algorithm worked correctly. The one exception (antigen 3, radius 4) appears to be a Type I error, due to statistical variation, because its χ^2 value was less than the critical value when the experiment was repeated. One such error in 20 tests is to be expected at p=0.05. The data used were from the same 100,000 simulations used to make the plots of Figure 4.4. Not enough clones were generated at radius 0 (eight total in 100,000 simulations) to perform the test.

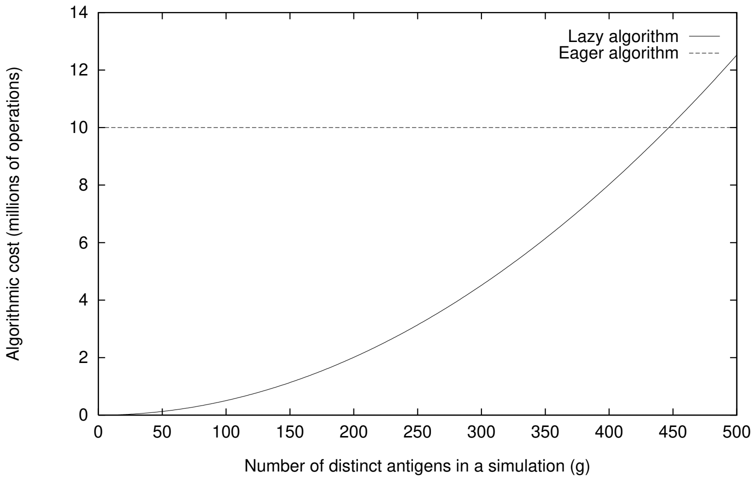

Figure 4.5: A comparison of the algorithmic cost of creating the B cell repertoire by the lazy and eager algorithms. The algorithmic cost was measured as the sum of the number of clones generated plus the number of checks that a clone was within the ball of stimulation of an antigen. Calculations were done for a realistic-size repertoire with $n = 10^7$ and $p = 10^{-5}$. The lazy algorithm costs less than the eager algorithm when there are less than 447 distinct antigens in a simulation, and costs 1,000 times less when there are less than 10 distinct antigens in the simulation.

When there are more than 10 distinct antigens in a realistic-size simulation, most of the algorithmic cost of the lazy method is in the g^2 comparisons of new clones with previously added antigens. In simulations involving hundreds of antigens, this g^2 cost could be reduced by various methods. One method is only to compare clones against antigens that are within distance $2r$ of the antigen for which clones are being generated. The algorithm still works correctly because antigens at greater than $2r$ distance cannot have intersecting balls of stimulation. In this case, the g^2 comparisons become a worst case, and the actual number of comparisons depends on the distances between the antigens in the simulation. Another method to reduce the g^2 comparisons is to generate clones in a ball larger than a ball of stimulation and thus avoid lazy generation for any future antigens whose balls of stimulation fall completely within the previously generated larger balls. This second method is effective when the antigens are tightly clustered.

4.5 Discussion

We have described an algorithm that uses lazy evaluation to generate only the subset of clones that can be stimulated by the antigens introduced into a simulation. Because this subset is typically a tiny proportion of the clone repertoire, the algorithm permits the efficient simulation of realistic-size repertoires. Correctness of the algorithm was checked by showing that, in a test case of 10 overlapping antigens, the algorithm produced clones in the same distributions as an eager algorithm. Analysis of the algorithm showed, in simulations of realistic-size repertoires involving less than 10 distinct antigens, that less than 0.01% of the expressed repertoire was created at less than 0.1% of the cost of creating a complete repertoire. We have implemented a lazy simulation of the humoral immune response that uses a realistic-size repertoire with a steady-state size of 10^7 B cell clones and a turnover of 5×10^5 B cell clones every 6 simulated hours (Smith *et al.*, 1997b). Simulations of the sequential infection by three antigens that have overlapping balls of stimulation, over a simulated period of 200 days, takes less than 2 minutes of CPU time, running in Lisp, on a Sun Ultra.

The algorithm we described is specific for models in which receptors are represented as strings of symbols and affinity is calculated as a function of the Hamming distance between receptors. The method could also be applied to other representations of receptors and other methods of calculating affinity, by changing the calculation of the probability distribution of clones within a ball of stimulation and the method of generating of clones within a ball of stimulation. The method is applicable to both *agent based* models in which each cell is represented individually, and to differential equation based models in which each clone is represented by a differential equation.

The method is also applicable to simulations of some associative memory and neural network models, including the Sparse Distributed Memory (SDM) of Kanerva (1988), that have similar mechanisms to the ones described here for the immune system (Smith *et al.*, 1996). Danforth (1997) used a lazy-like method, and a modified SDM learning rule (Danforth, 1991), to improve the performance of SDM. He added at most one *hard loca-*

tion (the SDM equivalent of a clone) on each write to the memory, at the exact location of the write. This is in contrast to the cluster of hard locations that would be added by our method. Both methods significantly reduce the number of hard locations in a simulation (compared to an equivalent eager simulation) and distribute hard locations in accordance with the distribution of addresses used to write to the memory. Danforth's method modifies the behavior of the SDM; our method leaves the behavior unchanged, and modifies the implementation to allow larger memories to be simulated.

General immune system models that include clones with receptors have been simulated with the order of 10^3 clones (DeBoer & Perelson, 1991; Celada & Seiden, 1996; Detours *et al.*, 1996). Lattice based cellular models that use only one or two bits to represent the concentration of highly simplified clones, and measure affinity by neighborhood on the lattice, have simulated 10^4 clones (DeBoer *et al.*, 1992a), and 10^8 clones (Stauffer & Sahimi, 1994) (the latter on a Cray-YMP). The lazy evaluation method presented here is the first to permit realistic-size repertoires of 10^7 to 10^8 clones for general immune system models.

Chapter 5

Annual vaccination against influenza: an *in machina* study*

Abstract

We have performed computer simulations to study the efficacy of annual vaccination against influenza. We generated vaccines and epidemic strains at many combinations of antigenic distances to each other. Simulated individuals were vaccinated at the start of one influenza season, revaccinated at the start of a subsequent season, and challenged with an epidemic virus during the second season. For many combinations of antigenic distances among the vaccine and epidemic strains, two vaccinations provided more protection than one. However, at some combinations of antigenic distances, the first vaccination reduced the effectiveness of the second by clearing it before it produced protective antibodies. Thus, in some cases, that might be common in practice, two annual vaccinations were less protective than a single vaccination. In this study the antigenic distances among the first vaccine, second vaccine, and epidemic strains, played the major role in determining protection.

*A prior version of this chapter was published as Smith *et al.* (1997b)

5.1 Introduction

Antigenic drift of the influenza virus exposes the population to new but related influenza variants on an annual basis. Thus, components of the influenza vaccine are updated, sometimes yearly, to maintain a reasonable correspondence between the vaccine and epidemic strains. Public heath recommendations are for at-risk populations to receive yearly vaccinations (CDC, 1996). Millions of people in the United States receive annual influenza vaccination; the major categories are the elderly, persons at high risk of death or severe illness with influenza infection, and health care workers.

Vaccine efficacy in young healthy first-time vaccinees is 70-90% effective (Davenport, 1973; Hoskins *et al.*, 1973; Feery *et al.*, 1979). However, efficacy in individuals who have been vaccinated multiple times has varied considerably and has called into question the recommendation for annual vaccination. A study at Christ's Hospital, a boys boarding school in England, showed that first-time vaccinees were well protected, whereas multiply-vaccinated boys were no better protected than unvaccinated boys (Hoskins *et al.*, 1979). Similar results were found in trials in geriatric patients and hospital staff in Melbourne, Australia (Feery *et al.*, 1979). Contrary results were found in a Houston, Texas study in which multiple-vaccinees were slightly better protected than first-time vaccinees (Keitel *et al.*, 1988). Vaccine efficacy in the elderly has also varied widely (Beyer *et al.*, 1989). The reasons are not clear, though they are thought to include reduced immunocompetance due to age and possibly the effects of multiple vaccinations.

It is known that the closeness of the antigenic match between the vaccine strain and the epidemic virus is important for vaccine effectiveness—this is why components of the vaccine are updated as the antigen drifts. In this study we have investigated whether the antigenic distances of a first vaccine strain to a second vaccine strain, and of the first vaccine strain to the epidemic strain, can account for variations in attack rates among two-time vaccinees.

All experiments reported here were performed *in machina*. Like any model system, a computer model trades off accuracy for controllability, observability, speed, and lower

Category	Num. Groups	Num. in each group	Vaccine 1 (year 1) (dose on day 0)	Vaccine 2 (year 2) (dose on day 365)	Epidemic challenge (year 2 flu season) (dose on day 425)
Never vaccinated[a]	1	40			500
Vaccinated in year 1 only[b]	8	80	1,000		500
Vaccinated in year 2 only[c]	1	80		1,000	500
Vaccinated in years 1 & 2[d]	31	40-42	1,000	1,000	500

Table 5.1: The timing and dose of vaccinations and epidemic challenge. Each category corresponds to a different vaccine strategy, and each group within a category corresponds to different antigenic distances among the vaccine and epidemic strains. [a]One group was never vaccinated. [b]Eight groups were vaccinated in year 1 and challenged during the year 2 influenza season—each group corresponded to challenge with a different epidemic strain with the vaccine1-epidemic antigenic distance varying from 0 to 7. [c]One group was vaccinated in year 2 and challenged 2 months later with an epidemic strain distance 2 from the vaccine2 strain. [d]Thirty-one groups were vaccinated in year 1, vaccinated again in year 2, and challenged with an epidemic strain during the year 2 influenza season—each group corresponded to different combinations of vaccine1-vaccine2 distances from 0 to 7 and vaccine1-epidemic distances 0 to 7, the vaccine2-epidemic distance was 2.

cost. The computer model allows us to test the effects of annual vaccination over many combinations of antigenic distances among the vaccine and epidemic strains. The computer model also allows us to isolate the effects of antigenic distance from other effects such as antigenicity of the vaccine, immunocompetence of the vaccinee, virulence and transmissibility of the wildtype, and compliance in long term trials. The danger of the *in machina* approach is that it might not faithfully represent relevant aspects of the immune system and thus might give misleading results. The model has been validated by replicating existing simpler experiments, and parameters of the model have been derived from data important in the cross-reactive immune response (Smith *et al.*, 1997d).

5.2 Materials and Methods

Experimental design. Forty-three groups in four categories were were injected with vaccines and epidemic strains with different combinations of antigenic distances to each other according to Table 5.1. The timing of the injections corresponded to vaccinations at the beginning of two influenza seasons and epidemic challenge two months into the second

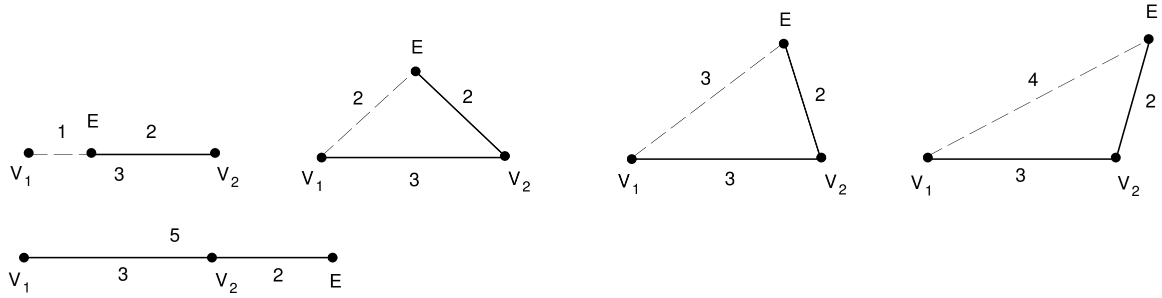

Figure 5.1: For each pair of vaccines (V_1 and V_2), epidemic strains (E) were generated at distance 2 from vaccine2 and at all geometrically feasible distances less than 7 from vaccine1. Here we show five combinations of antigenic distances among the vaccine and epidemic strains when the vaccine1-vaccine2 distance was 3 and the vaccine2-epidemic distance was 2.

season. For each member of each group, the viral load, and antibody quantity and affinities for each antigen, were measured every 6 hours. In addition, prior to each vaccination and epidemic challenge, and at the peak of each response, the number, affinity for each antigen, and clonal history of each B cell involved in the response were recorded. If the viral load exceeded 1,500 units it was deemed to have passed a "disease threshold" and the simulated organism was considered symptomatic. The attack rate within a group was defined as the proportion of the group in which the maximum viral load exceeded the disease threshold.

Vaccine and epidemic strains. In total 39 strains were generated—8 for use as monovalent vaccines and 31 for use as epidemic virus. The 31 epidemic strains were necessary to cover all possible combinations of antigenic distances of an epidemic strain to the two vaccine strains. Figure 5.1 shows the five possible combinations of antigenic distances among the vaccine and epidemic strains when the vaccine1-vaccine2 distance was 3 and the vaccine2-epidemic distance was 2. The vaccine strains were nonreplicating, the epidemic strains replicated every 6 hours.

Computer model. The computer model is a highly simplified vertebrate humoral immune system, it includes B cells, plasma cells, antibodies, memory B cells, and antigens. T-help is modeled implicitly by assuming that it is available whenever necessary. Each B cell, plasma cell and memory B cell is modeled as a separate entity within the simulation. In this way the model is *agent based* and related to that of (Seiden & Celada, 1992). Because of the large number of antibodies in a real immune system, each antibody in the model corresponds to a large number of real antibodies, similarly each antigen in the model corresponds to a large number of real antigens. When antigens are introduced into the simulation, B cells with sufficient affinity have a chance to bind the antigens. B cells with antigen bound are stimulated to divide, and on division have some chance of mutation in their antibody receptor, and some chance of differentiation into a memory or plasma cell. Plasma cells secrete antibodies, which have a chance of binding antigen depending on their affinity for the antigen. When antigens have more than a threshold number of antibodies bound they are removed from the simulation. Homologous antigens have antigenic distance zero, and antigenic distance increases as the antigens become less cross-reactive. Antigens at antigenic distance seven are effectively non-cross-reactive. A more detailed description of the model is given in Appendix C.

5.3 Results

Figure 5.2 shows the maximum viral load in each experiment in each group. Viral loads above a disease threshold are plotted in black, hence the proportion of black in each subplot indicates the attack rate in each group. Each group was challenged with epidemic virus 2 months into the second simulated influenza season. The attack rate was 100% in the group that was never vaccinated (Figure 5.2a). The attack rate was 58% in the group vaccinated once, at the start of the second influenza season (Figure 5.2b). Attack rates varied from 4 to 100% in groups vaccinated once at the start of the first influenza season (Figure 5.2c)—when the vaccine1 and epidemic strains were identical (antigenic distance 0), the attack rate was 0%, and the attack rate increased as the vaccine1-epidemic antigenic distance increased until the attack rate was 100% at vaccine1-epidemic distances 5, 6, and 7. Attack rates varied from 0 to 83% in groups vaccinated twice, once before the first influenza season, and again before the second (Figure 5.2d)—the attack rate depended on the vaccine1-vaccine2 antigenic distance, and the vaccine1-epidemic distance (the vaccine2-epidemic distance was fixed at 2).

The additional year between vaccination and challenge increased the attack rate from 58% to 89% for first time vaccinees when the vaccine-epidemic distance was 2 (groups 2;-,- Figure 5.2b and -;2,- Figure 5.2c).

Receiving vaccine2, at the start of the second influenza season, always lowered attack rates of the epidemic challenge in the second season, even in groups that had received vaccine1 at start of the first season. This can be seen be comparing a row of Figure 5.2d with the corresponding row of Figure 5.2c (a row corresponds to groups in which the vaccine1-epidemic distance was the same).

Attack rates in groups that received vaccine1 and vaccine2 (Figure 5.2d) were sometimes lower, and sometimes higher, than that in the group that received only vaccine2—even though the timing, dose, and vaccine2-epidemic distance was the identical.

Negative Interference. Rows of Figure 5.2d, which represent different vaccine1-vaccine2 distances and a constant vaccine1-epidemic distance, show higher attack rates when vaccine1 and vaccine2 were close to each other. We call this negative interference of vaccine1 on vaccine2, and example is show in Figure 5.3 (virus and antibody) and Figure 5.4 (B cells). Antibodies raised in response to vaccine1 cross-reacted, with medium affinity and medium-high quantity, with vaccine2 (Figure 5.3b). These same antibodies had only low affinity for the epidemic strain (Figure 5.3c). Vaccine2 was quickly cleared by the cross-reactive antibodies from vaccination1, and only slightly increased the quantity of antibodies that cross-reacted with the epidemic virus (negative interference). As a result the epidemic viral load grew beyond the disease threshold. The B cell snapshot at the peak of the response to vaccine1 (Figure 5.4a, b, and c) shows B cell clones raised by vaccine1 that cross-reacted with vaccine2, but not with the epidemic strain. The snapshot at the peak of vaccination2 (Figure 5.4d, e, and f) shows the response was dominated by the cross-reactive clones from vaccination1 and no new major clones were generated by vaccination2. It was not likely that vaccination1 would produce clones that cross-reacted with the epidemic strain because the vaccine1-epidemic distance was 4, which his fairly

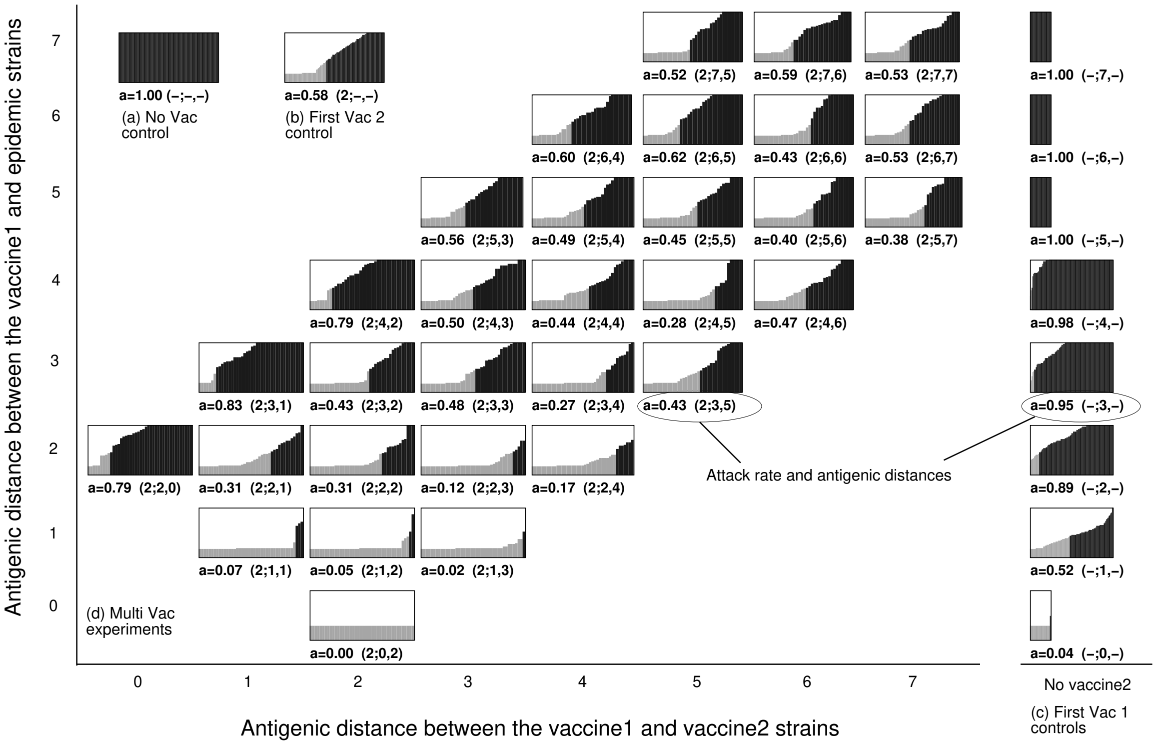

Figure 5.2: A summary of the maximum viral load in each experiment. Each subplot represents the experiments in a group. Beneath each subplot is the attack rate, a, and the antigenic distances among the strains in the form $ev_2; ev_1, v_1v_2$, where ev_2 is the epidemic-vaccine2 distance, ev_1 is the epidemic-vaccine1 distance, and v_1v_2 is the vaccine1-vaccine2 distance. Each subplot is comprised of a vertical line for each experiment in a group, the height of each vertical line indicates the maximum viral load during the experiment. The experiments in each group are plotted in order of increasing maximum viral load. Viral loads above the disease threshold are plotted in black; thus, the width of the black region indicates the attack rate in each group. (a) Exposure to the epidemic challenge, without prior vaccination, caused disease in all cases. (b) The attack rate was 58% when the vaccine was given 2 months before the epidemic challenge. (c) Attack rates varied from 4 to 100% when the vaccine was given 1 year 2 months before the epidemic challenge, depending on the antigenic distance between the vaccine and epidemic strains. (d) Attack rates varied between 0 to 83% when the epidemic challenge came after two annual vaccinations.

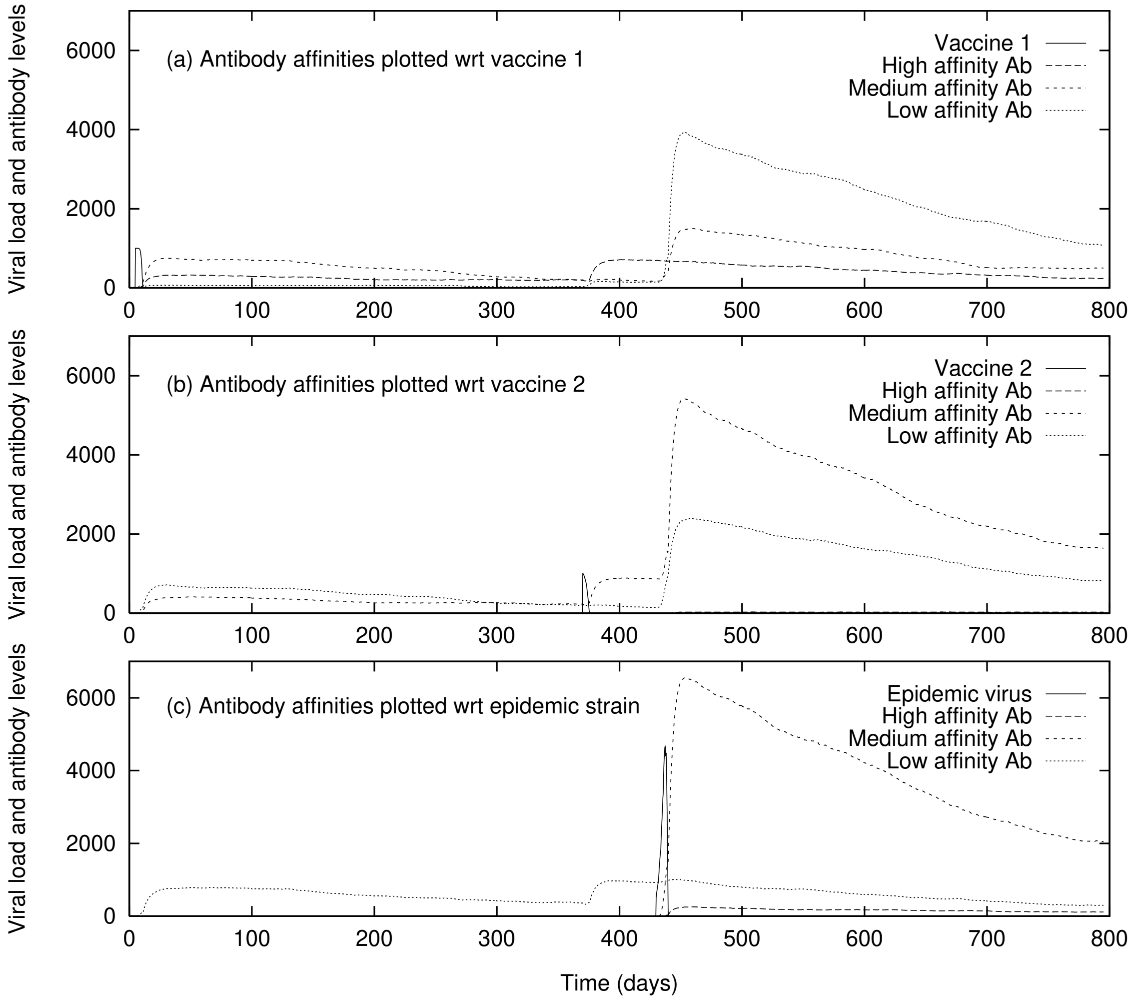

Figure 5.3: An example of negative interference of vaccine1 on vaccine2. An experiment from group 2;4,2 is shown, in which the vaccine2-epidemic distance was 2, the vaccine1-epidemic distance was 4, and the vaccine1-vaccine2 distance was 2. An analysis of the B cells for the same experiment is shown in Figure 5.4. (a) The response to vaccine1 produced a mixture of medium and high affinity antibodies. Measured wrt vaccine2 (panel b), the antibodies were a mixture of medium and low affinity, and measured wrt the epidemic virus (panel c) were low affinity. (b) Vaccine2 boosted the medium affinity antibodies, and measured wrt the epidemic virus it boosted the quantity but not the affinity of antibodies. (c) The epidemic virus was not cleared by the preexisting low affinity antibodies and passed the disease threshold.

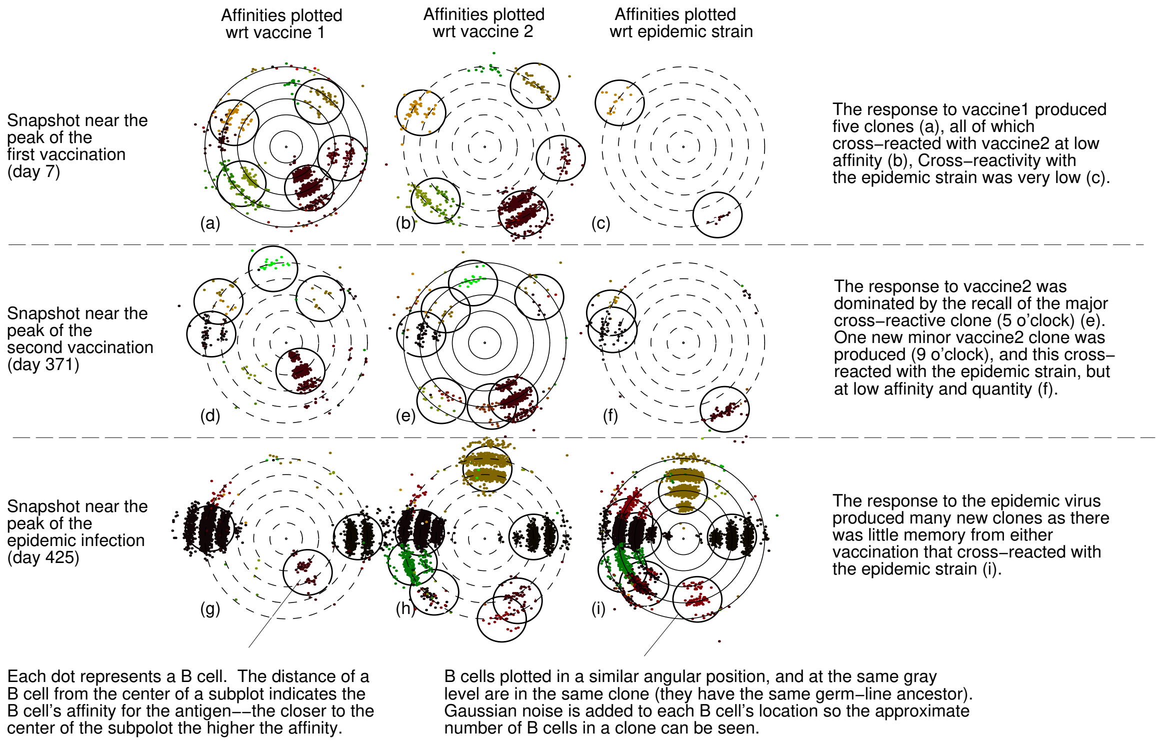

Figure 5.4: An example of negative interference of vaccine1 on vaccine2 causing vaccine2 failure. This is the B cell analysis of the experiment shown in Figure 5.3. The major vaccine clone, which also cross-reacted with vaccine2, dominated the vaccine2 response and prohibited the generation of new clones by vaccine2 that might have been cross-reactive with the epidemic strain. Because there were few memory clones from wither vaccination that cross-reacted with the epidemic strain, the response to the epidemic infection was like a primary response and the maximum viral load exceeded the disease threshold.

large; however, vaccine1 did have an influence on the epidemic because vaccine1 clones cleared vaccine2 before vaccine2 produced new clones that were quite likely to have cross-reacted with the epidemic strain because the vaccine2-epidemic distance was 2.

Positive Interference. Columns of Figure 5.2d, which represent different vaccine1-epidemic distances and a constant vaccine1-vaccine2 distance (Figure 5.1), show lower attack rates when vaccine1 and the epidemic strain were close to each other. We call this positive interference of vaccine1 on the epidemic challenge. Figures 5.5 and 5.6 show a combination of negative and positive interference. Antibodies raised in response to vaccine1 cross-reacted strongly with vaccine2 and the epidemic strain. Vaccine2 was mostly cleared by these cross-reactive antibodies, only one new memory clone was produced, and the increase in antibody levels was mostly due to boosting preexisting clones (negative interference). These preexisting clones and antibodies also cross-reacted with the epidemic virus (positive interference), hence the virus was quickly cleared. Figure 5.6 shows that B cells raised in response to vaccine1 cross-reacted with both vaccine2 and the epidemic strain. Vaccination2 boosted these clones. Because there were many cells cross-reactive with the epidemic, antibody secreted by some of these cells cleared the epidemic strain before the caused disease.

A summary of the B cell data for each experiment, averaged within each group, is shown in the cellular analysis summary (Table 5.2). This cellular analysis shows, not unexpectedly, that the number of vaccine1 cells that cross-reacted with the epidemic strain was proportional to the vaccine1-epidemic distance (Table 5.2 Column 4 and Figure 5.7a). Also, the attack rate was inversely proportional to the number of B cells that cross-reacted with the epidemic strain (Table 5.2 Columns 7 and 8, and Figure 5.7b). Thus, positive interference of vaccine1 on the epidemic appears to be correlated with the number of vaccine 1 clones that cross-reacted with the epidemic.

The cellular analysis also shows, not unexpectedly, that the number of vaccine1 cells that cross-reacted with vaccine2 was inversely proportional to the vaccine1-vaccine2 distance (Table 5.2 Column 2 and Figure 5.7a). It also shows that when more vaccine1 cells cross-reacted with vaccine2, fewer new cells were generated in response to vaccine2 (Table 5.2 columns 2 and 3, and Figure 5.7c). Thus, negative interference of vaccine1 on vaccine2 appears to be correlated with the number of cells, produced in response to vaccine1, which cross-reacted with vaccine2.

Original Antigenic Sin. Among B cells that cross-reacted with the epidemic strain, when the vaccine1-epidemic distance was less than 4, a greater proportion were initially raised in response to vaccine1 than to vaccine2 (Table 5.2 columns 5 and 6). The effect was more pronounced when the vaccine1-vaccine2 distance was small.

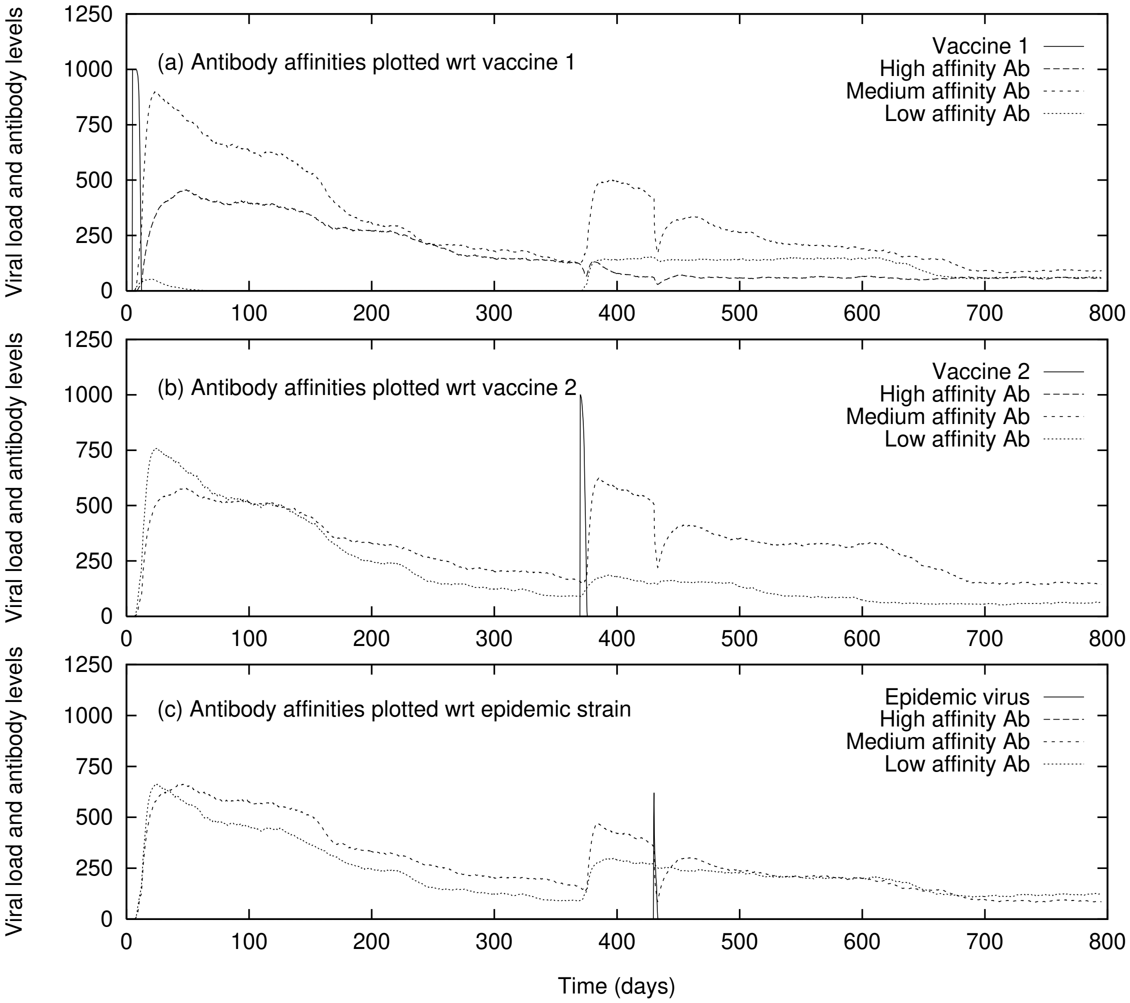

Figure 5.5: An example of negative and positive interference by vaccine1. An experiment from group 2;2,2 is shown, in which the vaccine2-epidemic distance was 2, the vaccine1-epidemic distance was 2, and the vaccine1-vaccine2 distance was 2. An analysis of the B cells for the same experiment is shown in Figure 5.6. Note, the vertical axis scale is different from that in Figure 5.3. (a) The response to vaccine1 produced a mixture of medium and high affinity antibodies. Measured wrt vaccine2 (panel b) and the epidemic strain (panel c) , the antibodies were a mixture of medium and low affinity. (b) Vaccine2 boosted the medium affinity antibodies, and and this also boosted the medium affinity antibodies measured wrt the epidemic virus. (c) The epidemic virus was quickly cleared by the preexisting medium affinity antibodies, and this did little to further boost the antibody levels.

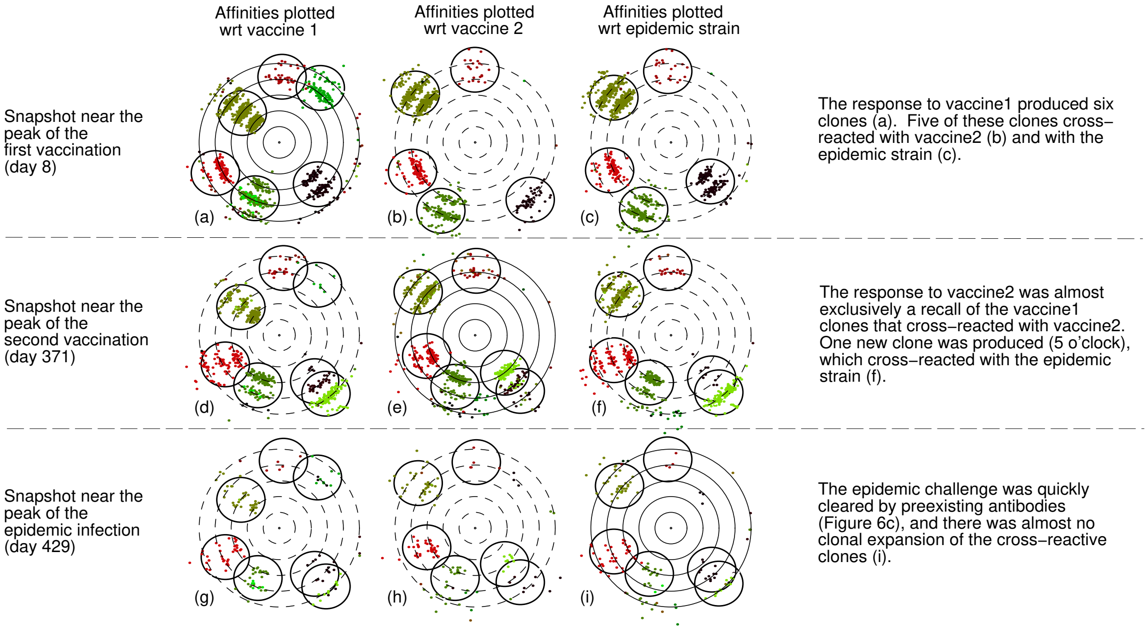

Figure 5.6: A example of both positive and negative interference by vaccine1. This is the B cell analysis of the experiment shown in Figure 5.5. Most of the clones generated by the response to vaccine1 cross-reacted with both vaccine2 and the epidemic strain. The response to vaccine2 boosted the vaccine1 clones and thus there was sufficient medium affinity antibodies to protect against the epidemic challenge. Vaccine1 negatively interfered with vaccine2—there was only one new clone generated, but it also positively interfered with the epidemic strain so the epidemic challenge was quickly cleared.

Antigenic dists	Num memory cells†		Num memory cells in $(V_1 + V_2) \times E$‡				Attack rate§
$ev_2; ev_1, v_1v_2^*$	$V_1 \times V_2$	New V_2	1°	1° after 2°	new 2°	total	
(col 1)	(col 2)	(col 3)	(col 4)	(col 5)	(col 6)	(col 7)	(col 8)
2;0,2	17	36	84	93	9	102	0.00
2;1,1	40	13	43	46	2	49	0.07
2;1,2	17	35	37	50	6	56	0.05
2;1,3	8	74	38	43	19	62	0.02
2;2,0	80	5	16	10	1	11	0.79
2;2,1	41	13	20	23	3	27	0.31
2;2,2	22	34	18	24	8	32	0.31
2;2,3	10	59	25	34	17	50	0.12
2;2,4	5	82	19	21	20	41	0.17
2;3,1	37	14	6	8	3	11	0.83
2;3,2	21	35	9	20	8	28	0.43
2;3,3	9	63	8	16	11	26	0.48
2;3,4	3	81	11	19	19	39	0.27
2;3,5	1	95	5	5	19	24	0.42
2;4,2	19	41	3	5	8	13	0.79
2;4,3	5	75	3	7	16	23	0.50
2;4,4	1	92	3	4	21	24	0.44
2;4,5	2	96	5	10	22	32	0.28
2;4,6	0	102	3	2	20	23	0.48
2;5,3	5	75	1	1	20	21	0.56
2;5,4	5	89	1	3	22	25	0.49
2;5,5	1	101	2	4	24	28	0.45
2;5,6	0	107	1	1	25	26	0.40
2;5,7	0	105	3	2	32	33	0.37
2;6,4	3	91	1	1	18	20	0.60
2;6,5	1	96	1	4	17	20	0.62
2;6,6	1	100	2	3	24	27	0.42
2;6,7	0	103	1	0	23	23	0.53
2;7,5	2	100	1	0	26	26	0.52
2;7,6	1	100	1	1	24	25	0.59
2;7,7	0	102	1	0	24	24	0.53

Table 5.2: A summary of the number of B cells produced and their cross-reactivities for groups that were vaccinated in both years. In each case, the number of cells are the medium and high affinity memory B cells averaged over the 40-42 experiments in each group. The experimental groups are collected according to rows of Figure 5.2. *The antigenic distances between the epidemic and vaccine1 strains (ev_1), the epidemic and vaccine2 strains (ev_2), and the vaccine1 and vaccine2 strains (v_1v_2). †The number of memory B cells produced by vaccination1 that cross-reacted with vaccine2 (col 2), and the number of new memory B cells produced by vaccination2 (col 3). ‡The number of memory B cells that cross-reacted with the epidemic strain that were: produced by vaccination1 (col 4), produced by vaccination1 after boosting by vaccination2 (col 5), produced by vaccination2 (col 6), and in total (col 7). §The proportion of experiments in a group in which the maximum viral load exceeded the disease threshold (col 8).

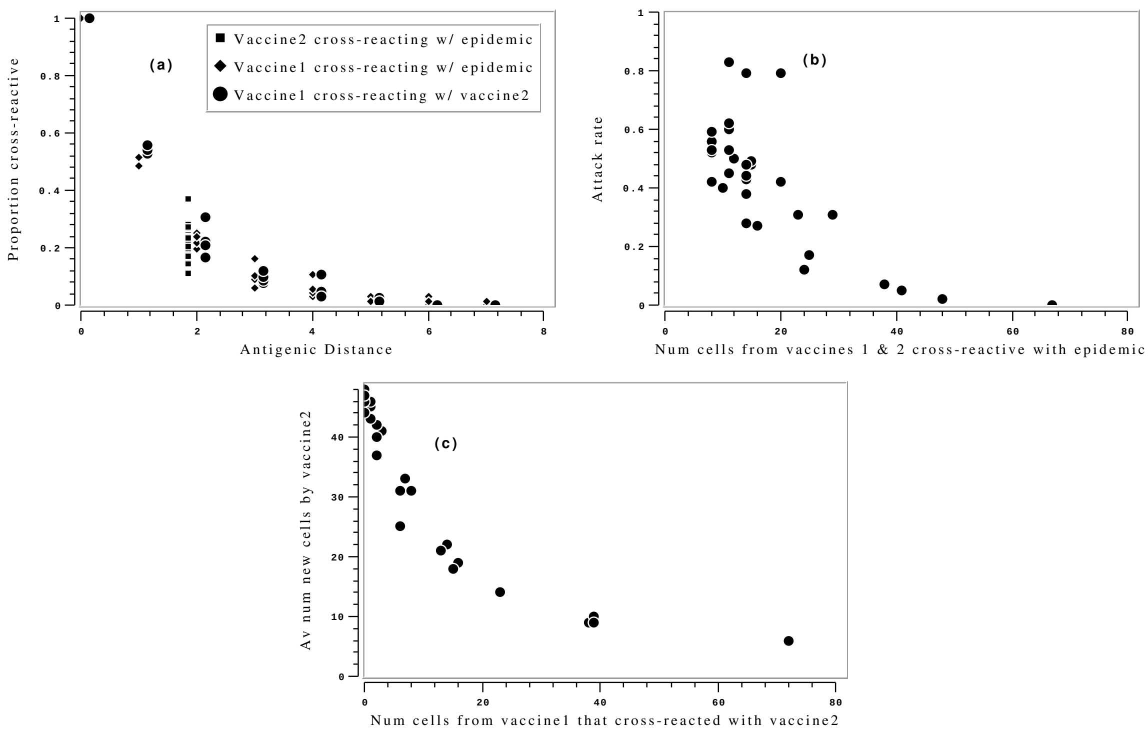

Figure 5.7: Correlations in the cellular analysis (Table 5.2). (a) The average proportion of B cells that cross-reacted with two antigens was inversely proportional to the antigenic distance between the antigens. (b) The attack rate of the epidemic virus was inversely proportional to the average number of B cells, generated by the vaccinations, that cross-reacted with the epidemic strain. (c) The average number of new B cells produced by vaccination2 was inversely proportional to the average number of B cells, produced by vaccination1, that cross-reacted with vaccine2.

5.4 Discussion

Our results indicate that for individuals vaccinated in two successive years, the antigenic distances of the first vaccine to the second vaccine, and of the first vaccine to the epidemic strain significantly affected attack rates. These results offer an explanation for the incongruous findings in field trials of annual influenza vaccination. When the vaccine1-vaccine2 antigenic distance was low, vaccine1 *negatively interfered* with vaccine2 by clearing it before it induced an immune response, and thus inhibited production of potentially protective antibodies against the upcoming epidemic strain. However, when the vaccine1-epidemic distance was low, vaccine1 *positively interfered* with the epidemic strain because antibodies raised to vaccine1 cross-reacted with the epidemic strain and helped to clear it. Thus, attack rates varied in annual vaccinees depending on the combination of negative and positive interference induced by vaccine1 which in turn depended on the vaccine1-vaccine2 and vaccine1-epidemic antigenic distances.

We found, as would be expected, that attack rates for first time vaccinees increased as the antigenic distance between the vaccine and epidemic strain increased. We also found, as would be expected, that attack rates were higher when there was a longer time between vaccination and challenge. We also found that attack rates during the second influenza season in groups vaccinated before the first influenza season were lowered by a second vaccination before the second influenza season.

Immune suppression by circulating antibodies, as seen in our study, has also been reported for influenza vaccines in humans (Howells *et al.*, 1973). The degree of suppression appears to be due to the amount of circulating antibodies (Hobson *et al.*, 1973; Robinson *et al.*, 1997).

In our model system, homologous vaccine boost prior to the second influenza season failed to elicit significant rise in antibody levels, and this coupled with the antibodies having fallen below protective levels resulted in a high attack rate. Failure of homologous vaccination to boost after 2 weeks (Hobson *et al.*, 1973) and after 6 months (Powers *et al.*, 1984) has been seen in human trials. However, in the latter study titers had not fallen below protective levels. We have previously performed experiments, similar to those reported here, but in which antibody levels returned close to zero levels before revaccination (Smith *et al.*, 1997b). In those experiments a homologous second vaccination provided good protection. Thus, our results depend on the persistence of antibodies and whether that persistence remains above protective levels. In reality, antibody persistence is different for different influenza antigens, for example, it has been found that antibody persistence was lower for the H1N1 component compared with the H3N2 and B components of a trivalent vaccine Powers *et al.* (1984).

Antibody levels and persistence also appears to be affected by whether exposure was by natural infection or by vaccination. In our model we also see a difference, with antibody levels and persistence much greater for epidemic infection above the disease threshold (Figure 5.3c). However, when the epidemic virus was cleared before it caused disease it had little effect on antibody levels (Figure 5.5). Vaccine design strives for persistent high antibody titers; however, perversely, if the titer remained protective during the influenza season, it would be advantageous for it to fall during the rest of the year to reduce negative interference of subsequent revaccinations.

Our results predict that two-time vaccinees will have a higher attack rate than first-time vaccinees when the vaccine1-vaccine2 distance is low and vaccine1-epidemic distance is high; that they will have lower attack rates if vaccine1-epidemic distance is low; and will have similar attack rates if vaccine1 is distant to both vaccine2 and the epidemic strain. Some rough testing of these predictions is possible by examining the data from the outbreaks at Christ's Hospital in 1974 and 1976 (Hoskins *et al.*, 1976; Hoskins *et al.*, 1979). Table 5.3 shows the hemagglutination inhibition (HAI) assay titers for the vaccine and epidemic strains relevant to the Christ's Hospital study. Relative HAI titers can be roughly related to antigenic distance, with low (log) difference in titers indicative of low antigenic distance, and high (log) difference indicative of high distance. For the 1974 outbreak, vaccine1 was A/HK/68, vaccine2 was A/Eng/72, and the epidemic strain was A/PC/73. The relative HAI titer difference between vaccine1 and vaccine2 was low (1 log), suggesting a

Virus	Sera			
	A/HK/68	A/Eng/72	A/PC/73	A/Vic/75
A/HK/68	1280	960	80	30
A/Eng/72	640	1280	640	80
A/PC/73	$<$10	40	320	40
A/Vic/75	30	40	20	640

Table 5.3: Hemagglutination inhibition titers between influenza strains similar to the vaccine and epidemic strains of the 1974 and 1976 outbreaks at Christ's Hospital. Titers were extracted from a larger table in Both *et al.* (1983).

low vaccine1-vaccine2 distance and the potential for negative interference of vaccine1 on vaccine2. The relative HAI titers between vaccine1 and the epidemic strain was high (7 logs for epidemic virus in vaccine1 sera, and 4 for vaccine1 in epidemic sera), suggesting high to medium vaccine1-epidemic distance and thus low positive interference of vaccine1 on the epidemic strain. Thus, our results would predict a higher attack rate for two-time vaccinees than for first-time vaccinees vaccinated at the beginning of the influenza season. This is what was found with attack rates of 3% in first-time vaccinees and 11% in two-time vaccinees. Note, in this comparison the vaccine2-epidemic distance, vaccine2 dose, and characteristics of the epidemic virus such as virulence do not have to be considered because one- and two-time vaccinees received the same vaccine2 and were challenged with the same epidemic strain.

For the 1976 outbreak at Christ's Hospital, vaccine1 was A/Eng/72, vaccine2 was A/PC/73, and the epidemic strain was A/Vic/75. It is more difficult to estimate antigenic distances for this outbreak because of assymetries in the HAI titers (for example, vaccine1 virus in vaccine2 sera gave a titer of 640 whereas vaccine2 virus in vaccine1 sera gave a titer of 40), and apparent changes in antigenicity (for example, vaccine2 virus in vaccine2 sera gave a lower titer (320) than vaccine1 virus in vaccine1 sera (1280)). Perhaps we can say that the vaccine1-vaccine2 distance was medium, and thus there may have been some negative interference, and that vaccine1-epidemic distance was low, so there maybe have been little positive interference, and thus we might predict a higher attack rate for two-time vaccinees compared with first-time vaccinees. This is what was found with attack rates of 22% in two-time vaccinees and 13% in first-time vaccinees. A further complicating factor in this comparison is that we simulated only two vaccinations whereas some boys in the study had three vaccinations, and some boys also had natural infections (clinical and subclincal) to previous epidemics.

The Melbourne studies (Feery *et al.*, 1979), as with the Christ's Hospital study, found higher attack rates in two-time vaccinees compared with first-time vaccinees. However, they did not report the strains of previous vaccinations. We would predict low vaccine1-vaccine2 distance and a high vaccine-1-epidemic distance. The Houston study (Keitel *et al.*, 1988) reported slightly lower attack rates in two-time vaccinees than in first-time vaccinees. They did report the vaccine strains, but we do not know the HAI titers. We would predict either a low vaccine1-vaccine2 distance with low vaccine1-epidemic distance, or a high vaccine1-vaccine2 distance and medium to high vaccine1-epidemic distance.

A limitation of our model is that it assumes genetic distance and antigenic distance are the same. This is out of necessity because the general mapping from sequence to folded protein is not understood. In some situations this assumption, though approximate, is not unreasonable. For example, Champion *et al.* (1975) showed that for azurins, lysozymes, and alpha subunits of tryptophan synthetase, that sequence difference was correlated with the degree of antigenic difference. However, for some antigenic determinants, a single amino acid change can cause a large change in antigenic difference. Table 5.8a shows the number of amino acid differences in antigenic sites A, B and C of the influenza H3 hemagglutinin gene of the vaccine and epidemic strains relevant to the Christ's Hospital outbreaks in 1974 and 1976. Table 5.8c shows one possible mapping of the HAI titers of Table 5.3 into antigenic distances. A comparison of Tables 5.8a and 5.8c shows an approximate correspondence between genetic and antigenic distance for the hemagglutinin of these influenza strains.

This approximate correspondence between genetic and antigenic distance allows us

	HK	Eng	PC	Vic
HK	–	4	7	10
Eng		–	3	5
PC			–	3
Vic				–

(a) Genetic distances

	HK	Eng	PC	Vic
HK	–	0.5	4.0	5.5
Eng	1.0	–	1.0	4.0
PC	5.0	3.0	–	3.0
Vic	4.5	4.0	5.0	–

(b) Antigenic distances

	HK	Eng	PC	Vic
HK	–	0.8	4.5	5.5
Eng		–	2.0	4.0
PC			–	4.0
Vic				–

(c) Averaged antigenic distances

Figure 5.8: Genetic and approximate antigenic distances among virus similar to those in the Christ's Hospital vaccine and epidemic strains. HK is A/Hong Kong/8/68, Eng is A/England/42/72, PC is A/Port Chalmers/1/73, and Vic is A/Victoria/3/75. (a) Number of amino acid differences in antigenic sites A, B, and C of the H3 hemagglutinin gene (extracted from data in (Both *et al.*, 1983)). (b) One, of many, possible interpretations of the antigen distances from the HAI titers of Table 5.3. In this case we took the $\log_2$ difference of a row entry with the diagonal element of that row. (c) The same antigenic distances as in (b), but averaged across the diagonal. Comparing tables a and c shows an approximate correspondence between genetic and antigenic distance among these strains.

to estimate how often we might see higher attack rates in annual vaccinees compared with first-time vaccinees. If vaccine1 and vaccine2 are fairly close genetically, and if this corresponds to being fairly close antigenically, then vaccine1 will negatively interfere with vaccine2 and the attack rate may be high if the vaccine1-epidemic distance is also high. If vaccine1, vaccine2, and the epidemic strain are from the same evolutionary path, then it is likely that the epidemic strain will have the same mutations from vaccine1 as those seen in vaccine2. Also, new mutations in the epidemic strain are likely to be at sites conserved between vaccine1 and vaccine2 because if the vaccine1-vaccine2 distance is low there are more conserved sites than modified ones. Indeed, all major H3N2 epidemic strains between 1968 and 1980 had this pattern of accumulative mutations in previously conserved sites (Both *et al.*, 1983). Thus, the vaccine1-epidemic distance is likely to be greater than the vaccine1-vaccine2 distance and thus there is likely to be more negative than positive interference by vaccine1. This argument, based on an approximate correspondence between genetic and antigenic distance, suggests that higher attack rates in multiple vaccinees compared with first-time vaccinees might be fairly common in practice.

Wet biology is, of course, never as simple as *in machina* biology—our model system abstracts away many details of the immune system and influenza virology and pathology, and factors known to have an effect on influenza vaccination and pathogenesis are ignored by the model, including age, virus virulence, vaccine immunogenicity, and immunocompetance. However, even given the simple nature of the model, our experimental results appear to reflect some of the complex phenomena observed in field trials of influenza vaccine, and offer an explanation of apparently contradictory results in trials of annual vaccination.

Our major result is that the antigenic distance between a prior vaccine and a subsequent vaccine, and the distance between the prior vaccine and a subsequent epidemic virus, and can significantly influence the protection offered by annual vaccination. Wet experiments will need to be done to test the significance of our results. Our results suggest that field trials of influenza vaccines should record the vaccination history and prior infection history of study volunteers. Our results also suggest that if a choice is available among otherwise equivalent vaccine strain candidates, that a strain as far as possible from the previous vaccine strain would be most effective in previously vaccinated individuals.

Chapter 6

Further work

In this chapter I review directions in which the work presented so far can proceed, and I outline some preliminary results in those directions. In section 6.1 I use the results from chapter 5 to address a specific question of importance for influenza vaccine strain selection: "Should the vaccine strain be updated if it is already fairly close to the expected epidemic strain." In section 6.2 I do a mathematical analysis of the effects of prior exposure on vaccine efficacy. In section 6.3 I discuss multivalent vaccines, and in section 6.4 I outline wet experiments that could be done to test and refine the theoretical results of this dissertation.

6.1 Vaccine Strain Selection

An important question in selecting the influenza vaccine strain is "If the existing vaccine strain is reasonably close to the expected epidemic strain, should the vaccine strain be updated to the expected epidemic strain, or should the vaccine remain the same?" (Cox, 1997).

We performed *in machina* experiments to examine three annual vaccinations and measured the attack rates in the second and third influenza seasons. We compared three vaccine update strategies. The first two were "stay" in which the vaccine is not updated, and "follow" in which the vaccine is updated. The third strategy, "surround," is of our own design and attempts to incorporate the best of stay and follow. The surround-vaccine strategy is to choose a strain that is as close to the epidemic estimate as the stay-vaccine would be, but is as far from the previous vaccine as possible. Thus, vaccine-surround attempts to minimize the effects of antibody-mediated suppression of the second vaccine by the first vaccine. Also, because of the high dimensional nature of shape space, vaccine-surround is also likely to be father from a subsequent vaccine and thus interfere less with it.

We examined combinations of these strategies over three influenza seasons. The vaccine strain for the first year (vaccine1) was the same in all groups. In the second year we selected vaccine strains according to the stay, follow, and surround strategies, and different groups were given a different vaccine. In the third year all groups were given a vaccine chosen by the follow strategy. Thus, the combinations of strategies tested were follow-follow, stay-follow, and surround-follow.

Figures 6.1, 6.2, and 6.3 show three different sets of antigenic distances between the three epidemic strains, and the three vaccine strain selection strategies. The approximate correspondence between genetic and antigenic distance discussed in chapter 5 allows us to characterize Figures 6.1, 6.2, and 6.3 in terms of the evolutionary path of the virus and to estimate which path is most likely. If we accept the rough genetic-antigenic correspondence, then the antigenic distances in Figure 6.1 would most likely be caused by mutations in the epidemic virus that are at previously unmutated locations (with respect to the epidemic virus in the first year). Such *accumulative* mutations are most likely because there are more unmutated than mutated locations. The antigenic distances of Figure 6.2 would correspond to accumulative mutations between the first and second years, and a combination of accumulative and *sequential* mutations (mutations at locations that have previously been mutated) between the second and third years. Conversely, Figure 6.3 would correspond to a combination of accumulative and sequential mutations between the first and second years, and accumulative mutations between the second and third years. We label the evolutionary path of Figure 6.1 accumulative-accumulative, of Figure 6.2 accumulative-sequential, and of Figure 6.3 sequential-accumulative.

Attack rates for the second influenza season were taken from the experiments of chapter 5 (Figure 5.2). Further experiments were run to determine the attack rates when the vaccine2-epidemic distance was 1 and 3 (Figure 6.4). Attack rates for the third season have been approximated by ignoring the effects of vaccine1 and any epidemic challenge in the second season, and were also read from Figures 5.2 and 6.4. Hence, results for the third season reflect a separate set of experiments that did not receive vaccine1 and were not challenged in the second season. Further work would also look at simulated individuals who received all the three vaccinations.

Table 6.1 shows the attack rates for the most likely antigenic distances among the epidemic strains—the accumulative-accumulative configuration (Figure 6.1). We see that the average attack rates, for simulated individuals previously vaccinated with vaccine1 and then vaccinated with vaccine2 and challenged in the second influenza season, were 54% and 51% for the follow and surround strategies respectively. The average attack rate for the stay strategy was significantly worse at 87%. In the third influenza season, the average attack rates were 39% for the stay-follow and surround-follow strategies, and 51% for the follow-follow strategy. Stay-follow and surround-follow had the same attack rates because the antigenic distances between the vaccines and among the vaccines and epidemic strains were the same (Figure 6.1). Thus, on average over both seasons, follow-follow and surround-follow offered about the same protection (surround-follow may be a little better), and stay-follow offered worse protection.

Table 6.2 shows attack rates for a less common evolutionary path of the epidemic virus, the accumulative-sequential path (Figure 6.2). Average attack rates for the second influenza season were the same as for the accumulative-accumulative experiments above because the evolutionary path of the virus was the same from the first to second seasons. Attack rates in the third season were approximately 20% for each strategy. These attack rates were lower than those seen when the virus evolved accumulative-accumulative because the vaccine2-epidemic3 distance was lower and thus there was more positive trans-

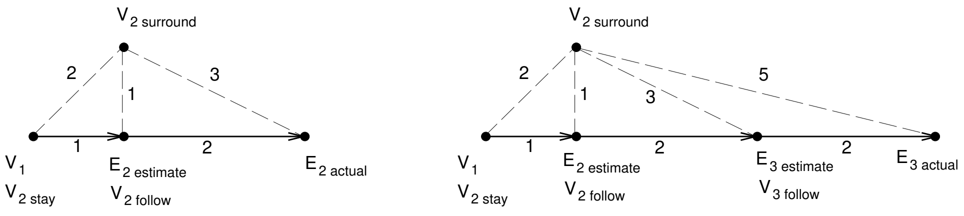

(a) Epidemic 2 (b) Epidemic 3

Figure 6.1: The antigenic distances among vaccines and epidemic virus for: (a) the second influenza season, and (b) the third season. Bold, arrowed, lines indicate the evolution of the virus, which in this case was likely to have been caused by accumulative mutations between each influenza season.

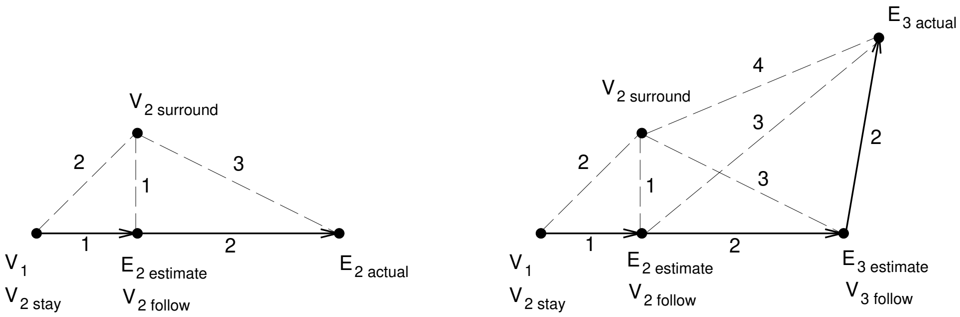

(a) Epidemic 2 (b) Epidemic 3

Figure 6.2: A similar situation to the one described in Figure 6.1, but with an evolutionary path of the epidemic virus that has accumulative mutations between the first and second years, and a combination of accumulative and sequential mutations (as discussed in the main text) between the second and third years.

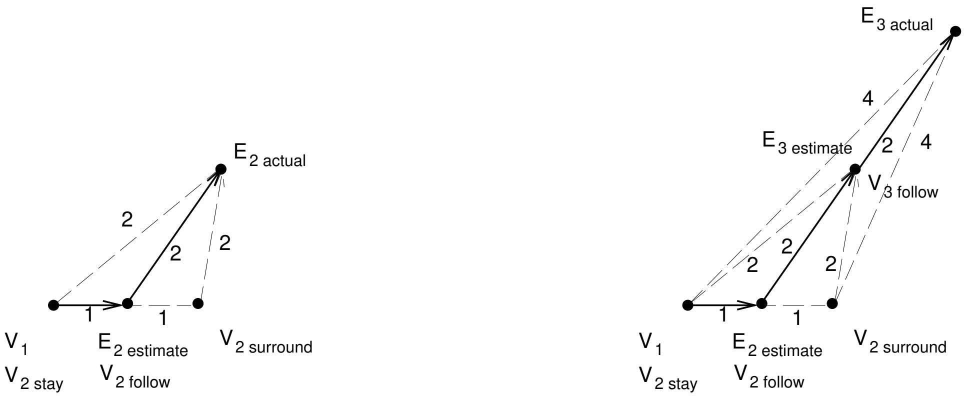

(a) Epidemic 2 (b) Epidemic 3

Figure 6.3: A similar situation to the one described in Figure 6.1, but with an evolutionary path of the epidemic virus that has a combination of accumulative and sequential mutations between the first and second years, and accumulative mutations between the second and third years.

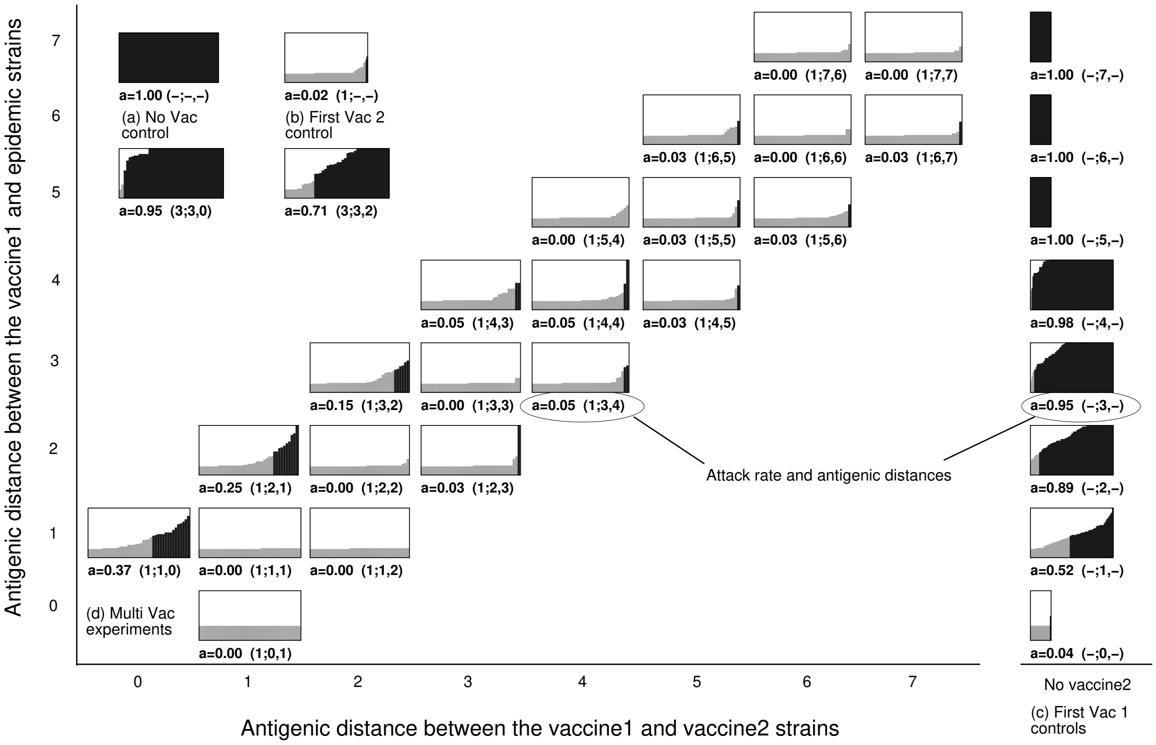

Figure 6.4: Attack rates at various combinations of antigenic distances between vaccine1 and vaccine2, and of vaccine1 and vaccine2 to the epidemic virus. This figure shows related data to that in Figure 5.2 and is it structured the same way. This figure shows attack rates when the vaccine2-epidemic distance was 1 and 3, whereas Figure 5.2 shows data when the vaccine2-epidemic distance was 2.

		Strategy		
		Follow-Follow	Stay-Follow	Surround-Follow
			Epidemic 2	
		$\underline{V_{2follow}}$	$\underline{V_{2stay}}$	$\underline{V_{2surround}}$
$E_{2e-2a} = 1$	$V_1 - E_{2e} = 1$	0.25 $_{1;2,1}$	0.79 $_{2;2,0}$	0.31 $_{2;2,2}$
$E_{2e-2a} = 2$	$V_1 - E_{2e} = 1$	0.83 $_{2:3,1}$	0.95 $_{3;3,0}$	0.71 $_{3;3,2}$
		(av 0.54)	(av 0.87)	(av 0.51)
			Epidemic 3	
		$\underline{V_{3follow}}$	$\underline{V_{3follow}}$	$\underline{V_{3follow}}$
$E_{3e-3a} = 1$	$E_{2e-3e} = 1$	0.25 $_{1;2,1}$	0.15 $_{1;3,2}$	0.15 $_{1;3,2}$
$E_{3e-3a} = 1$	$E_{2e-3e} = 2$	0.15 $_{1;3,2}$	0.05 $_{1;4,3}$	0.05 $_{1;4,3}$
$E_{3e-3a} = 2$	$E_{2e-3e} = 1$	0.83 $_{2;3,1}$	0.79 $_{2;4,2}$	0.79 $_{2;4,2}$
$E_{3e-3a} = 2$	$E_{2e-3e} = 2$	0.79 $_{2;4,2}$	0.56 $_{2;5,3}$	0.56 $_{2;5,3}$
		(av 0.51)	(av 0.39)	(av 0.39)
			Combined epidemics 2 and 3	
		(av 0.52)	(av 0.63)	(av 0.45)

Table 6.1: Attack rates in previously vaccinated simulated individuals for various antigenic distances between the epidemic estimated and actual strains for the second and third influenza seasons. The evolution of the epidemic virus had accumulative mutations in both years (Figure 6.1). Each attack rate is subscripted with antigenic distances in the form $x; y, z$, where x is the vaccine2-epidemic distance, y is the vaccine1-epidemic distance, and z is the vaccine1-vaccine2 distance. Average attack rates (av) are shown for each strategy in each season, and combined over both seasons.

		Strategy		
		Follow-Follow	Stay-Follow	Surround-Follow
			Epidemic 2	
		$\underline{V_{2follow}}$	$\underline{V_{2stay}}$	$\underline{V_{2surround}}$
$E_{2e-2a} = 1$	$V_1 - E_{2e} = 1$	0.25 $_{1;2,1}$	0.79 $_{2;2,0}$	0.31 $_{2;2,2}$
$E_{2e-2a} = 2$	$V_1 - E_{2e} = 1$	0.83 $_{2:3,1}$	0.95 $_{3;3,0}$	0.71 $_{3;3,2}$
		(av 0.54)	(av 0.87)	(av 0.51)
			Epidemic 3	
		$\underline{V_{3follow}}$	$\underline{V_{3follow}}$	$\underline{V_{3follow}}$
$E_{3e-3a} = 1$	$E_{2e-3e} = 1$	0.00 $_{1;1,1}$	0.00 $_{1;2,2}$	0.00 $_{1;2,2}$
$E_{3e-3a} = 1$	$E_{2e-3e} = 2$	0.00 $_{1;2,2}$	0.00 $_{1;3,3}$	0.00 $_{1;3,3}$
$E_{3e-3a} = 2$	$E_{2e-3e} = 1$	0.31 $_{2;2,1}$	0.43 $_{2;3,2}$	0.43 $_{2;3,2}$
$E_{3e-3a} = 2$	$E_{2e-3e} = 2$	0.43 $_{2;3,2}$	0.50 $_{2;4,3}$	0.50 $_{2;4,3}$
		(av 0.19)	(av 0.23)	(av 0.23)
			Combined epidemics 2 and 3	
		(av 0.37)	(av 0.55)	(av 0.37)

Table 6.2: This table is similar to Table 6.1 except it shows data when the evolutionary path of the epidemic virus is accumulative between the first and second influenza seasons, and a combination of sequential and accumulative between the second and third seasons.

fer from vaccine2 to epidemic3. Again, on average over both seasons, follow-follow and surround-follow offered the same protection, and stay-follow offered worse protection.

Table 6.3 shows the attack rates for the sequential-accumulative path (Figure 6.3). This path is also less likely than the accumulative-accumulative path. Similarly to the accumulative-accumulative second season, average attack rates for the follow and surround strategies were lower than for the stay strategy. Attack rates during the third season were identical for each strategy. Again, on average over both seasons, follow-follow and surround-follow offered the same protection, and stay-follow offered worse protection.

For first-time vaccinees, when the viral evolution was accumulative-accumulative or accumulative-sequential, attack rates for vaccine-stay and vaccine-surround groups during

		Strategy		
		Follow-Follow	Stay-Follow	Surround-Follow
			Epidemic 2	
		$\underline{V_{2follow}}$	$\underline{V_{2stay}}$	$\underline{V_{2surround}}$
$E_{2e-2a} = 1$	$V_1 - E_{2e} = 1$	0.00 $_{1;1,1}$	0.37 $_{1;1,0}$	0.00 $_{1;1,2}$
$E_{2e-2a} = 2$	$V_1 - E_{2e} = 1$	0.31 $_{2:2,1}$	0.79 $_{2;2,0}$	0.31 $_{2;2,2}$
		(av 0.16)	(av 0.58)	(av 0.16)
			Epidemic 3	
		$\underline{V_{3follow}}$	$\underline{V_{3follow}}$	$\underline{V_{3follow}}$
$E_{3e-3a} = 1$	$E_{2e-3e} = 1$	0.25 $_{1;2,1}$	0.25 $_{1;2,1}$	0.25 $_{1;2,1}$
$E_{3e-3a} = 1$	$E_{2e-3e} = 2$	0.15 $_{1;3,2}$	0.15 $_{1;3,2}$	0.15 $_{1;3,2}$
$E_{3e-3a} = 2$	$E_{2e-3e} = 1$	0.83 $_{2;3,1}$	0.83 $_{2;3,1}$	0.83 $_{2;3,1}$
$E_{3e-3a} = 2$	$E_{2e-3e} = 2$	0.79 $_{2;4,2}$	0.79 $_{2;4,2}$	0.79 $_{2;4,2}$
		(av 0.51)	(av 0.51)	(av 0.51)
			Combined epidemics 2 and 3	
		(av 0.34)	(av 0.60)	(av 0.34)

Table 6.3: This table is similar to Table 6.1 except it shows data when the evolutionary path of the epidemic virus is a combination of sequential and accumulative between the first and second influenza seasons, and accumulative between the second and third seasons.

the second season were higher than for vaccine-follow groups. This was because vaccine-follow resulted in a closer match between the vaccine and epidemic strains.

In summary, in the previously vaccinated, follow-follow and surround-follow offer about the same protection, with surround-follow doing a little better (though this may not be statistically significant). Both strategies perform better than stay-follow. In first-time vaccinees, follow is always the best strategy. Even though follow-follow and surround-follow have similar averages, they are quite different strategies: Follow-follow minimizes the distance of each vaccine selection to the epidemic virus, and thus it maximizes positive interference; surround-follow maximizes the distances among vaccine strains, and thus it minimizes negative interference. We could run more experiments, so we can tell statistically if surround-follow is really any better than follow-follow in the model. However, what really needs to happen is to investigate *in vivo* whether maximizing positive interference is more or less effective than minimizing negative interference. An experiment to test this is outlined in section 6.4.

6.2 Estimation of Protection based on Antigenic Distances

The results of Chapter 5 and Smith *et al.* (1997b) on prior vaccination and prior infection on influenza vaccination found that protection was primarily determined by the antigenic distances between the prior, vaccine and epidemic. In order to investigate this further, we now remove as many details of the immune response as possible and see what can be predicted by a mathematical analysis using only the antigenic distances between antigens. The analysis below applies to the experiments in Smith *et al.* (1997b) in which the antibody levels returned close to zero levels before each challenge.

Simple Analysis. First, assume a primary immune response always clears the antigen and generates a single memory clone whose members have similar affinities. This clone, with equal probability, lies anywhere within the ball of stimulation of the antigen. Second, assume that if a memory clone lies anywhere within the ball of stimulation of an

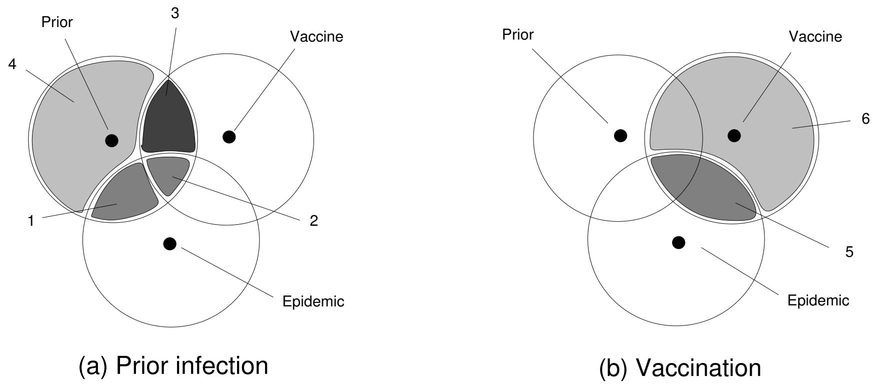

Figure 6.5: The distances between the prior, vaccine and epidemic correspond to the antigenic distances between the antigens. The balls of stimulation around each antigen indicate an affinity threshold within which B cells can be simulated by the antigen. B cells in the intersection of balls of stimulation of 2 or more antigens are thus cross-reactive with those antigens. Clones generated by the prior infection, (a), will be in regions 1 through 4, and depending on which region they are in, they cross-react with either or both of the vaccine and epidemic. Similarly, clones generated by the vaccination, (b), will be in regions 5 or 6.

antigen, it is sufficient to clear the antigen, and no new memory clone is produced.

By the first assumption, a prior infection will generate a single clone that will be in either region 1, 2, 3, or 4 of Figure 6.5a. By the second assumption, if the clone is in region 1 or 2, it cross-reacts with the epidemic and protects against epidemic challenge. If the clone is in region 3, it does not protect against epidemic challenge, but does cross-react with the vaccine, and will clear the vaccine; the vaccine will not generate its own clone, and there will be no protection against the epidemic challenge. If the clone is in region 4, it does not protect against the epidemic challenge, and neither does it interfere with the vaccination, and thus the vaccination will generate a memory clone. If this clone is in region 5 (Figure 6.5b), it protects against the epidemic challenge; if it is in region 6, there is no cross-reactivity with the epidemic and thus no protection. Thus we can write

$$\begin{aligned} P(\text{protection}) &= P(\text{prior clone is in region 1 or 2}) + \\ &\quad P(\text{prior clone is in region 4}) \times P(\text{vaccine clone is in region 5}). \end{aligned}$$

Because we assume that a clone can, with equal probability, be anywhere within the ball of stimulation of an antigen, the probability that a clone is in a region can be determined by knowing the size of a region relative to the size of a ball of stimulation. The relative sizes depend on the antigenic distances between the three antigens and geometric properties of the space. The relative size could be determined by labeling B cells with the antigens they cross-react with, and grouping them into the regions of Figure 6.5. For the model, we can directly calculate the number of different possible antibody receptors within a region and within a ball of stimulation (using an extension to three balls of the calculations in Appendix A). Thus, the above equation can be written as

$$P(\text{protection}) = \frac{\text{Vol(region } 1+2)}{\text{Vol}(P)} + \left(\frac{\text{Vol(region } 4)}{\text{Vol}(P)} \times \frac{\text{Vol(region } 5)}{\text{Vol}(V)}\right), \qquad (6.1)$$

where $\text{Vol}(P) = \text{Vol(region } 1+2+3+4)$ and $\text{Vol}(V) = \text{Vol(region } 5+6)$. The probability of protection can be calculated from this formula for the 31 combinations of prior, vaccine and epidemic cross-reactivities in Smith *et al.* (1997b). Figure 6.6a compares the predicted probability of protection given by this very simple analysis with the observed probability of protection in the *in machina* experiments. There is a reasonable agreement, especially given the very simple nature of this analysis. This confirms that, at least for the *in machina* model, the cross-reactivities are the major factor in the effect of prior infection on vaccine efficacy.

Complex Analysis. The simple analysis was deliberately as simple as we could make it. We now pursue a somewhat more complex analysis to get more predictive power. For the complex analysis, the two assumptions of the simple analysis are relaxed. The part of the first assumption, that only 1 clone is generated by a primary response, is relaxed by letting $P_{a,b,c,d}$ indicate a prior infection that results in a clones in region 1, b clones in region 2, c clones in region 3 and d clones in region 4, and letting $V_{e,f}$ indicate a vaccination that results in e clones in region 5 and f clones in region 6. The probability of $P_{a,b,c,d}$ can be

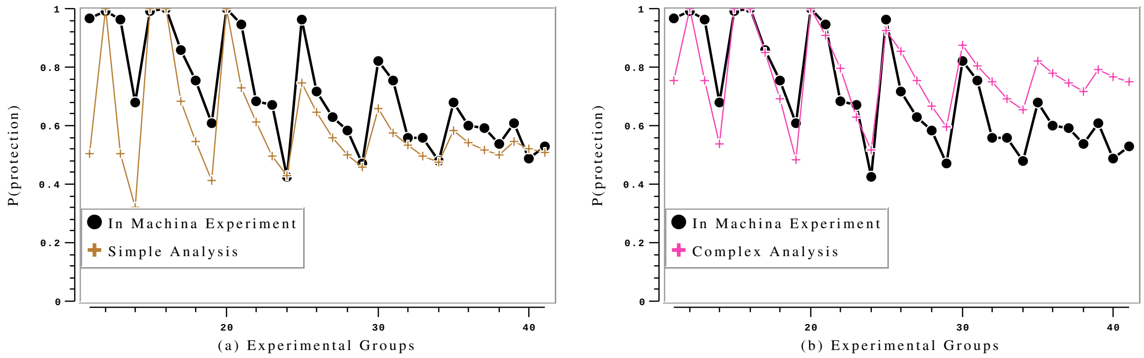

Figure 6.6: The observed (*in machina*) and predicted vaccine efficacy for (a) the simple analysis (Equation 6.1) and (b) the complex analysis (Equation 6.2), for each of the 31 experimental groups.

written directly from the multinomial theorem[1]

$$\begin{aligned} P(P_{a,b,c,d}) &= \binom{a+b+c+d}{a,b,c,d} \times \\ &\quad P(\text{prior clone is in region 1})^a \times \\ &\quad P(\text{prior clone is in region 2})^b \times \\ &\quad P(\text{prior clone is in region 3})^c \times \\ &\quad P(\text{prior clone is in region 4})^d \end{aligned}$$

where $\binom{a+b+c+d}{a,b,c,d}$ is the multinomial coefficient giving the number of ways to divide $a+b+c+d$ objects into 4 groups of a, b, c, and d objects. Similarly, the probability of $V_{e,f}$ is

$$P(V_{e,f}) = \binom{e+f}{e,f} \times P(\text{vaccine clone is in region 5})^e \times P(\text{vaccine clone is in region 6})^f.$$

Allowing the prior infection and vaccination to produce any number of clones gives the opportunity to relax the second assumption. For example, the number of clones produced by the vaccine could be a function of the number of clones in the intersection of the prior and vaccine. For this analysis we shall assume that the prior infection produces two clones, and that if there are no prior clones in regions 2 or 3 then the vaccine also produces two

[1]The multinomial theorem is a generalization of the binomial theorem to more than two variables.

clones (otherwise it produces no clones), and that a single clone in regions 1, 2, or 5 protects against the epidemic. We then have

$$\begin{aligned} P(\text{protection}) &= P(>0 \text{ clones in regions } 1,\ 2 \text{ or } 5) \\ &= 1 - P(0 \text{ clones in regions } 1,\ 2 \text{ or } 5) \end{aligned}$$

There are three ways to have zero clones in regions 1, 2, or 5: (i) both prior clones are in region 3, they do not cross-react with the epidemic and they do inhibit the vaccine from producing any clones, (ii) 1 prior clone is in region 3 and 1 is in region 4, they do not cross-react with the epidemic and the clone in region 3 inhibits the vaccine, or (iii) both prior clones are in region 4, they do not cross-react with vaccine or epidemic, but both the vaccine clones are in region 6 and thus do not overlap the epidemic. Thus,

$$P(\text{protection}) = 1 - \left(P(P_{0,0,0,2}) + P(P_{0,0,1,1}) + P(P_{0,0,2,0}) \times P(V_{0,2})\right). \tag{6.2}$$

This predicted probability of protection is compared to the observed probability of protection for the 31 prior strains in Figure 6.6b.

These mathematical predictions of vaccine efficacy based on the antigenic distances between the prior, vaccine and epidemic correlate well with the results from the model (Figure 6.6). The accuracy of the mathematical predictions indicated that, in the model, the antigenic distances between the antigens were the dominant factors in determining the protection conferred by vaccination after a prior infection (given a fixed vaccine to epidemic antigenic distance). Further analysis would take into account antibody levels, and could then be applied to the results of annual vaccination in chapter 5.

6.3 Multivalent Vaccines

Rapid antigenic drift is a property of many viruses, including influenza virus, human immunodeficiency virus, and hepatitis C virus. As a result of their high mutation rate, thousands of strains of these viruses coexist in a *species swarm* (or *quasispecies*) (Eigen, 1993).

Vaccination against species swarms is difficult because of the need to provide broad immunity to the many strains, and because new strains constantly emerge.

Depending on the diversity of the species swarm, a single vaccine strain may or may not protect against all members of the swarm. For influenza, a single vaccine strain usually does a good job (in first-time vaccinees) in protecting against the swarm.[2] The diversity of the HIV species swarms is too great for a single HIV vaccine strain (directed against the V3 loop). Thus, it is thought that an HIV vaccine will have to be multivalent. The valency of a vaccine is sometimes limited by requiring sufficient quantities of each component to induce an immune response, while having a limited overall quantity of vaccine to reduce toxicity. Thus, because the diversity of the HIV species swarm is so great, a single vaccination may not be able to contain sufficient strains to provide protection against all wildtype strains. This, coupled with the emergence of new viral strains. suggests that HIV vaccination may have to consist of a series of vaccinations. Hence our results from chapter 5 may be applicable.

We have done preliminary *in machina* experiments with multivalent vaccines, and have interesting results regarding the distribution of clones. Multivalent vaccines may also be be useful in influenza vaccination, where perhaps an influenza vaccine could contain strains from both the follow and surround strategies.

6.4 Wet experiments

This section describes wet experiments that could be done to test and expand on the results of chapters 3 and 5. I have no experience in wet biology, and I imagine actual experiments could be better designed than the ones I suggest. I include them to convey that my results can be tested with current experimental methods.

Intersection Volume. The derivation of shape space parameters from immunological data could be improved by results from experiments that directly measured the number

[2]The influenza vaccine is actually trivalent, with one strain directed against each of the three currently co-circulating antigenically distinct species swarms (H3N2, H1N1, and B).

of B cells in the intersection of balls of stimulation of antigens at various antigenic distances. Such results could improve the parameter choice of the model, and be used in the mathematical analysis of the cross-reactive immune response (Section 6.2)

One version of the experiment would take pairs of antigens at various antigenic distances to each other. These could be different myoblobins (East *et al.*, 1980), bacterial azurins (Champion *et al.*, 1975), or strains of influenza. The antigens would then be labeled for subsequent sorting by FACS (Fluorescence Activated Cell Scanning and Sorting). Two of the antigens would then be mixed with the B cell repertoire from a naive mouse (one that has not seen antigens). B cells would bind antigens to which they had affinity. The FACS could then sort the antigen-labeled B cells into 4 categories: those with one antigen bound, those the other antigen bound, those with both antigens bound, and those with no antigens bound. We could then calculate the number of cells in the intersection of balls of stimulation as a proportion of the number of cells in a ball of stimulation.

This experiment could be performed with three or more antigens instead of two. In the three antigen case, the cells would be sorted into eight groups, and the relative sizes of the eight intersection possibilities between three antigens could be measured (Figure 6.5). A further variant would be to use B cells from mice that had been exposed to one or more of the antigens. This would give an idea of the number and distribution of cells in the memory population. Such measurements would be very useful in improving the accuracy of the model and mathematical analysis.

Annual Influenza Vaccination. *In vivo* experiments to test the effects of annual influenza vaccination would be quite straightforward (Katz, 1997). The experiments could be done in mice. Human influenza virus is usually not pathogenic in mice, but some strains are, and one such strain would be chosen and used as the epidemic virus in all experiments. Vaccine strains would be selected at varying antigenic distances between each other, and to the epidemic virus. Distances would be taken from the hemagglutination inhibition assay (Table 5.3). The CDC has samples of many strains strains of influenza , and it is common practice to amplify samples and use them as vaccines in experiments at the CDC. The mice would be vaccinated and challenged according to Table 5.1. Vaccine and challenge dosage would be taken from other influenza vaccination studies in mice (Katz *et al.*, 1997), and the time between vaccinations would be set depending on the longevity of anti-influenza antibodies in mice. At intervals during the experiment, blood samples could be taken and antibody levels measured to be compared with the *in machina* antibody levels (Figures 5.3 and 5.5). After the epidemic challenge, viral load would be assessed in the lungs using the method described in Katz *et al.* (1997).

The results from such experiments would be a test of the predictions of chapter 5. The results would also show the relative effects of positive and negative interference, and could be used to make the model more quantitative. This would make the experiments comparing vaccine update strategies (Section 6.1) more accurate, and thus potentially quantitatively useful in the vaccine strain selection process.

Chapter 7

Conclusions

Although the model abstracts away from many of the details of the immune system, it appears to capture sufficient details to make a contribution to understanding annual influenza vaccination, and influenza vaccine design. The results offer a potential explanation for previously incongruous reports of highly varying attack rates in annual vaccinees by showing how immunological memory to previous vaccines can interfere, both positively and negatively, with subsequent vaccination. The degree, and sign, of the interference depended on the antigenic differences between the vaccine strains and epidemic strains used in the experiments. Currently, new strains for the influenza vaccine are chosen to be close to the expected epidemic strains. The results reported here suggest that vaccine strains should also be chosen to be distant from previous vaccine strains. A collaboration has started with the US Centers for Disease Control, Influenza Branch, to test these results.

Contributions to computer science include identifying immunological memory as a member of the class of sparse distributed associative memories. This tells us why immunological memory is associative—because it is sparse and distributed. The immune system is just beginning to be used as an information processing metaphor, and computational devices based on the immune system, usually associative memories, are beginning to be researched—such work has focused on idiotypic networks as the source of power and interest in the immune system. I have shown that immunological memory is associative regardless of whether it uses idiotypic networks to maintain memories. This does not mean that idiotypic networks should not be investigated as information processing systems in their own right, but it does change the perspective of their importance in the associative memory behavior of the immune system.

The model was used to study annual vaccination against influenza; however, it has many other potential applications. These include the study of the HIV pathogenesis, and the design of multivalent vaccines against influenza, HIV, and other antigenically variable pathogens.

Appendix A

Intersection Volume in Hamming Shape Space

Consider an n-dimensional Hamming space with alphabet size k. Let I and J be points (strings of n symbols) in the space at Hamming distance s from each other. Let K be a point at distance i from I and j from J, and let $N_{i,j}$ be the number of all such points. Figure A.1 shows the three strings I, J, and K, structured in a way to illustrate that the symbols of K can be partitioned into five groups. These strings can, without loss of generality, be manipulated to fit this template, because the space has an automorphism which maps any three points to these templates; the order of presentation of the dimensions, and the choice of symbols for each dimension, do not alter any of the aspects of the space that interest us.

The partitions a, b, c, d, and e of Figure A.1 can be described in words as follows:

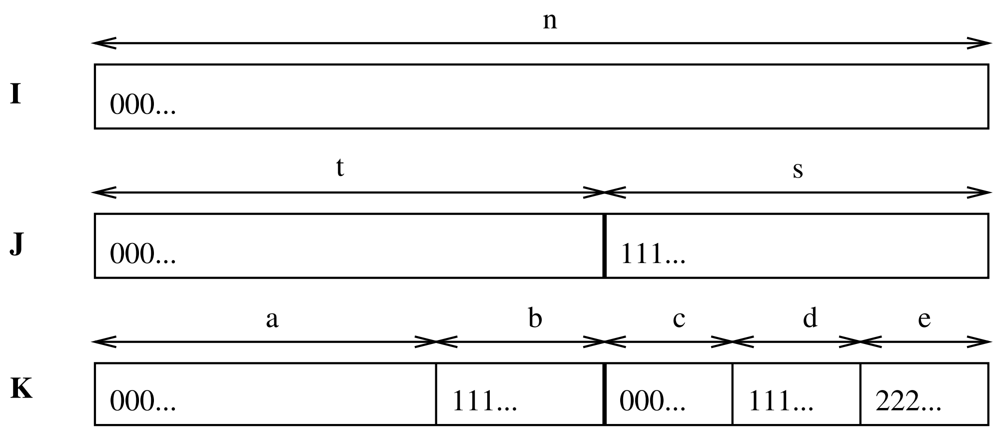

Figure A.1: This figure shows the five groupings of the symbols of K, and how these groups relate to the groupings in I and J.

a. those that are the same as both I and J.

b. those that are different from I and J in a place where I and J are the same.

c. those that are the same as I in a place where J differs from I.

d. those that are the same as J in a place where I differs from J.

e. those that are different from both I and J in a place where I and J differ.

The Hamming distance between two strings is the number of symbols that are different between the strings. The Hamming distance between I and J is s, the Hamming distance between K and I is the sum of b, d and e, and the Hamming distance between K and J is the sum of b, c and e (Figure A.1).

Thus for K to be Hamming distance i from I and j from J we must have (Figure A.1)

$$i = b + d + e, \tag{A.1}$$

and

$$j = b + c + e. \tag{A.2}$$

Similarly the distance, s, between I and J is the sum of the sizes of the partitions c, d and e, thus we have

$$s = c + d + e, \tag{A.3}$$

and

$$t = a + b. \tag{A.4}$$

Because of equations (A.3) and (A.4) and that the length of the strings is n, we get

$$n = t + s. \tag{A.5}$$

Let C be the set of 5-tuples, $\{a, b, c, d, e\}$, that satisfy equations (A.1), (A.2), (A.3), (A.4) and (A.5). Then,

$$N_{i,j} = \sum_{\{a,b,c,d,e\}\epsilon C} \binom{t}{a, b} 1^a (k-1)^b \binom{s}{c, d, e} 1^c 1^d (k-2)^e,$$

where k is the number of symbols in the alphabet.

If we write the multinomials as binomials, and substitute in a rearrangement of equation (A.5) for t we get

$$N_{i,j} = \sum_{\{b,d,e\}\epsilon C0} \binom{n-s}{b} (k-1)^b \binom{s}{d} \binom{s-d}{e} (k-2)^e.$$

The five equations, (A.1) through (A.5), constrain the values of the five free variables of a, b, c, d and e, to one degree of freedom, i.e. the choice of either a, b, c, d or e, will determine the remaining four values. If we choose d as the free variable, then

by (A.2) minus (A.3) we get

$$b = d + j - s, \tag{A.6}$$

and by (A.6) into (A.1) we get

$$e = i + s - 2d - j, \tag{A.7}$$

which gives

$$N_{i,j} = \sum_{0 \le d \le s} \binom{n-s}{d+j-s} (k-1)^{d+j-s} \binom{s}{d} \binom{s-d}{i+s-2d-j} (k-2)^{i+s-2d-j}.$$

Let r_0 and r_1 be the radii of the Hamming balls[1] about I and J respectively. Then the intersection volume is the sum of $N_{i,j}$ for all $0 \leq i \leq r_0$ and $0 \leq j \leq r_1$, thus

$$I(n, k, s, r_0, r_1) = \sum_{\substack{0 \leq i \leq r_0 \\ 0 \leq j \leq r_1}} N_{i,j}. \tag{A.8}$$

[1] A Hamming ball is the set of points that are within a distance r of a particular point. We call r the radius of the Hamming ball. The *ball* and *radius* terminology is by analogy with the usual, Euclidean, notion of balls and radii.

Appendix B

Intersection Volume in Euclidean Shape Space

The volume of the intersection of two Euclidean balls of stimulation can be calculated as the sum of the two shaded segments in Figure B.1. Beyer (1981) gives formulas for 2- and 3-dimensional segments; here we derive the volume of n-dimensional segments.

The volume of a segment is the integral, along the line S_1S_0, from the circumference of the ball to the line AB. The integrand is an $n-1$ dimensional ball with radius $\sqrt{r^2-(r-x)^2}$, where x is the distance from the circumference along S_1S_0. Thus, for a segment of width x',

$$\text{Segment}\ (n,r,x') = \int_0^{x^0} \text{Ball}\ \left(n-1, \sqrt{r^2-(r-x)^2}\right)\ dx,$$

where

$$\text{Ball}(n,r) = \mathrm{C}(n)r^n$$

and

$$\mathrm{C}(n) = \frac{2\pi^{(n/2)}}{n\Gamma(n/2)} = \frac{2^n\pi^{((n-1)/2)}((n-1)/2)!}{n!}.$$

Thus

$$\text{Segment}(n,r,x') = \mathrm{C}(n-1)\int_0^{x^0}\left(r^2-(r-x)^2\right)^{(n-1)/2}\ dx$$

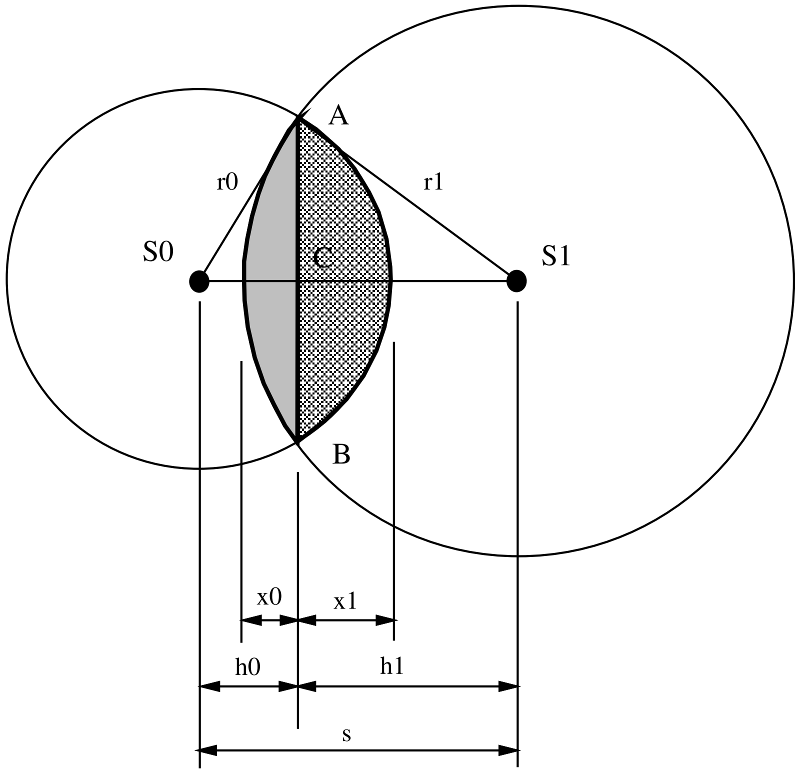

Figure B.1: The two shaded segments in this figure, when added together, form the intersection of the balls. The volume of a segment is calculated by integrating along the line S_0S_1. The key to the calculation is that the integrand is a ball in the next lower dimension whose radius is the distance from S_0S_1 to the circumference of the segment's circle (which varies as x moves along S_0S_1 during the integration).

The intersection is the sum of the S_0 segment and the S_1 segment, i. e. ,

$$I(n, r_0, r_1, s) = \text{Segment}(n, r_0, x_0) + \text{Segment}(n, r_1, x_1)$$

where

$$x_0 = \min(2r_0, 2r_1, \max(0, x'_0)),$$

$$x_1 = \min(2r_0, 2r_1, \max(0, x'_1)),$$

$$x'_0 = r_0 - h_0,$$

$$x'_1 = r_1 - h_1,$$

$$h_0 = \frac{s^2 - (r_1^2 - r_0^2)}{2s},$$

and

$$h_1 = s - h_0.$$

Figure B.2 plots the Euclidean intersection, as a function of sequence difference for 1, 2, 3, 5, 10 and 20 dimensions, with $\hat{r} = 0.5$.

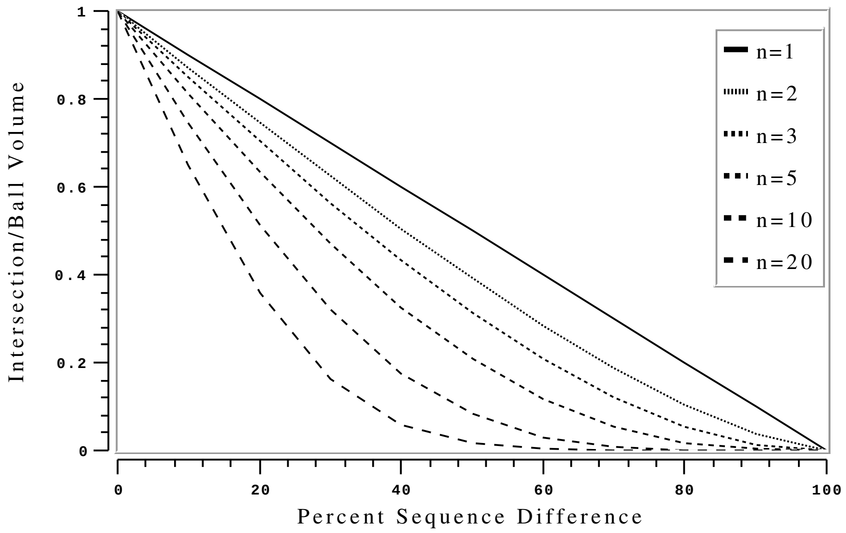

Figure B.2: The intersection volume as a function of the sequence difference for Euclidean balls in 1, 2, 3, 5, 10 and 20 dimensions, with $\hat{r} = 0.5$.

The left hand side of equation 3.4, in the main text, is derived as follows

$$\frac{\mathrm{Ball}(n, \hat{r})}{\mathrm{Ball}(n, 1)} = \frac{\mathrm{C}(n)\hat{r}^n}{\mathrm{C}(n)1^n} = \hat{r}^n.$$

Appendix C

Description of the Model

The model simulates an animal-sized B cell repertoire of 10^7 to 10^8 B cells (Köhler, 1976; Klinman *et al.*, 1976; Klinman *et al.*, 1977). The expected lifetime for an unstimulated B cell is 4.5 days. New B cells, with randomly generated antibody receptors, are generated at a rate of 560,000 per day on average to maintain the B cell repertoire in steady state. B cell and antibody receptors and antigen are modeled as strings of symbols that can loosely be thought of as the amino acids of a binding site. The mapping between sequence and shape is not fully understood, so for the purposes of the model we assume that sequence and shape are equivalent. The affinity between antibodies and antigens is proportional to the number of symbols that are complementary between their receptors. We define the antigenic distance between antigens as the number of symbols in which their receptors differ. The length of the receptor (20 symbols) and the number of distinct symbols at each location (4) were chosen (Smith *et al.*, 1997d) to give the following properties: a potential repertoire of 10^{12} B cells, a 1 in 10^5 chance of a B cell responding to a particular antigen (Edelman, 1974; Nossal & Ada, 1971; Jerne, 1974), and with an expressed repertoire of 10^7 B cells (Köhler, 1976; Klinman *et al.*, 1976; Klinman *et al.*, 1977) two antigens cease being cross-reactive when they have more than about 35% sequence difference (Champion *et al.*, 1975; East *et al.*, 1980). Thus, effectively, there are eight degrees of cross-reactivity in our model corresponding to antigenic distances 0 through 7. Due to the very large number of antibody molecules in a real immune response, each antibody in the simulation represents a large number of real antibodies. T-help is modeled implicitly by assuming that it is always available whenever it is needed.

During each 6 hour time period, each B cell gets a chance to bind with a unit of antigen which is selected at random from all antigens in the simulation.[1] The affinity of the B cell for the antigen is 10^{r-d} where d is the mutation, or Hamming,[2] distance between the strings representing the B cell antibody receptor and the antigen epitope, and r is the distance within which a B cell can be stimulated by an antigen. We set r=5, which means about 1 in 10^5 B cells can bind any particular antigen (Smith *et al.*, 1997d; Edelman, 1974; Nossal & Ada, 1971; Jerne, 1974). The probability that a B cell will bind an antigen is 0.1 times the ratio of this affinity to the average affinity of any antibodies bound to the antigen, or 1.0, whichever is the smaller. If there are no antibodies bound to the antigen, a random B cell (but one that has some affinity for the antigen) is selected, and its affinity is used in place of the average antibody affinity.

When a B cell has bound antigen for 6 hours it is stimulated to divide. On cell division the B cell antibody receptor has a 0.005 probability of a mutation in a digit that represents the receptor. B cell differentiation is approximated by each daughter cell having a 0.05 probability of differentiating into a plasma cell and a 0.05 probability of differentiating into a memory cell. Memory B cells have a half-life longer than the duration of the simulation. When memory B cells bind antigen and divide, both daughter cells revert to naive B cells. Plasma cells have a 75% chance of having a half-life of 3 days, and a 25% chance of being long lived with an expected half-life of 200 days. (Actual plasma cell half lives have been seen up to 100 days; however, we set the half-life 200 days to make keep

[1]The selection method for B cell-antigen encounters is more complex when more than 1 antigen are present in the simulation at the same time. However, this does not occur in the experiments reported in this paper.

[2]The Hamming distance between two receptors is the number of places where the receptors differ. This can also be thought of as the mutation distance. For example, if the four equivalence classes of amino acids represented by the symbols A through D, and receptors are represented by strings of 20 symbols, the Hamming distance between receptors CC$\underline{\text{B}}$DD$\underline{\text{B}}$BCCCAB$\underline{\text{D}}$CCDADAD and CC$\underline{\text{A}}$DD$\underline{\text{D}}$BCCCAB$\underline{\text{A}}$CCDADAD is 3 because they differ in the three underlined locations.

titers closer to experimentally observed levels.) Plasma cells secrete 2 units of antibody every 6 hours. Free antibodies have a chance to bind antigens every 6 hours. For each unit of antibody, an antigen is selected at random. If the antigen is not bound to a B cell the antibody binds with the antigen if it is within binding threshold. Unbound antibodies have a half-life of 10 days. When an antigen has 2 or more units of antibodies bound it is removed from the system. No more than 2 units of antibodies can to bind to any particular antigen.

The immune response and clearance of an two vaccinations and an epidemic challenge, that takes over 450 simulated days, takes about 2 minutes of CPU time, running in Franz Lisp, on a Sun Ultra 2/2300. An implementation technique called *lazy evaluation* is used to efficiently simulate the animal-size B cell repertoire (Smith *et al.*, 1997c). The model and simulator written in Common Lisp and the user interface is written in Tcl/TK and Blt. Figures 5.4, 5.3, 5.6 and 5.5 were taken almost directly from the user interface. The model, simulator, and user interface are available on request.

REFERENCES

Ada, G. L. (1993). Vaccines. In: *Fundamental Immunolgy, Third Edition* (Paul, W. E., ed.) chapter 37, pp. 1309–1352. Raven Press, New York.

Albus, J. S. (1981). *Brains, Behavior, and Robotics*. Byte Books, Peterborough, NH.

Aleksander, I., Thomas, W. V. & Bowden, P. A. (1984). Wisard-a radical step forward in image recognition. *Sensor Review* **4**(3), 120–124.

Amit, A. G., Mariuzza, R. A., Phillips, S. E. V. & Poljak, R. J. (1986). Three-dimensional structure of an antigen-antibody complex at 2.8 angstrom resolution. *Science* **233**, 747–753.

Angelova, L. A. & Shvartsman. (1982). Original antigenic sin to influenza in rats. *Immunology* **46**, 183–188.

Berek, C. & Milstein, C. (1988). The dynamic nature of the antibody repertoire. *Immunol. Rev.* **105**, 5–26.

Beyer, W. E. P., Palache, A. M., Baljet, M. & Masurel, N. (1989). Antibody induction by influenza vaccines in the elderly: A review of the literature. *Vaccine* **7**, 385–394.

Beyer, W. H. (1981). *CRC Standard Mathematical Tables, 26th Edition*. CRC Press, Florida.

Both, G. W., Sleigh, M. J., Cox, N. J. & Kendal, A. P. (1983). Antigenic drift in influenza virus H3 hemagglutinin from 1968 to 1980: Multiple evolutionary pathways and sequential amino acid changes at key antigenic sites. *J. Virol.* **48**, 52–60.

Burnet, F. M. (1959). *The Clonal Selection Theory of Immunity*. Cambridge Univerity Press, London.

CDC. (1996). Prevention and control of influenza: recommendations of the advisory committee on immunization practices (ACIP). *Morbidity and Mortality Weekly Report* **45**.

Celada, F. & Seiden, P. E. (1996). Affinity maturation and hypermutation in a simulation of the humoral immune response. *Eur. J. Immunol.* **26**, 1350–1358.

Champion, A. B., Soderberg, K. L., Wilson, A. C. & Ambler, R. P. (1975). Immunological comparison of azurins of known amino acid sequence: Dependence of cross-reactivity upon sequence resemblance. *J. Mol. Evol.* **5**, 291–305.

Commuri, S., Jagannathan, S. & Lewis, F. L. (1997). CMAC neural network control of robot manipulators. *J. Robotic Systems* **14**, 465–482.

Cox, N. J., (1997). Personal communication.

Danforth, D. (1990). An empirical investigation of sparse distributed memory using discrete speech recognition. In: *Proc. Intnl. neural network conf. (Paris)* pp. 183–186, MA. Kluwer Academic.

Danforth, D. G. (1991). Total recall in distributed associative memories. Technical Report TR 91.03, Research Institute for Advanced Computer Science, NASA Ames Research Center.

Danforth, D. G., (1997). Personal communication of work performed at the Research Institute for Advanced Computer Science, NASA Ames Research Center.

Dannenberg, R. B., Fraley, C. L. & Velikonja, P. (1992). A functional language for sound synthesis with behavioral abstraction and lazy evaluation. In: *Computer Generated Music* (Baggi, D., ed.). IEEE Computer Society Press.

Davenport, F. M., Hennessy, A. V. & Francis, T. (1953). Epidemiologic and immunologic significance of age distribution of antibody to antigenic variants of influenza virus. *J. Exp. Med.* **98**, 641–656.

Davenport, F. M. (1973). Control of influenza. *Med. J. Aust.* (Supplement), 33–38.

DeBoer, R. J. & Perelson, A. S. (1991). Size and connectivity as emergent properties of a developing immune network. *J. Theoret. Biol.* **149**, 381–424.

DeBoer, R. J., Hogeweg, P. & Perelson, A. S. (1992). Growth and recruitment in the immune network. In: *Theoretical and Experimental Insights into Immunology* (Perelson, A. S. & Weisbuch, G., eds) pp. 223–247. Springer-Verlag, Berlin.

DeBoer, R. J., Segel, L. A. & Perelson, A. S. (1992). Pattern formation in one and two dimensional shape space models of the immune system. *J. Theoret. Biol.* **155**, 295–333.

Detours, V., Sulzer, B. & Perelson, A. S. (1996). Size and connectivity of the idiotypic network are independent of the discreteness of the affinity distribution. *J. Theoret. Biol.* **183**, 409–416.

Deutsch, S. & Bussard, A. E. (1972). Original antigenic sin at the cellular level. I. Antibodies produced by individual cells against cross-reacting haptens. *Eur. J. Immunol.* **2**, 374–378.

Dunne, P. E., J.Gittings, C. J. & Leng, P. H. (1993). Sequential and parallel strategies for the demand-driven simulation of logic circuits. *Microprocessing and microprogramming* **1**, 591–525.

East, I. J., Todd, P. E. & Leach, S. J. (1980). Original antigenic sin: Experiments with a defined antigen. *Mol. Immunol.* **17**, 1539–1544.

Edelman, G. M. (1974). Origins and mechanisms of specificity in clonal selection. In: *Cellular Selection and Regulation in the Immune System* (Edelman, G. M., ed.) pp. 1–38. Raven Press, New York.

Eigen, M. (1993). Viral quasispecies. *Scientific American* **269**(1), 32–39.

Eisen, H. N., Little, J. R., Steiner, L. A., Simms, E. S. & Gray, W. (1969). Degeneracy in the secondary immune response: Stimulation of antibody formation by cross-reacting antigens. *Israel J. Med. Sci.* **5**, 338–351.

Elliott, C. & Hudak, P. (1997). Functional reactive animation. In: *Proc. ACM SIGPLAN International Conference on Functional Programming (ICFP '97).*

Farmer, J. D., Packard, N. H. & Perelson, A. S. (1986). The immune system, adaptation, and machine learning. *Physica D* **22**, 187–204.

Fazekas de St. Groth, S. & Webster, R. G. (1966). Disquisitions of original antigenic sin. II. Proof in lower creatures. *J. Exp. Med.* **124**, 347–361.

Fazekas de St. Groth, S. & Webster, R. G. (1966). Disquisitions of original antigenic sin. I. Evidence in man. *J. Exp. Med.* **124**, 331–345.

Feery, B. J., Evered, M. G. & Morrison, E. I. (1979). Different protection rates in various groups of volunteers given subunit influenza virus vaccine in 1976. *J. Inf. Dis.* **139**, 237–241.

Fish, S., Zenowich, E., Fleming, M. & Manser, T. (1989). Molecular analysis of original antigenic sin. I. Clonal selection, somatic mutation, and isotype switching during a memory B cell response. *J. Exp. Med.* **170**, 1191–1209.

Forrest, S. & Perelson, A. S. (1991). Genetic algorithms and the immune system. In: *Parallel Problem Solving from Nature* (Schwefel, H. & Maenner, R., eds) pp. 320–325. Springer-Verlag, Berlin.

Francis, T. (1953). Influenza, the newe acquayantance. *Ann. Intern. Med.* **39**, 203–221.

Friedman, D. P. & Wise, D. (1976). CONS should not evaluate its arguments. In: *Automata, Languages and Programming* (Michaelson, S. & Milner, R., eds) pp. 257–284, Edinburgh. Edinburgh University Press.

Gerhard, W. (1978). The analysis of the monoclonal immune response to influenza virus. III. The relationship between stimulation of virus-primed precursor B cells by heterologous viruses and reactivity of secreted antibodies. *J. Immunol.* **120**, 1164–1168.

Gibert, C. J. & Routen, T. W. (1994). Associative memory in an immune-based system. In: *Proceedings of the Twelfth National Conference on Artificial Intelligence* pp. 852–857, Cambridge, MA. AAAI Press/The MIT Press.

Gilden, R. V. (1963). Antibody responses after successive injections of related antigen. *Immunology* **6**(30), 30–36.

Henderson, P. & Morris, J. M. (1976). A lazy evaluator. In: *Proc. 3rd Annual ACM symposium on Principles of Programming Languages* pp. 95–103, New York. ACM.

Hightower, R. R., Forrest, S. & Perelson, A. S. (1995). The evolution of emergent organization in immune system gene libraries. In: *Proceedings of the Sixth International Conference on Genetic Algorithms* (Eshelman, L. J., ed.) pp. 344–350, San Francisco, CA. Morgan Kaufman.

Hobson, D., Baker, F. A. & Curry, R. L. (1973). Effect of influenza vaccines in stimulating antibody in volunteers with prior immunity. *Lancet* **ii**, 155–156.

Hopfield, J. J. (1982). Neural networks and physical systems with emergent collective computational abilities. *Proc. Nat. Acad. Sci. (Biophysics)* **78**(8), 2554–2558.

Hoskins, T. W., Davis, J. R., Allchin, A., Miller, C. L. & Pollock, T. M. (1973). Controlled trial of inactivated influenza vaccine containing the A/HongKong strain during an outbreak of influenza due to the A/England/42/72 strain. *Lancet* **ii**, 116–120.

Hoskins, T. W., Davis, J. R., Smith, A. J., Allchin, A. & Miller, C. L. (1976). Influenza at Christ's Hospital: March, 1974. *Lancet* **i**, 105–108.

Hoskins, T. W., Davis, J. R., Smith, A. J., Miller, C. L. & Allchin, A. (1979). Assessment of inactivated influenza-A vaccine after three outbreaks of influenza A at Christ's Hospital. *Lancet* **i**, 33–35.

Howells, C. H. L., Evans, A. D. & Vessilinova-Jenkins, C. (1973). *Lancet* **i**, 1436.

Hudak, P., Peyton Jones, S. L., Wadler, P. *et al.* (1992). Report on the functional programming language Haskell: A non-strict, purely functional language: Version 1.2. *ACM SIGPLAN Notices* **27**, 1–163.

Inman, J. K. (1978). In: *Theoretical Immunology* (Bell, G., Perelson, A. & Pimberly, G., eds) page 243. Marcel Decker, Inc., New York.

Ivanyi, J. (1972). Recall of antibody synthesis to the primary antigen following successive immunization with heterologous albumins. A two-cell theory of the original antigenic sin. *Eur. J. Immunol.* **2**(4), 354–359.

Jaeckel, L. A. (1989). An alternative deisgn for a sparse distributed memory. Technical Report TR 89.28, Research Institute for Advanced Computer Science, NASA Ames Research Center.

Jaeckel, L. A. (1989). A class of designs for a sparse distributed memory. Technical Report TR 89.30, Research Institute for Advanced Computer Science, NASA Ames Research Center.

Jenner, E. (1798). *An Inquiry into the Causes and Effects of the Variolae Vaccinae*. Low, London.

Jerne, N. K. (1974). Clonal selection in a lymphocyte network. In: *Cellular Selection and Regulation in the Immune System* (Edelman, G. M., ed.) pp. 39–48. Raven Press, New York.

Kanerva, P. (1988). *Sparse Distributed Memory*. MIT Press, Cambridge, MA.

Kanerva, P. (1992). Sparse distributed memory and related models. In: *Associative Neural Memories: Theory and Implementation* (Hassoun, H. M., ed.) chapter 3. Oxford University Press.

Katz, J. M., Lu, X., Young, S. A. & Galphin, J. C. (1997). Adjuvant activity of the heat-labile enterotoxin from enterotoxigenic *escherichia coli* for oral administration of inactivated influenza virus vaccine. *J. Infect. Dis.* **175**, 352–363.

Katz, J. M., (1997). Personal communication.

Keitel, W. A., Cate, T. R. & Couch, R. B. (1988). Efficacy of sequential annual vaccination with inactivated influenza virus vaccine. *Am. J. Epidemiol.* **127**, 353–364.

Klinman, N. R., Press, J. L., Sigal, N. H. & Gerhart, P. J. (1976). The acquisition of the B cell specificity repertoire: the germ-line theory of predetermined permutation of genetic information. In: *The Generation of Antibody Diversity* (Cunningham, A. J., ed.) pp. 127–150. Academic Press, New York.

Klinman, N. R., Sigal, N. H., Metcalf, E. S., Gerhart, P. J. & Pierce, S. K. (1977). *Cold Spring Harbor Symp. Quant. Biol.* **41**, 165.

Köhler, G. (1976). Frequency of precursor cells against the enzyme beta-galactosidase: an estimate of the BALB/c strain antibody repertoire. *Eur. J. Immunol.* **6**, 340–347.

Kohonen, T. (1984). *Self-organization and associative memory*. Springer-Verlag, New York.

Leder, P. (1991). The genetics of antibody diversity. In: *Immunology: Recognition and Response* (Paul, W., ed.) pp. 20–34. W. H. Freeman, New York.

Lodish, H., Baltimore, D., Berk, A., Zipursky, S. L., Matsudaira, P. & Darnell, J. (1995). *Molecular Cell Biology*. Scientific American Books, New York.

Lucas, S. M. (1995). Rapid best-first retrieval from massive dictionaries by lazy evaluation of a syntactic neural network. In: *Proc. IEEE Intnl. Conf. on Neural Networks* pp. 2237–42, New York, NY. IEEE.

Mackay, C. R. (1993). Immunological memory. *Adv. Immunol.* **53**, 217–265.

Manevitz, L. M. & Zemach, Y. (1997). Assigning meaning to data: using sparse distributed memory for multilevel cognitive tasks. *Neurocomputing* **14**, 15–39.

Marr, D. (1969). A theory of cerebellar cortex. *J. Physiology* **202**, 437–470.

Matzinger, P. (1994). Immunological memories are made of this? *Nature* **369**, 605–6.

Nara, P. L. & Goudsmit, J. (1990). Clonal dominance of the neutralizing response to the hiv-1 v3 epitope; evidence for original antigenic sin during vaccination and infection in animals including humans. In: *Vaccines (Cold Spring Harbor Eighth Annual Meeting), Vol. 91, Modern Approaches to New Vaccines including Prevention of AIDS* (Chanock, R. M., ed.). Cold Spring Harbor, NY.

Nossal, C. J. V. & Ada, G. L. (1971). *Antigens, Lymphoid Cells and The Immune Response*. Academic Press, New York.

Percus, J. K., Percus, O. E. & Perelson, A. S. (1993). Predicting the size of the T cell receptor and antibody combining region from consideration of efficient self-nonself discrimination. *Proc. Natl. Acad. Sci. USA* **90**, 1691–1695.

Perelson, A. S. & Oster, G. F. (1979). Theoretical studies of clonal selection: Minimal antibody repertoire size and reliability of self- non-self discrimination. *J. Theoret. Biol.* **81**, 645–670.

Perelson, A. S., Hightower, R. & Forrest, S. (1996). Evolution and somatic learning in V-region genes. *Res. Immunol.* **147**, 202–208.

Powers, R. D., Hayden, F. G., Samuelson, J. & Gwaltney Jr, J. M. (1984). Immune response of adults to sequential influenza vaccination. *J. Med. Virol.* **14**, 169–175.

Prager, R. W. & Fallside, F. (1989). The modified Kanerva model for automatic speech recognition. *Comptuer Speech and Language* **3**(1), 61–81.

Robinson, H. L., Boyle, C. A., Feltquate, D. M., Morin, M. J., Santoro, J. C. & Webster, R. G. (1997). DNA immunization for influenza virus studies using hemagglutinin- and nucleoprotein-expressing DNAs. *J. Infect. Dis.* **176** (Supplement 1), 50–55.

Sabourin, M. & Mitiche, A. (1993). Modeling and classification of shape using a Kohonen associative memory with selective multiresolution. *Neural Networks* **6**, 275–283.

Segel, L. A. & Perelson, A. S. (1988). Computations in shape space: A new approach to immune network theory. In: *Theoretical Immunology, Part Two, SFI Studies in the Sciences of Complexity* (Perelson, A. S., ed.) pp. 321–343. Addison-Wesley, Reading, MA.

Seiden, P. E. & Celada, F. (1992). A model for simulating cognate recognition and response in the immune system. *J. Theoret. Biol.* **158**, 329–357.

Smith, D. J., Forrest, S. & Perelson, A. S. (1996). Immunological memory is associative. In: *Workshop Notes, Workshop 4: Immunity Based Systems, Int. Conf. on Multiagent Systems* pp. 62–70, Kyoto, Japan.

Smith, D. J., Forrest, S., Ackley, D. H. & Perelson, A. S. (1997a). Geometric interpretations of the cross-reactive immune response. *In Preparation* .

Smith, D. J., Forrest, S., Ackley, D. H. & Perelson, A. S. (1997b). Modeling the effects of prior infection on vaccine efficacy. In: *IEEE Intnl. Conf. on Systems, Man, and Cybernetics* pp. 363–368, Orlando, Florida. IEEE.

Smith, D. J., Forrest, S., Ackley, D. H. & Perelson, A. S. (1997c). Using lazy evaluation to simulate realistic-size repertoires in models of the immune system. *Submitted to Bull. Math. Biol.* and *Santa Fe Institute Working Paper 97-09-078* and *Chapter 4 of this dissertation* .

Smith, D. J., Forrest, S., Hightower, R. R. & Perelson, A. S. (1997d). Deriving shape space parameters from immunological data. *J. Theoret. Biol. (in press)* and *Santa Fe Institute Working Paper 97-03-017* and *Chapter 3 of this dissertation* .

Smith, D. J. (1994). A literature review of original antigenic sin. Technical Report TR 94–10, University of New Mexico, Albuquerque, NM.

Stauffer, D. & Sahimi, M. (1994). High-dimensional simulation of simple immunological models. *J. Theoret. Biol.* **166**, 289–297.

Tew, J. G. & Mandel, T. E. (1979). Prolonged antigen half–life in the lymphoid follicules of antigen–specifically immunized mice. *Immunology* **37**, 69–76.

Tew, J. G., Phipps, P. R. & Mandel, T. E. (1980). The maintenance and regulation of the humoral immune response. persisting antigen and the role of follicular antigen–binding dendritic cells. *Immunol. Rev.* **53**, 175–211.

Turner, D. A. (1979). A new implementation technique for applicative languages. *Software—Practice and Experience* **9**, 31–49.

Turner, D. A. (1985). Miranda: a non-strict functional language with polymorphic types. In: *Proc. Int'l Conf. on Functional Programming and Computer Architecture, Nancy, Lecture Notes in Computer Science 201* (Jouannaud, J.-P., ed.) pp. 1–16, Berlin. Springer-Verlag.

Virelizier, J. L., Allison, A. C. & Schild, G. C. (1974). Antibody responses to antigenic determinants of influenza virus hamagglutinin. II. Original Antigenic Sin: A bone marrow-derived lymphocyte memory phenomenon modulated by thymus-derived lymphocytes. *J. Exp. Med.* **140**, 1571–1578.

Weisbuch, G. & Oprea, M. (1994). Capacity of a model immune network. *Bull. Math. Biol.* **56**, 899–921.

Willshaw, D. (1981). Holography, associative memory, and inductive generalization. In: *Parallel Models of Associative Memory* (Hinton, G. E. & Anderson, J. A., eds) pp. 83–104. Erlbaum, New Jersey.

Yarchoan, R. & Nelson, D. L. (1984). Specificity of in vitro anti-influenza virus antibody production by human lymphocytes: Analysis of original antigenic sin by limiting dilution cultures. *J. Immunol.* **132**, 928–935.

Yoshino, T., Smith, D. J. & Matzke, D. J. (1987). An RTL simulator based on functional programming. *Texas Instruments Technical Journal* **4**(3).